ESTIMATION OF RUNOFF COEFFICIENT ACCORDING TO SOIL MOISTURE USING GIS TECHNIQUES

A. I. Crăciun[1], I. Haidu[1], Zs. Magyari-Sáska[1], A. I. Imbroane[1]

ABSTRACT:
This study aims the analysis of the role that the soil water content has in evaluating the runoff in a small watershed (≈ 10km^2) situated in mountain area – Stolna Basin (Apuseni Mountains). From meteorological point of view a model developed by Soil Conservation Service (SCS) from USA will be used, model that is based on hydrologic balance, by which the infiltration depth (cumulative infiltration) can be estimated. Also, the runoff depth can be estimated. In the same time, in order to obtain a spatial representation of these hydrological processes, the SCS equation will be integrated in GIS medium. So, it will be necessary, first to create a raster database for the next parameters: soil texture, hydrological soil group, slope, land use, CN index, maximum capacity of retention, loss due to interception and evapotranspiration etc. In the end, medium values of the runoff coefficient will be computed in the basin for different periods of the year.

Key words: *runoff coefficient, soil moisture, GIS, SCS method, Stolna (Apuseni Mountains)*

1. INTRODUCTION

Runoff coefficient represents one of the principal means to characterize the runoff, showing the ratio rainfall / runoff for different periods and areas. Analysis scale through this coefficient starts from a single pluviometrical event with a certain duration (ex: one hour – hourly runoff coefficient) and can continue to the yearly level or even multiannual (yearly or multiannual runoff coefficient). In this paper, we want to study the influence that soil water content has in evaluating the hillslope runoff. For detection of the runoff differences during a year, a monthly analysis of the side runoff will be realized.

The main objectives of this research consist in:

- developing a GIS algorithm for estimating the cumulative infiltration (infiltration depth) using a distributed parameter model;
- computation of runoff coefficients on monthly scale, taking in account the soil water content;

For this study, a hydrographic basin located in East of Gilău Massif (Stolna Basin) on the contact with Vlaha-Hăşdate depression was chosen. Stolna Basin has a surface of approximately 9,7 Km^2 and a drainage length of 30 km, its principal stream being the left affluent of Feneş river (**Fig. 1**).

[1] *"Babeş-Bolyai" University, Faculty of Geography,400006 Cluj-Napoca, Romania*

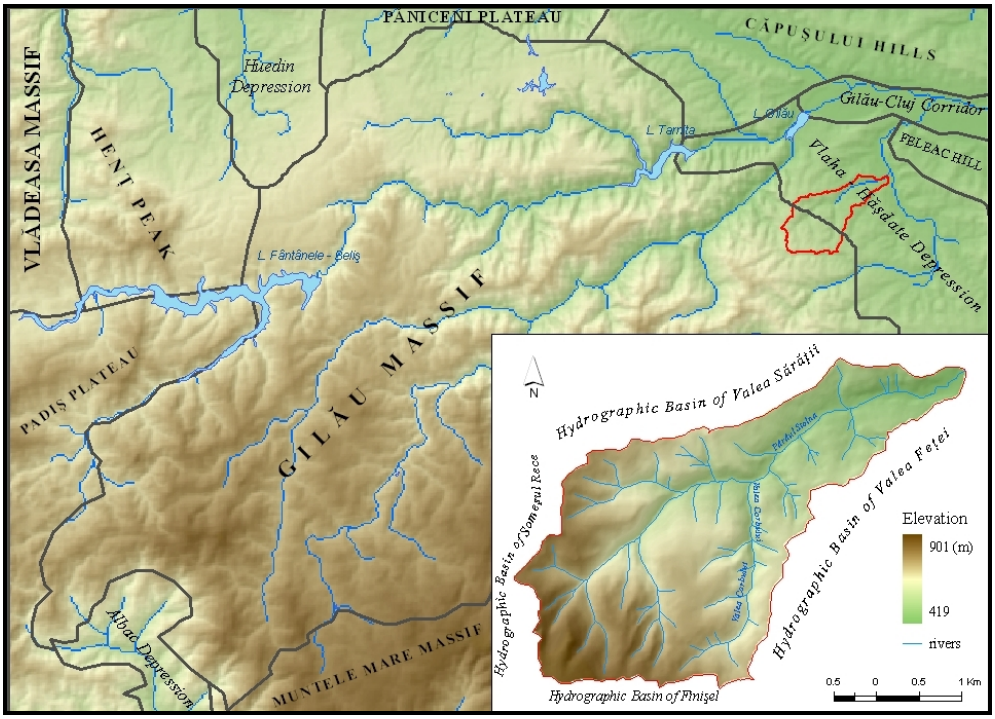

Fig. 1 Elements of studied watershed location

2. METHODOLOGY

a) Description of methods used

Methodological, an algorithm was created based on a classical method implemented in GIS (SCS-CN – Soil Conservation Service-Curve Number) in order to estimate the cumulative infiltration and the runoff.

In order to estimate the infiltration ratio – cumulative infiltration (F, [mm]), SCS (Soil Conservation Service) proposes a relation depending on the quantity of precipitation intercepted by the basin (P), initial abstractions (I_a), maximum capacity of retention (S). In its original form, the model is based on using the next equations (*Musy, Higy , 1998*):

$$F = \frac{S \cdot (P - I_a)}{P - I_a + S} \qquad S = \frac{25.400}{CN} - 254 \qquad I_a = 0{,}2 \cdot S \tag{1}$$

- where:

P – quantity of precipitation;
S – maximum capacity of retention;
I_a – initial abstractions (evapotranspiration, vegetation retentions, other retentions);
CN – f (soil, vegetation, land use, soil moisture conditions)

*

Studying the model, some weaknesses were observed which have asked for some improvements, we believe, of the presented method.

The most important problem is represented by not taking into account the slope and runoff capacity that characterized each area. From this consideration, we find useful to integrate in the equation a *theoretical runoff coefficient* (α) estimated in function of slope, soil texture, land use. So, the equation of cumulative infiltration would have the next form:

$$F = \frac{S \cdot (P - I_a)}{P - I_a + S} \cdot (1 - \alpha) \tag{2}$$

Another remark considering the use of the relation to determinate $\mathbf{I_a}$ parameter (initial abstractions due to evapotranspiration, vegetation retentions, other retentions) goes to obtaining some overdone values, because it analyses the process from a static point of view, without taking into account the fact that a part of that water quantity retained initially will be drained and it will reach the soil later. This fact should impose its multiplication with a coefficient (β) which illustrates the water retention capacity at vegetation level or a coefficient that shows the lag drainage as a fraction of initial abstractions on vegetation in function of different land uses. So, the equation of I_a parameter would have the next form:

$$I_a = 0{,}2 \cdot S \cdot \beta \tag{3}$$

Evaluation of ***runoff depth*** was realized by using an equation based on balance, having the next form:

$$Q = P - F - I_a \tag{4}$$

Later, using the rapport runoff depth / precipitation depth, the runoff coefficient (C) will be obtained:

$$C = \frac{Q}{P} \tag{5}$$

b) GIS contribution for soil moisture estimation

The first step of the algorithm consists in an initial database acquisition (data series measured to the meteorological stations, pedological maps, terrain and laboratory studies, topographical maps etc.); the next component of the algorithm refers to georeferencing the initial cartographic database and generating a vector database.

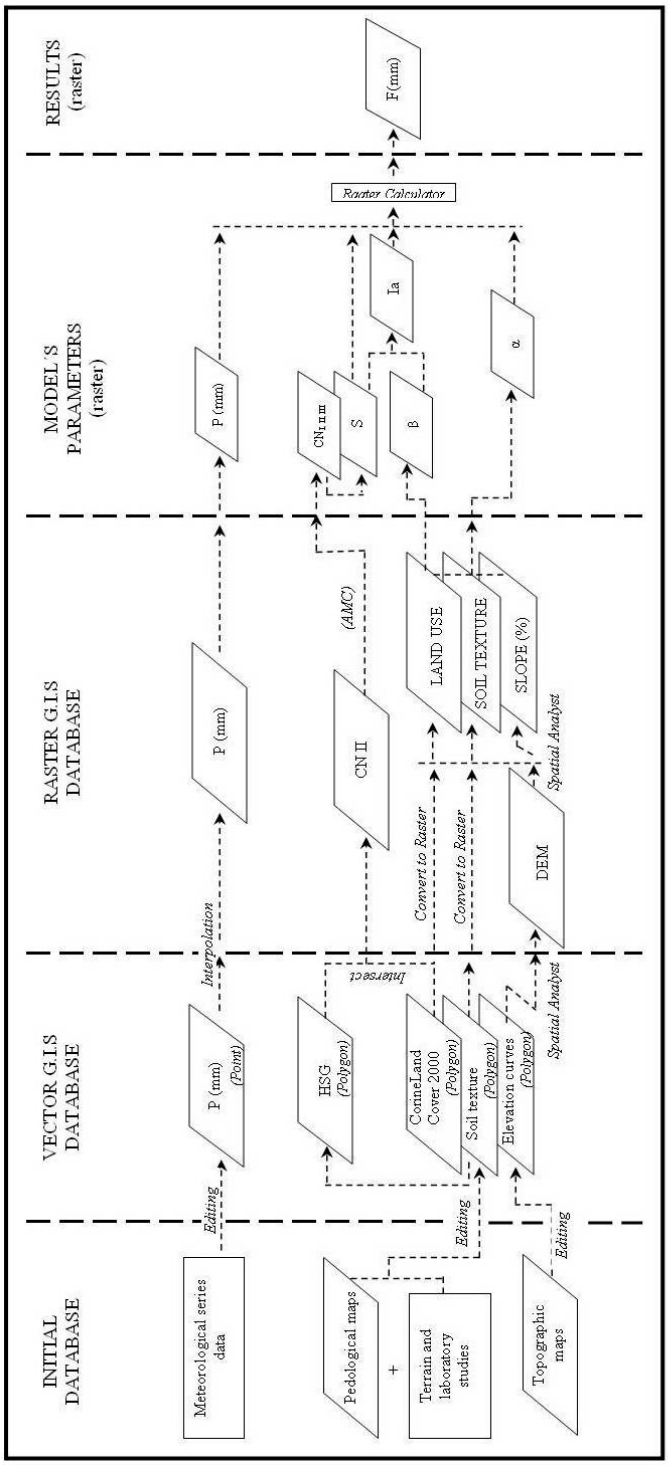

[P (mm) – precipitations; HSG – hydrologic soil group; CN II – Curve Number Index for standard antecedent moisture conditions; AMC – Antecedent Moisture Conditions; $CN_{I, II, III}$ – corrected Curve Number Index; S – maximum retention capacity; Ia – initial abstractions; α –theoretical runoff coefficient; F (mm) cumulative infiltration]

Fig. 2 GIS algorithm in order to estimate the cumulative infiltration using the SCS method

The derived database, containing raster layers, obtained by using some spatial analysis functions (conversions, interpolation functions, reclassification, map algebra etc.), is the most consistent in that it may concern the geographical information generated and, of course, is definetly important in evaluating the model parameters (**Fig. 2**). In the present study this database was realized at a spatial resolution of 10m. In table 1 we present the sources used for create this database.

Table 1. ***GIS functions used for create the derived database***

Layer	**Source**	**GIS functions used**
Digital Model Elevation	Topographic map 1:25.000	- *Sketch Tool; Topo to Raster*
Slope	DEM exploring	- *Surface Analysis → Slope*
Soil	Pedologic map 1:200.000	- *Sketch Tool; Covert to Raster*
Landuse	CLC 2000 database	- *Covert to Raster*

In what it may concern the ***P*** parameter (precipitation amount) the values registered at the nearest meteorological station (Cluj-Napoca, aprox. 12 km) have been taken into account. Being a small watershed with no monitoring, from meteorological point of view, by a network that can measure the precipitation spatialisation, the values registered at Cluj-Napoca station have been considered medium on basin.

The parameter ***α*** was obtained according to land use, slope and soil texture - Frevert tables (*Diaconu, Şerban, 1994*) – using a spatial analysis algorithm based on accessing some conversion functions vector-raster, reclassification, map algebra. Some of the recent studies about runoff coefficient spatialisation using Frevert indices are: *Păcurar (2005), Magyari-Saska (2008), Crăciun (2007), Bilaşco (2008).*

CN index is determined according to land use, soil hydrological group (A, B, C, D) and antecedent moisture conditions *(Chendeş, 2007; Crăciun, Haidu, Bilaşco, 2007; Crăciun, Haidu, 2009).*

As we mentioned at the beginning of this chapter, for evaluating the vegetation capacity to lag the drainage to soil for a part of water quantity initially stored, we propose to introduce a ***β*** coefficient. So, it starts from the idea that during a rain, a forest, for example, being in vegetation period, stores a very high quantity, but from this quantity, just a part contributes to define the **Ia** parameter, another part of it will reach the soil level and will contribute to the infiltration process. So, it was appreciated that from the water quantity stored by the forest, only 50 % consists in losses. In **table 2** we present the values proposed for β coefficient according to land use.

Table 2. ***Estimation of β coefficient according to landuse***

Landuse	**β**
Forest	0,5
Shrubbery	0,4
Grass / Pasture	0,3
Agricultural	0,2
Settlement	0,1

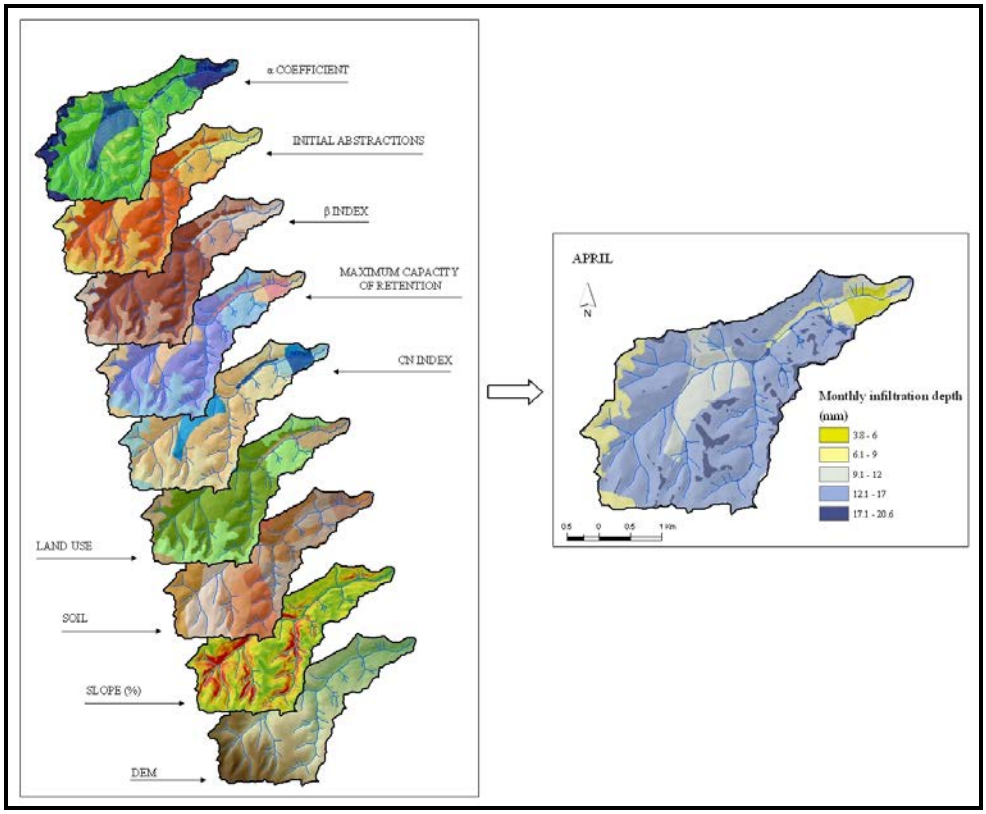

Fig. 3 Layers necessary for spatialisation of infiltration depth

Once the raster database was realized, by integrating in GIS medium of the equation presented, spatial representations of infiltration depth are obtained. In **fig. 3** we present the values obtained in April, taking into account the monthly multiannually precipitation amounts of Cluj-Napoca Station.

3. RESULTS

After obtaining the infiltration depth layers we pass to determine the runoff depth and than the runoff coeficient by applying the equations (4) and (5). In order to emphasize runoff differences in time first the monthly mean multiannual runoff depth (Q-mm) was modeled. Also, such modelings have been realized for two more recent years (2005, 2006). In **fig. 4** are presented the results obtained on a monthly multiannual scale. So, the months with the highest runoff depth are: May, June, July and August. The low values obtained in the beginning of spring could be explained by the fact that the study didn't take into account the snow water content. So, we emphasize that the results refer only to runoff generated by rain.

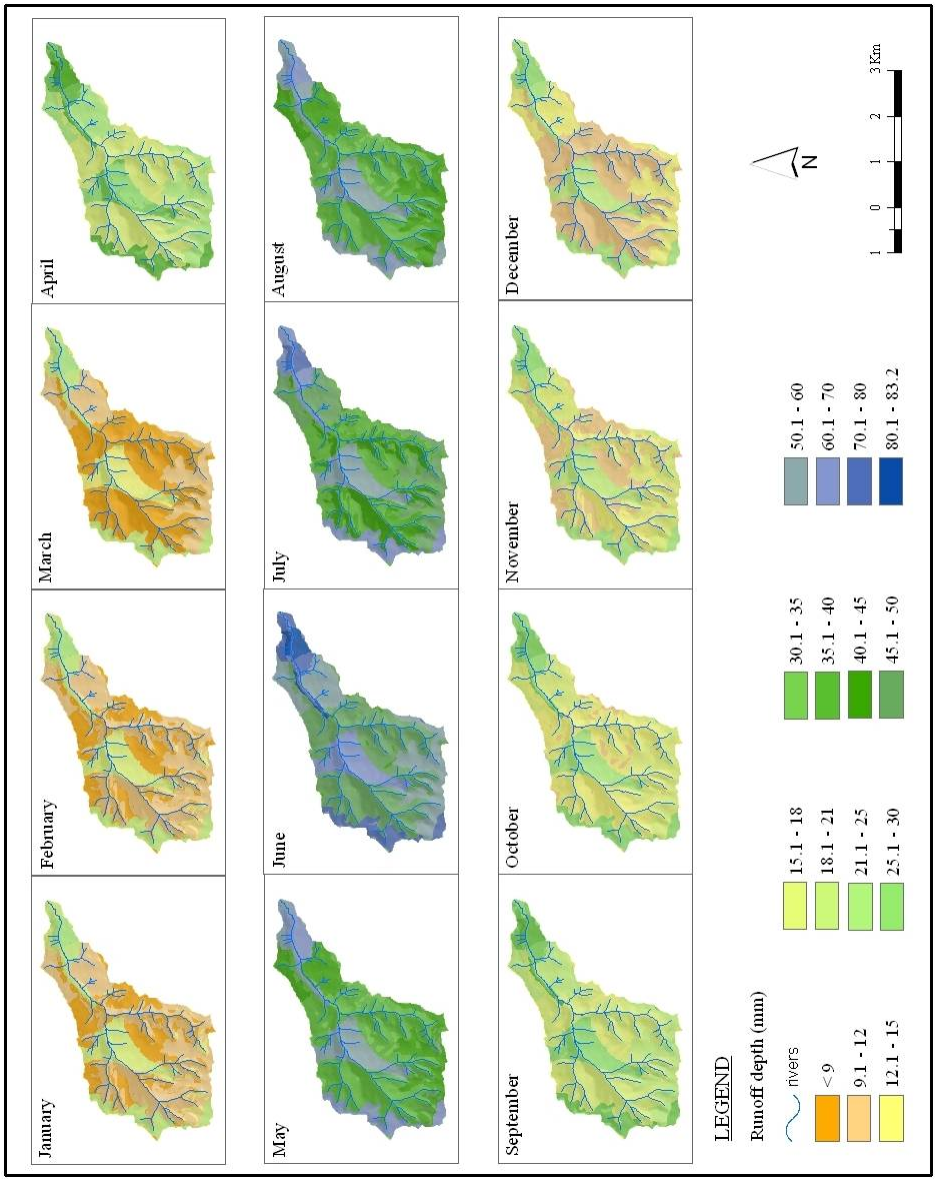

Fig. 4 The quantum of monthly runoff generated by rains

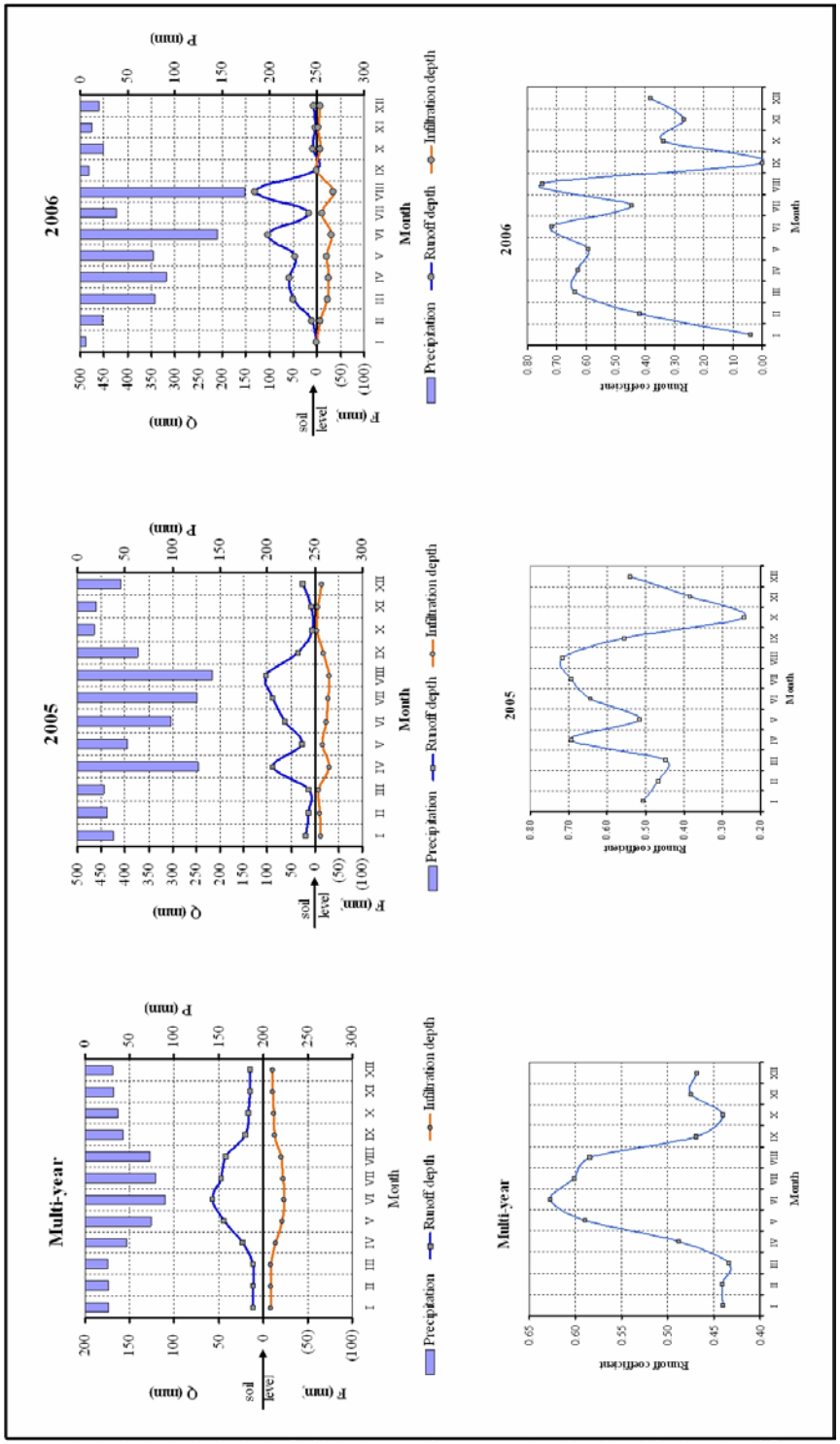

Fig. 5 Runoff characteristics generated by rains during a year

The results were syntethised by extracting the medium values for the infiltrated layer, the layer available for runoff and the runoff coefficient using a statistical function (Zonal Statistics) (**Fig. 5**).

At monthly multiannual scale, a raise of the runoff coefficient can be seen, from 0.44 in January to 0.63 in June, then a drop of this coefficient can be seen down to the value of 0.44 in october. A small raise of the runoff coefficient in the last two months of the year is explained by the lower losses caused by the interception and the evapotranspiration because the vegetation period ends.

Analyzing the results for two recent years (2005 and 2006), the medium runoff coefficient oscillates several times according, of course, to the recorded rainfall quantities. Therefore, in year 2005 a spring maximum is reached (0.69 in April) and a summer maximum (0.71 in august). Year 2006 also has a spring maximum (0.64 in March) and two summer maximum values (0.72 in June and 0.75 in august).

CONCLUSIONS

This study has determined a linear increase of the runoff coefficient along with the soil water content at multiannual level after correlating the monthly runoff coefficient with the infiltration layer. Years 2005 and 2006 are an exception because the distributions that were obtained are polynomial (Fig. 6) and the correlation coefficients that resulted (r) were bigger than 0.9.

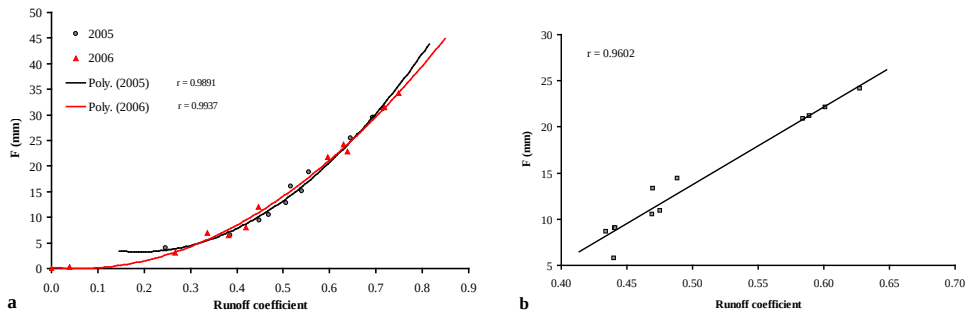

Fig. 6 Relation between soil moisture and yearly runoff coefficient (a) and multiannual (b) – (*points represents the months of the year*)

For a correct evaluation of the surface runoff, we consider that the soil water content should be accounted.

In mountain areas, because of the mostly thin soil profile, the clefts in the geological substrate should be accounted (especially in calcareous areas).

REFERENCES

Bilaşco Şt., Haidu I., (2006), *The Valuation of Maximum Runoff on Interbasinal Areas, Assisted by GIS*, Geographia Technica, ISSN 1842-5135, No.2, pag. 1-6, Cluj-Napoca.

Bilaşco Şt., (2008), *Model G.I.S de estimare a coeficientului de scurgere adaptat după Frevert*, Geographia Napocensis, Nr. 1, pag. 38-45.

Chendeş V., (2007), *Scurgerea lichidă şi solidă în Subcarpaţii de la curbură*, Teză de doctorat, Institutul de Geografie, Academia Română.

Crăciun A. I., Haidu I., Bilaşco Şt., (2007), *The SCS-CN model assisted by GIS – alternative estimation of the hydric runoff in real time*, Geographia Technica, ISSN 1842-5135, No.1, pag. 1-7, Cluj-Napoca.

Crăciun, A. I**.,** (2007)**,** *Use G.I.S to establish some parameters useful to measure the time of concentration and runoff coefficient***,** Geographia Technica, ISSN 1842-5135, No.2, pag. 12-19, Cluj-Napoca.

Crăciun A.I., Haidu I., (2009), *Estimation of soil water infiltration using CN (Curve Number) index and G.I.S techniques. Application: Săcuieu Hydrographic Basin*, Studia Universitatis Babeş-Bolyai, Series Geographia, ISSN: 1221-079X, no. 3, pag. 178-185.

Diaconu C., Şerban P., (1994), *Sinteze şi regionalizări hidrologice*, Edit. Tehnică, Bucureşti.

Magyari-Saska Zs., (2008), *Dezvoltarea algoritmilor S.I.G pentru calculul riscurilor geografice naturale. Aplicaţie la Bazinul Superior al Mureşului*, Teză de doctorat, UBB Cluj-Napoca.

Musy, A., Higy C., (1998), *Hydrologie appliquée*, Edit. H*G*A, ISBN: 973-98530-8-0, Bucureşti.

Păcurar V. D., (2005), *Utilizarea Sistemelor de Informaţii Geografice în modelarea şi simularea proceselor hidrologice*, Edit. Lux Libris, Braşov.

Acknowledgements. This work was supported by Grant PN-II-ID-No.517 and Grant BD-Cod 410 financed by CNCSIS Romania.

GIS IN DETERMINATION OF THE DISCHARGE HYDROGRAPH GENERATED BY SURFACE RUNOFF FOR SMALL BASINS

M. Domniţa[1], A. I. Crăciun[1], I. Haidu[1]

ABSTRACT:
A hydrograph model is proposed in which the watershed is decomposed into subareas represented by individual cells. The watershed response is found for each cell and these responses are convoluted to produce the watershed runoff hydrograph. The cell to cell flow path to the watershed outlet is determined from a digital elevation model. A flow velocity for each cell is calculated using Manning's formula and used in determining the travel time of water through each cell. In this paper a simplified approach is used: the rainfall intensity is considered constant thorough the rainfall event. The velocity field, considered spatially varying but time invariant, and the flow path to the outlet are used to determine the runoff time from each cell to the outlet of the watershed. The responses of each cell with the same travel time to the outlet are summed to produce the hydrograph. An example is shown for the 11 km^2 Pârâul Mare watershed in the Apuseni Mountains.

Keywords: *hydrograph, runoff, small basin, GIS, rational method*

1. INTRODUCTION

The unit hydrograph is a traditional method of representing the response at a watershed outlet to a rainfall event over the watershed. This method suffers from the limitation that the response function is considered constant over the watershed and does not consider the spatially distributed nature of the watershed properties (*Maidment, 1996*).

The representation of a watershed as a grid of cells allows the user to calculate the characteristics that determine a certain response for each cell of the grid. The question examined in this paper is how to extend the hydrograph method in order to use the spatially distributed characteristics of the watershed in calculating the response of the watershed to the rainfall event.

A GIS allows the user to determine the base characteristics of flow through the watershed using standard functions implemented in the system. Therefore, the flow path from each cell to the outlet can be determined and the flow length can be calculated easily. The only thing that needs special calculations is the speed of water passing through each cell and the time that the water needs to pass through this cell.

Using the flow path and the time of translation through each cell total time of runoff to the watershed outlet can be easily calculated. The response at the outlet at a certain time can be determined using the total time of runoff from each cell and the quantity of water runoff from each cell. The discharge at the outlet is calculated according to the intensity and duration of the rainfall event and the behavior of runoff in the watershed during and after this event.

The initial state of the watershed is considered to be a dry state and the discharge at the outlet is calculated without taking into account the discharge existing at the beginning of

[1] *„Babeş-Bolyai" University, Faculty of Geography, 400006 Cluj-Napoca, Romania.*

the rainfall. If the actual discharge before the rainfall can be measured, the result of this study can be summed with the measured discharge to obtain the estimation of total discharge during the rainfall.

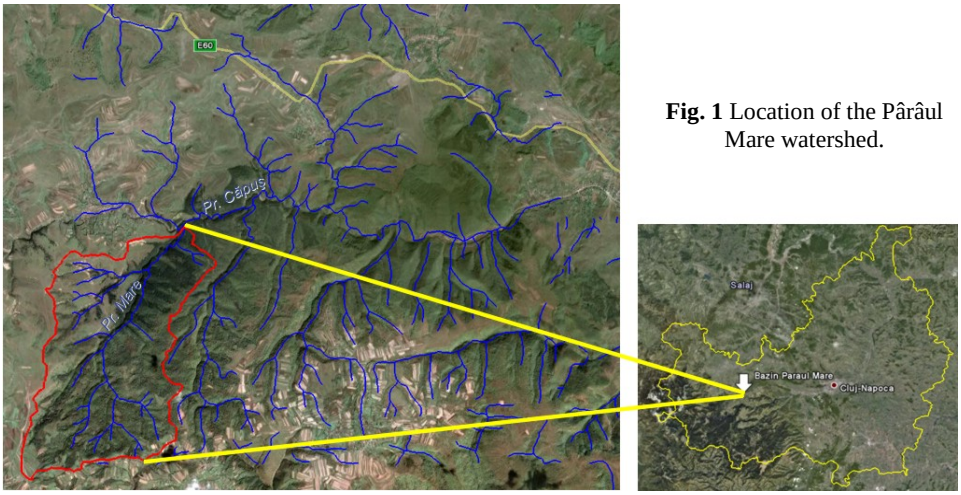

Fig. 1 Location of the Pârâul Mare watershed.

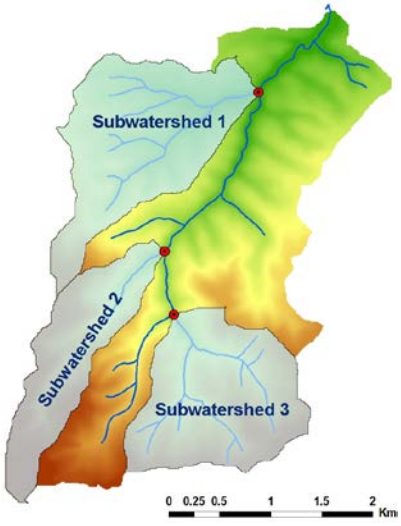

Fig. 2 Subwatersheds used for calculating the hydrographs

The usage of this model is presented on the Pârâul Mare watershed in the Apuseni Mountains. This watershed is located in the south-western region of the Cluj county, about 30 km west of Cluj-Napoca. This watershed is a small part of the Căpuș watershed and represents a zone with an area of ~11 km^2 . The location of the Pârâul Mare watershed related to the Cluj county and the Căpuș catchment can be seen in fig. 1.

The relief of the catchment is characteristic to low altitude mountains, with the land covered by forests and meadows. The altitude of the basin varies from 609 to 910 m (**Fig. 3a**). The slope of the hillslopes in the basin varies from 0 to 40 degrees (**Fig. 3b**).

The catchment does not include any major towns or communes, and the main landuse is characteristic to regions at this altitude. The land cover includes agricultural areas, broad-leaved and coniferous forests and pastures.

The rainfall event was a hypothetical storm event with a uniform rainfall intensity ower a known period of time.

The catchment and three subwatersheds were selected to calculate the hydrographs. The location and these subwatersheds are shown in **fig. 2**. The hydrographs were calculated for all four of the watersheds and shown on the same figure for comparison.

After the functions used in calculating and plotting the hydrographs were implemented, four of these hydrograph comparisons are presented with different rainfall intensities and different storm duration.

2. METHODOLOGY

2.1. Initial data processing

The data needed to apply the method described above was obtained from georeferencing and digitizing maps available for the zone where the model is applied. The most important piece of data that is needed to create any hydrological model is the digital representation of elevation (DEM).

A DEM can be obtained from different sources. The SRTM data offers worldwide elevation data at 90m resolution and USA elevation data at 30m resolution (NASA SRTM site). Another good source is the ASTER Global Digital Elevation Model (GDEM) released to the public in June 2009, which offers 30m resolution for the entire world. Also, different maps can be digitized to obtain a good DEM.

The DEM used in this study was obtained from digitizing the 1:25000 topographic maps of Romania. The digitized contours were converted to a GRID DEM with a 10m cell size. This DEM was used to obtain the slopes of the terrain in the studied region. The obtained DEM and the slopes of the region can be seen in **fig. 2**.

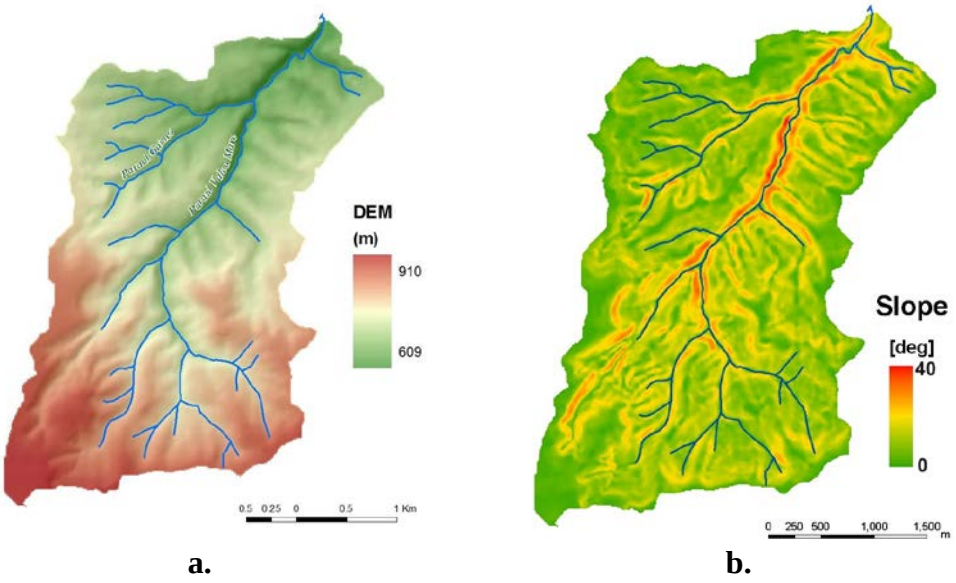

Fig. 3 DEM (a) and slope (b) of the Pârâul Mare watershed

Using the DEM, the terrain slope and the streams digitized in the area, some of the characteristics of the watershed can be calculated. Using a grid DEM cell to cell flow paths through the terrain can be defined by any common GIS. The most used algorithm is the 8 direction pour point algorithm which defines the flow from a cell to be in the direction of

the steepest descent to one of its eight neighbors (**Fig. 4**). Using the flow direction, the flow path and length can be determined directly from the terrain with other GIS functions (**Fig. 3**).

Using the flow direction grid the watershed corresponding to the user defined outlet can be delineated. The outlet defined for this watershed was placed at the confluence between Pârâul Mare and the Căpuş River, so the location where the model was applied includes all the surface of the Pârâul Mare watershed.

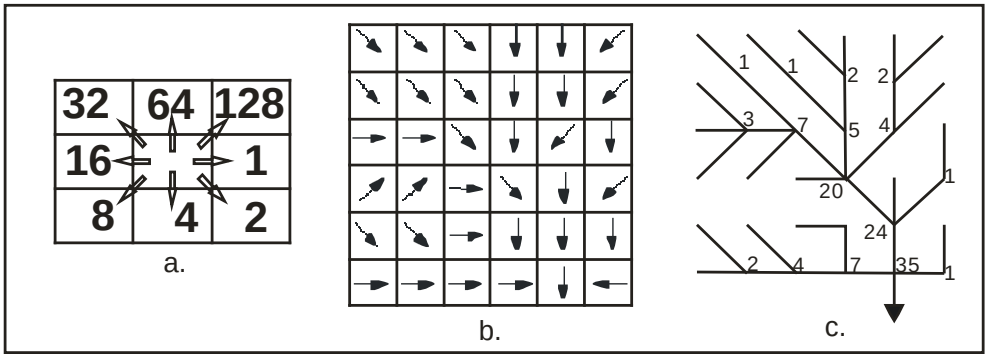

Fig. 4 Flow direction (a), flow direction grid (b), flow path (c)
(*after D. R. Maidment*)

The calculation of runoff speed and runoff curve numbers also requires data about the types of soil and the land use types in the watershed.

The curve number index (CN) was determined according to the land use and the hydrologic soil group. The land use was obtained from the CORINE Land Cover Databas (CLC2000)**,** created by the European Environment Agency. CLC data is available at 100 meters resolution for most European countries and offers data about land use. (CLC main page). The determined curve number index can be seen in **fig. 5b**.

The soils were digitized from the 1:200.000 topographic map and separated in 4 hydrologic soil groups (HSG) according to the infiltration capacity. The hydrologic soil groups were marked in the following way: Group **A** is sand, loamy sand or sandy loam types of soils. It has low runoff potential and high infiltration rates (>7.62 mm); Group **B** is silt loam or loam. It has a moderate infiltration rate when thoroughly wetted (3,81-7,62 mm); Group **C** soils are sandy clay loam. It has low infiltration rates when thoroughly wetted (1,27-3,81 mm); Group **D** soils are clay loam, silty clay loam, sandy clay, silty clay or clay. It has very low infiltration rates when thoroughly wetted (0-1,27 mm).

The runoff coefficient (α) is a parameter that will be used in the final calculation of discharge. The GRID that represents this parameter was generated according to the land use, slope and soil texture (Frevert tables) and can be seen in **fig. 5a**. The creation of this GRID was made using different spatial analysis functions available in GIS (raster reclassification, map algebra, conversions from shapefiles to raster). Some of the recent studies that deal with the spatial representation of the α coefficient include: *Păcurar (2005), Crăciun , (2007), Magyari-Saska (2008), Bilaşco (2008).*

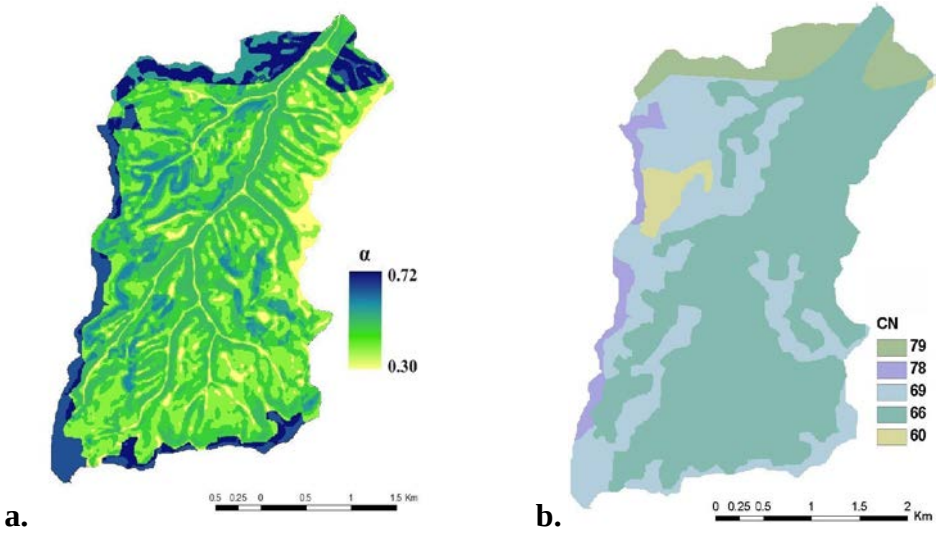

Fig. 5 Runoff coefficient (α) (a) and curve number index (b)

2.2 Travel time computation

The calculation of traveling time to the outlet from any cell needs information about the runoff speed through each cell. The runoff speed can be calculated using Manning's formula for open streamflow.

The Manning Equation is the most commonly used equation to analyze open channel flows. It is a semi-empirical equation for simulating water flows in channels and culverts where the water is open to the atmosphere, i.e. not flowing under pressure, and was first presented in 1889 by Robert Manning. The Manning Equation was developed for uniform steady state flow.

The Gauckler–Manning formula states:

$$V = 1/n * R_h^{2/3} * S^{1/2} \quad (1)$$

- where:

V - the cross-sectional average velocity (m/s)

N - Manning's roughness coefficient

S is the slope of the water surface (m/m)

R is the hydraulic radius (ft, m)

Manning's roughness coefficient (a coefficient for quantifying the roughness characteristics of the channel) can be obtained from tables available in literature according to the terrain on which the water flows (ex: *Chow, 1988*).

On the hillslopes, mean flow depth is used as an approximation of the hydraulic radius because the flow width is significantly larger than the flow depth (*Michaelides Katerina, 2002*)

The runoff speed on the hillslopes was calculated using the Gauckler-Manning formula in each cell. First, the Manning's n number was calculated according to the landuse and soil properties (**Fig. 6a**).

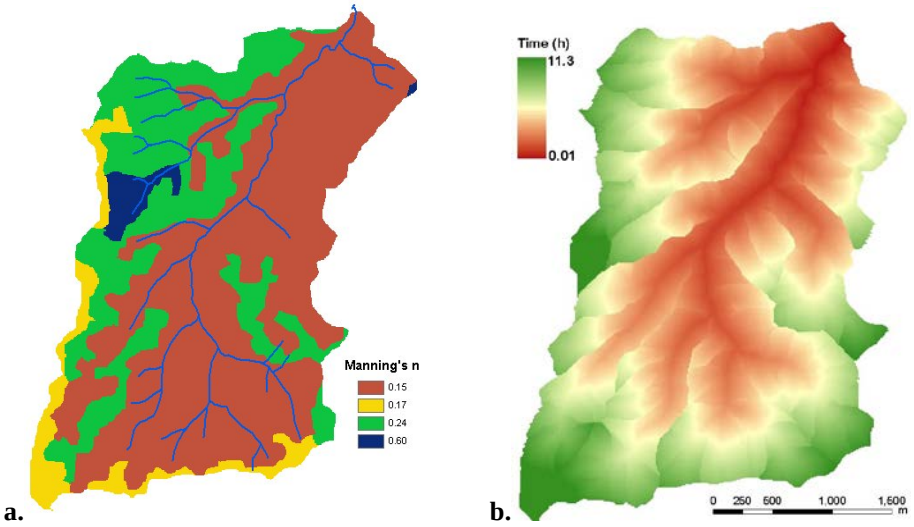

Fig. 6 Manning's n number (a), runoff travel time (b)

Once the flow velocity through each cell is known, the travel time through each cell can be estimated as

$$t = D / V \quad (2)$$

-where
t is the travel time through any given cell (s)
D is the distance traveled through that cell (m).
V is the equilibrium flow velocity through the same cell (m/s).

For orthogonal flow, the flow distance is the cell width (10 m), while for diagonal flow, it is the $\sqrt{2}$ times cell width which yields 14.41 m in this study.

At this point, the travel time through each cell, the flow direction and the flow path are all known. The cumulative travel time grid can be found by summing the travel times along the path of flow.

The calculation of the cumulative travel time and the flow velocity through each cell according to the flow length and Manning's equation was implemented in a SAGA GIS module by Victor Olaya (Olaya, 2004). This function was used to calculate the flow speed and total travel time through the watershed (**Fig. 6b**)

Using the calculated Manning's n number, the formula was applied for an average rainfall intensity of 12 mm/h (0.2 mm/min) and 60mm/h (1 mm/min). This allowed the calculation of the flow speed through each cell.

After applying Manning's formula, the cells which had a calculated flow speed lower than 0.05 m/s were automatically set at this value to avoid errors in calculating the

isochrones. The travel time through each cell led to easy calculation of the isochrones on the studied area.

When the travel time from each cell to the outlet is known, the isochrones can be determined by classifying the travel time grid in classes with a defined time interval (**Fig. 7**).

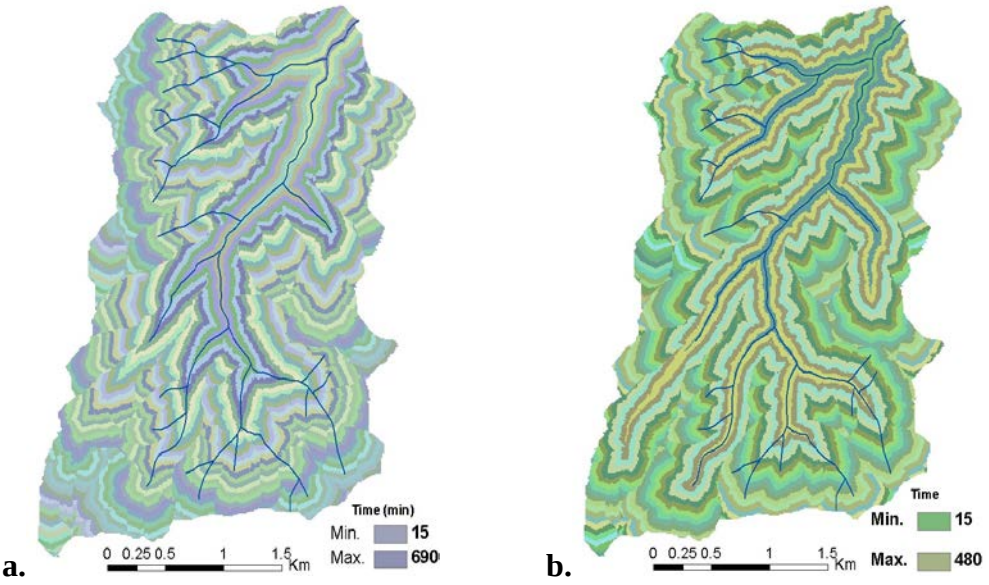

Fig.7 15 min isochrones for I= 0.2 mm/min (a) and 1 mm/min (b)

When the travel time from each cell is known, the isochrones can be calculated by classifying the travel time grid in classes representing a defined time interval. In fig 7 isochrones are shown for a rainfall intensity of 0.2 mm/min and 1 mm/min for the whole watershed.

2.3 Discharge calculation

Calculation of the discharge from the watershed was made using the *rational equation*. The Rational Method was first introduced in 1889. Although it is often considered simplistic, it still is appropriate for estimating peak discharges for small drainage areas of up to about 200 acres (80 hectares) in which no significant flood storage appears. The Rational equation is the simplest method to determine peak discharge from drainage basin runoff.

The rational method is appropriate for small watersheds (< 20 km^2) where the intensity of the rainfall can be considered constant in space and time (*Şerban and colab., 1989; Diaconu, Şerban , 1994*).

In this case, the rational method was applied according to the equation (*Păcurar, 2005*):

$$Q_{iz} = 0{,}167 \cdot S_{iz} \cdot i_m \cdot \alpha_{iz} \quad (3)$$

- where:
Q_{iz} – Peak discharge for each isochrone (m^3/s)
S_{iz} – Isochrone area (ha)
I_m – Rainfall intensity (mm/min)
α_{iz} – Rational method medium runoff coefficient

Using the grid that represents the isochrones and the runoff coefficient grid, the area of each isochrone and the medium runoff coefficient (α) for each isochrone was extracted. To obtain these values, the zonal statistics function from ArcView wto generate the tables containing the values automatically.

3. RESULTS

The discharge corresponding to each isochrone was determined using equation (3) and the tabular data obtained with Zonal Statistics, as presented. The tabular data was imported in Matlab to make the necessary operations and to plot the results.

The surfaces that contributes to runoff in each isochrone can be seen in the Time-Area Diagram (**Fig. 8 a,b**). The Time-Area diagrams were generated in OpenOffice.org.

The examples show the TAD for a hypothetical rainfall intensity of 10 mm/h (a) and 60 mm/h (b).

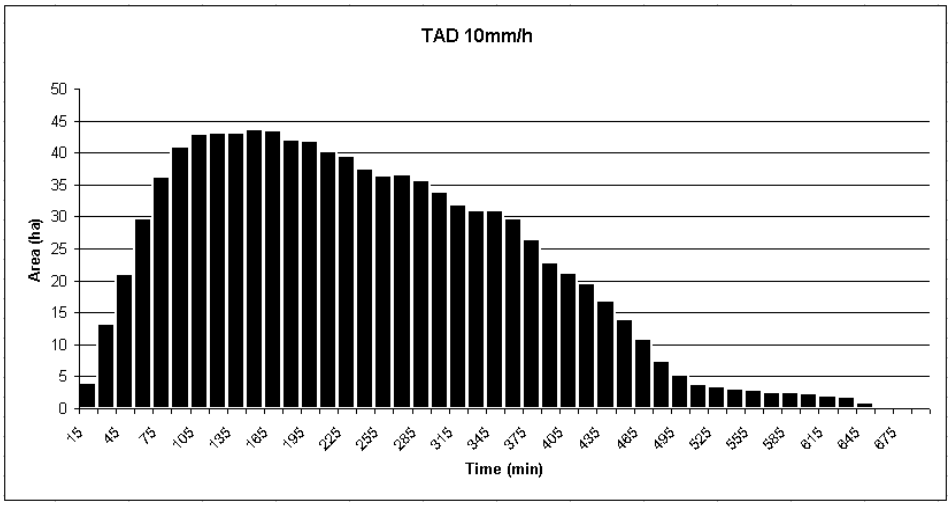

a.

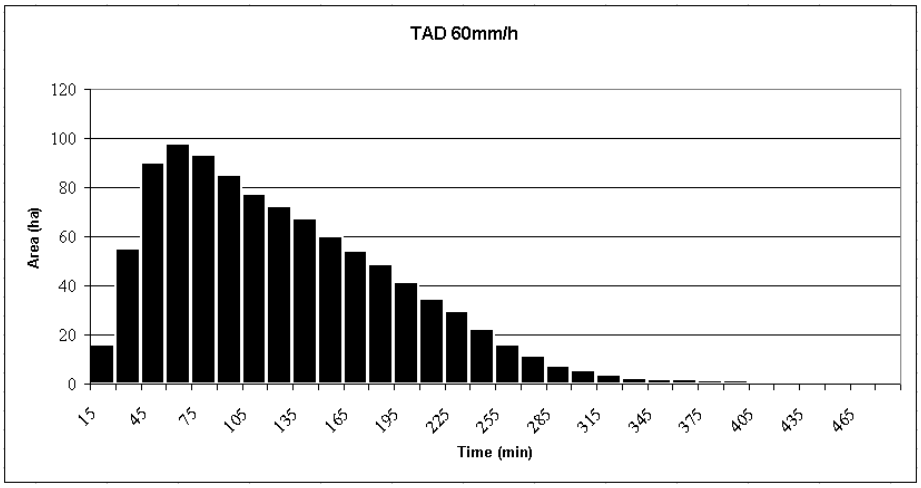

b.

Fig. 8 Time Area Diagrams for a rainfall intensity of 10 mm/h (a) and 60 mm/h (b)

The calculation of the final hydrographs was made by accumulating the discharge from each isochrone during the rainfall event. After the rain stops, the value of the discharge in each isochrone does not change anymore and the isochrones are eliminated in chronological order.

The calculated values of the cumulated discharge for certain points in time represent defined points within the hydrograph. These points are then interpolated to obtain the hydrograph corresponding to the associated rainfall.

Examples are presented in **fig. 9 a,b,c,d** for different rainfall intensities and rainfall durations. The hydrograph values from the watershed and the three subwatersheds are plotted on the same figure for comparison.

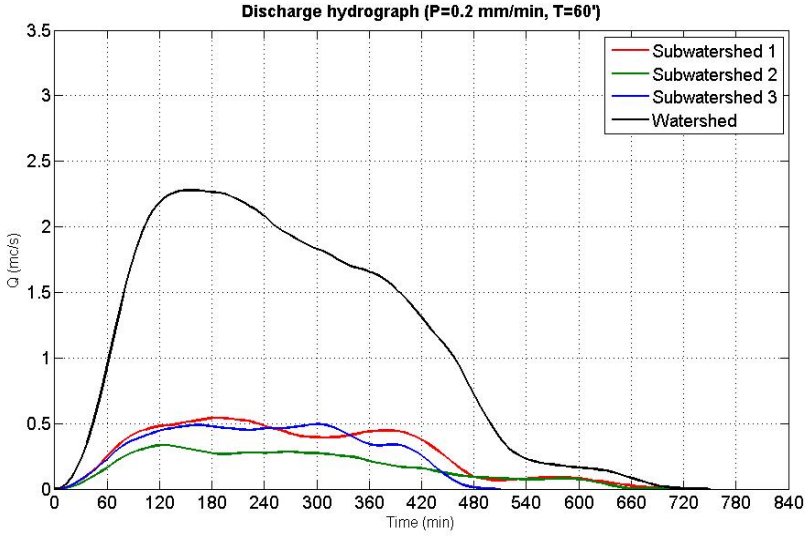

a.

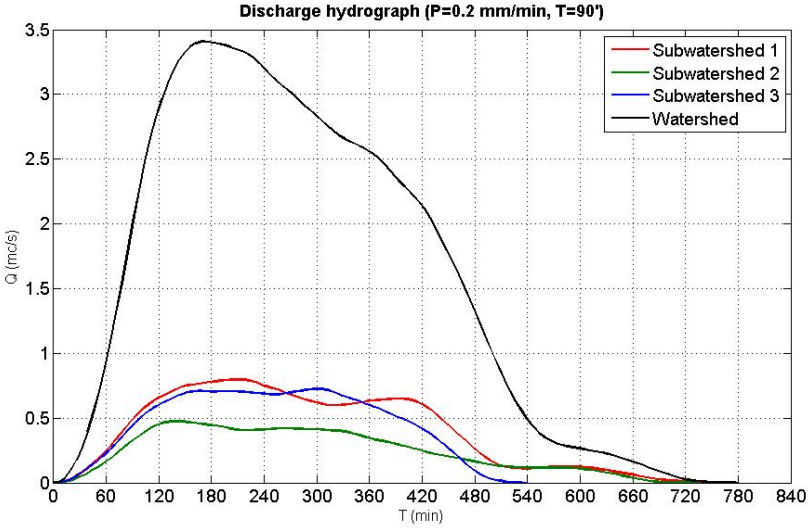

b.

Fig. 9 Discharge hydrograph, 0.2 mm rainfall for 60 min (a) and 90 min (b)

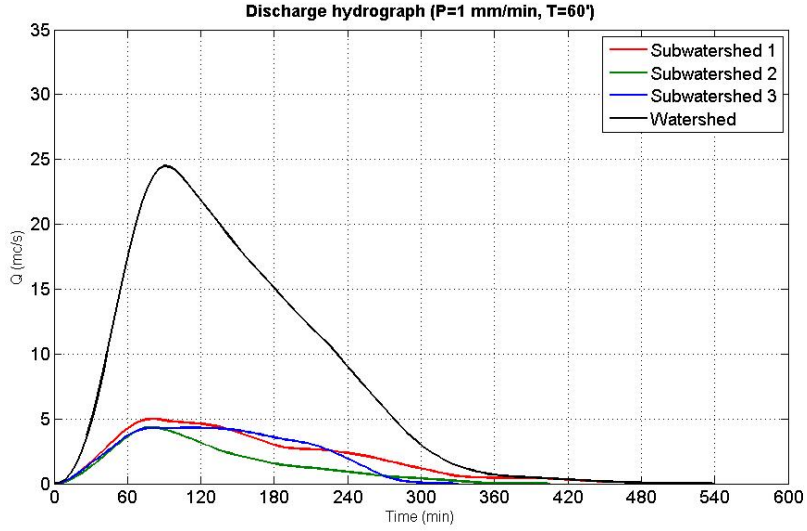

a.

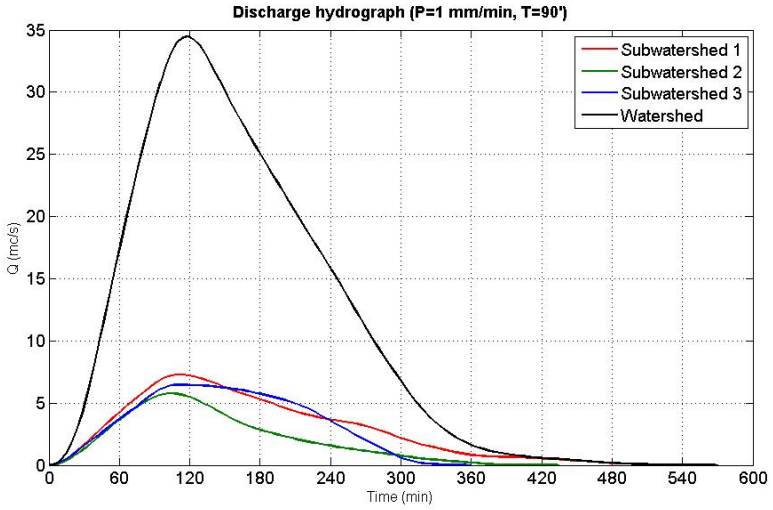

b.

Fig. 9 Discharge hydrograph, 1 mm rainfall for 60 min (c) and 90 min (d)

4. CONCLUSIONS

This paper allowed us to use and understand the hydrological functions that exist in different GIS packages and their usage. Different GIS packages offer different sets of functions that can be used in hydrological modelling of any kind.

Some of these functions were presented and used through this study to obtain the desired results (the hydrographs). The main data needed for the result was obtained in GIS using these functions as presented but the data needed some processing in other software packages to obtain the plots.

The data obtained by running the model (as shown in the last section) may be used effectively by regional authorities for taking decision on certain water resources projects. These include small structures on the river mainly for the use of the local community.

Some examples could be:

- Bridges, Culverts, and Aqueducts, which need knowledge about the anticipated high flood level
- Levees for flood protection, whose design can be made with results of this simulation and data about the shape of the stream bank.

The result of this study can be completed by adding some other parameters in calculation.

The first parameter that has to be taken into account is the soil antecedent moisture condition (AMC). This parameter affects the quantity and behavior of runoff on the hillslopes.

The second parameter should be related to the rainfall. Although the basin is small, the rainfall is never uniform in time and space. The rational method used is only appropriate for rainfall which is constant in both space and time, so using this parameter requires changing the main method of computing the discharge.

The model is oriented towards the use of regional level managers for taking a decision on local water resources related projects or estimating different events.

REFERENCES

Bilaşco Şt., Haidu I., (2006), *The Valuation of Maximum Runoff on Interbasinal Areas, Assisted by GIS*, Geographia Technica, ISSN 1842-5135, No.2, pag. 1-6, Cluj-Napoca.

Bilaşco Şt., (2008), *Model G.I.S de estimare a coeficientului de scurgere adaptat după Frevert*, Geographia Napocensis, Nr. 1, pag. 38-45.

Chanson, H. (2004), *The Hydraulics of Open Channel Flow*, Butterworth-Heinemann, Oxford, UK, 2nd edition, ISBN 978 0 7506 5978 9

Chow, V. T., Maidment, D. R. & Mays, L. W. (1988) *Applied Hydrology.* McGraw-Hill, New York

Crăciun, A. I.**,** (2007)**,** *Use G.I.S to establish some parameters useful to measure the time of concentration and runoff coefficient***,** Geographia Technica, ISSN 1842-5135, No.2, pag. 12-19, Cluj-Napoca.

Diaconu C., Şerban P., (1994), *Sinteze şi regionalizări hidrologice*, Edit. Tehnică, Bucureşti.

Maidment, D. R. (1993) Developing a spatially distributed unit hydrograph by using GIS, Application of Geographic Information Systems in Hydrology and Water Resources Management (ed. by K. Kovar & H. P. Nachtnebel), IASH Publ., 211**,** pag. 181-192.

Magyari-Saska Zs., (2008), *Dezvoltarea algoritmilor S.I.G pentru calculul riscurilor geografice naturale. Aplicaţie la Bazinul Superior al Mureşului*, Teză de doctorat, UBB Cluj-Napoca.

Michaelides Katerina, Wainwright, J. (2002) *Modelling the effects of hillslope-channel coupling on catchment hydrological response*, Earth Surface Processes and Landforms, 27, pag. 1441-1457.

Olaya, V. Hidrologia computacional y modelos digitales del terreno. Alqua. 536 pp. 2004

Păcurar V. D., (2005), *Utilizarea Sistemelor de Informaţii Geografice în modelarea şi simularea proceselor hidrologice*, Edit. Lux Libris, Braşov.

Şerban P., Stănescu Al. V., Roman P., (1989), *Hidrologie dinamică*, Editura Tehnică Bucureşti.

Official NASA SRTM site - http://www2.jpl.nasa.gov/srtm/

Corine Land Cover main page - http://dataservice.eea.europa.eu/dataservice/

Open Channel Flow and Pressure Pipe Flow - http://www.lmnoeng.com/literature.htm

Acknowledgements:

"Investing in people"! PhD scholarship, Project co-financed by the European Social Fund, SECTORAL OPERATIONAL PROGRAMME HUMAN RESOURCES DEVELOPMENT 2007 – 2013, Babeş-Bolyai University, Cluj-Napoca, Romania.

This work was also supported by Grant PN-II-ID-No.517 of CNCSIS Romania.

ETUDE DE LA VARIABILITE DES PRECIPITATIONS DANS L'EXTREME NORD DE MADAGASCAR ET ANALYSE DE L'ADAPTATION DES PRATIQUES CULTURALES SUR LE POURTOUR DE LA MONTAGNE D'AMBRE

A. Hong-Wa[1], J. Randrianarison[1]

ABSTRACT: Study of the rainfall variability in the north of Madagascar. Analysis of the agricultural adaptation around the Ambre Mountain

The analysis of rainfall trends in the region of the Montagne d'Ambre is done on a station with long time series. The study of precipitation shows a predominance of dry years. The frequency, intensity, persistence and speed of return of these phenomena are a major aspect of climate variability of extreme northern Madagascar. These climatic irregularities disrupt agricultural activities in rural areas and affect the cultivated area but also agricultural production. But given the aggressiveness and persistence of dry periods of the late 1990s, there is an adaptation of peasant farming practices around the Montagne d'Ambre. This is based on strategies for land development that emphasize less water demanding practices. This new form of development began to spread in the region.

Keywords: *Montagne d'Ambre, climate variability, drought, agriculture, adaptation*

RÉSUMÉ

L'analyse des tendances générales des pluies dans la région de la Montagne d'Ambre est effectuée sur une station possédant de longues séries chronologiques. L'étude de la précipitation montre une prédominance des années sèches. La fréquence, l'intensité, la persistance ainsi que la rapidité du retour de ces phénomènes constituent un aspect majeur de la variabilité du climat de l'extrême Nord Malgache. Ces irrégularités climatiques perturbent les activités agricoles en milieu rural et influent sur la superficie cultivée mais également sur la production agricole. Mais, face à l'agressivité et la persistance des périodes sèches de la fin de la décennie 1990, on remarque une adaptation des pratiques culturales paysannes sur le pourtour de la Montagne d'Ambre. Celle-ci repose sur des stratégies de mise en valeur des terres qui misent sur des pratiques moins exigeantes en eau. Cette nouvelle forme de mise en valeur commence à se répandre actuellement dans la région.

Mots Clés: *Montagne d'Ambre, Variabilité climatique, sècheresse, agriculture, adaptation*

1. INTRODUCTION

La région de la Montagne d'Ambre, un des versants naturels de Madagascar, se situe à l'extrême Nord de l'île entre la latitude 12°20' et 12°48' sud et la longitude 48°54' et 49°40' est. C'est un massif volcanique qui a la forme d'un cercle de 30 km de rayon. Sa superficie totale est de l'ordre de 3000 km^2. Une zone faîtière orientée nord-sud, s'étirant sur 30 km à une altitude supérieure à 900 m, sépare deux régions, orientale et occidentale. De la base au sommet, l'altitude augmente très lentement jusqu'à 300-400 m, puis elle croît plus rapidement jusqu'à 700-900 m. Cette partie basse du massif de l'Ambre est influencée

[1] *Université d'Antananarivo, Madagascar, e-mail: hongwa_allan@yahoo.fr; mt2_randrianarison@yahoo.fr*

par un climat tropical sec dont la partie orientale est sous le régime de l'alizé (1000<P<1500mm) et la partie occidentale est sous le régime de la mousson (1500<P<2000mm). Dans cette région, les variations saisonnières de précipitation sont très nettes caractérisant les deux saisons. La variabilité des précipitations n'est pas seulement saisonnière mais également interannuelle. La succession des années humides aux années sèches est un fait majeur de la variabilité du climat de la région. L'étude porte sur cet aspect du phénomène climatique qui semble avoir le plus d'impact sur l'agriculture. On remarque en effet, que du fait de la tendance à l'assèchement du climat durant cette dernière décennie, les pratiques culturales de cette zone sont en pleine mutation.

2. METHODES ET CHOIX DES DONNEES

2.1. Les méthodes utilisées

2.1.1. Variabilité interannuelle des précipitations

L'étude de la variabilité interannuelle des précipitations est basée sur l'analyse temporelle et la détection des périodes de changement de la tendance pluviométrique.

- *Variabilité dans le temps*

L'analyse des séries temporelles a pour objectif de voir la variabilité des pluies annuelles par rapport à la moyenne. Par cette méthode, il peut être dégagé la répartition dans le temps des années humides et des années sèches ainsi que leur fréquence. L'analyse des séries temporelles a été faite sur une série de 58 années entre 1950 et 2007.

- *Comparaison entre deux moyennes*

Cette méthode permet de voir l'existence d'une tendance générale des pluies vers la diminution ou l'augmentation.

-Etude de la tendance par les moyennes mobiles

Pour la détermination de la tendance générale des précipitations annuelles nous avons utilisé la méthode des moyennes mobiles. Le test des moyennes mobiles sur 20 années nous a permis de retenir celle calculée sur quinze ans. Celle –ci a permis de dégager une tendance générale tout en réduisant les fluctuations dues aux années extrêmes.

2.1.2. Caractérisation de la sècheresse

- *Méthode fondée sur l'expression du total pluviométrique annuelle en pourcentage de la normale*

Les données en pourcentage obtenues pour l'analyse ont été tirées de la formule X=IPx100 ou IP est l'Indice Pluviométrique de l'année étudiée.

L'analyse de l'intensité de la sècheresse est basée sur les conditions suivantes :

- Année très sèche : X<50% de la pluviosité normale ;
- Année sèche : 50%<X<70% ;
- Année de sècheresse modérée: 70%<X<95% ;
- Année normale : 95%<X<110% ;
- Année humide : 110%<X<125% ;
- Année très humide : X>125% ;

Où X représente la précipitation de l'année étudiée.

1.1.3. L'analyse d'impact de la sècheresse

Elle résulte des observations faites sur le terrain et d'une recherche de liaison entre la sècheresse observée et la production agricole ainsi que des méthodes utilisées par les ruraux pour faire face à la sècheresse.

2.2. Le choix des données

En raison de la quasi-disparition des stations pluviométriques dans la région de la Montagne d'Ambre, les données pluviométriques utilisées dans cette étude sont celles de la station d'Arrachart située dans la ville d'Antsiranana. Elles ont été collectées auprès du service de la Météorologie et de l'hydrologie d'Antsiranana. Nous sommes conscients que l'étude des phénomènes climatiques d'une seule station est assez audacieuse pour donner une signification aux phénomènes observés à toute une région, mais devant le fait nous ne pouvions que nous en tenir à ce choix. En dépit de cela, des tests de corrélation des données pluviométriques en période normale sur trois stations Andranofanjava, Anivorano-Nord et Arrachart à Antsiranana (cf.**fig1**) ont montré qu'il existe une corrélation positive entre les données qui est supérieure à 0,95. Cette forte corrélation nous permet d'extrapoler les résultats sur la région.

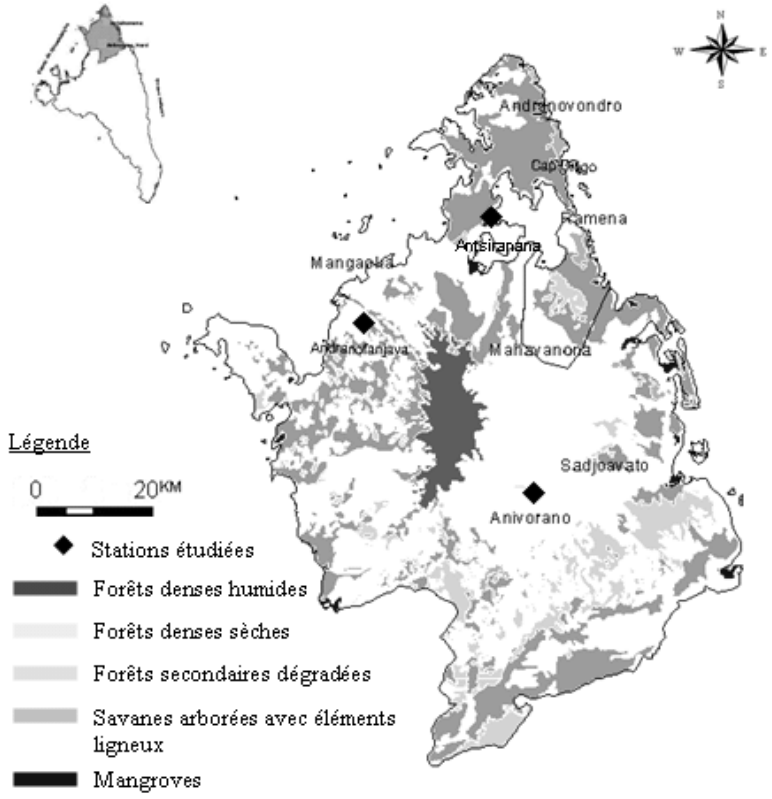

Fig. 1 Localisation des stations étudiés dans la région de la Montagne d'Ambre

3. VARIABILITE INTERANNUELLES DES PRECIPITATIONS DANS LA MONTAGNE D'AMBRE

3.1 Variabilité dans le temps

L'étude de la variabilité interannuelle des pluies est importante dans une région rurale car la pluie conditionne toute activité agricole. L'instabilité des flux d'eau apportés par les pluies annuelles qu'elles soient normales ou imputables au changement du climat est un phénomène qui mérite une attention particulière puisqu'elle influe sur les activités humaines.

L'analyse d'une série de précipitations pour une période de 58 ans (1950-2007) nous donne une idée sur leur variation. Les résultats observés montrent une succession de périodes sèches et de périodes humides. La **fig. 2** montre que la série comporte 27 années humides et 31 années sèches. La section des séries chronologiques par tranche de 10 ans indique déjà une tendance générale des précipitations pour la période étudiée. On peut y déceler l'existence de deux périodes pluviométriques:

-la première de 1950-1990;

-la seconde de 1990-2007.

L'année 1990 étant considérée comme celle partageant les deux périodes. L'analyse de cette rupture fera l'objet du paragraphe qui suit.

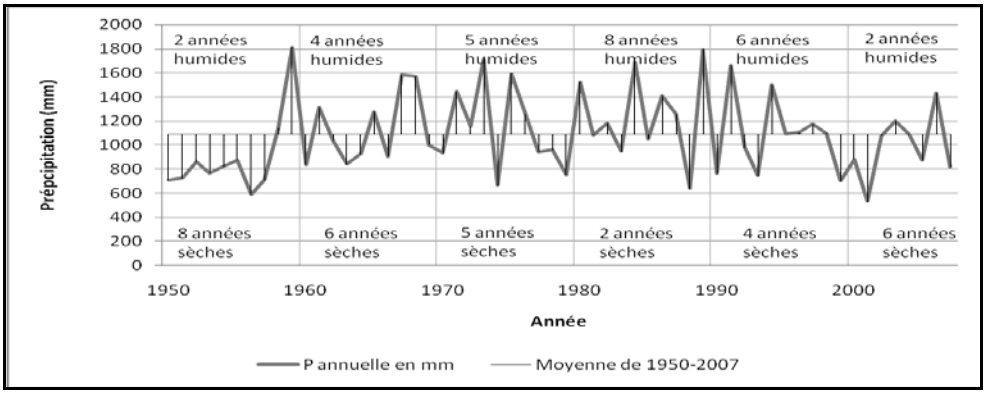

Fig. 2 Evolution des totaux pluviométriques annuels de la station d'Arrachart de 1950-2007

3.2 Comparaison entre deux moyennes

A partir de l'analyse de la variation interannuelle des précipitations, il a été constaté que l'année 1990 sépare deux périodes. Le résultat de la comparaison entre la période d'avant 1990 et celle d'après montre la tendance de la précipitation.

Tableau 1. ***Différence entre les moyennes pluviométriques annuelles des périodes 1950-1990 et 1990-2007 et identification des périodes de longues sécheresses par rapport à la normale***

	1ere période	2eme période
Moyenne	1098.6	1039.8
Rapport 1ere période/2eme période	1.1	
Année de plus grand déficit	1956	2001
Deficit en mm	507.7	508
Deficit en %	46%	49%
Périodes sèches les plus longues par rapport à la normale de 1961-90	1950-1958	1995-2002
Nombre d'année	9	8

Le tableau 1, indique que :

- La période de 1990-2007 est plus sèche que celle de 1950-1990 ;
- Chaque période a eu des intervalles de sècheresse prolongée pouvant parfois dépasser huit années.

3.3 Les Moyennes Mobiles

Le glissement de la moyenne en 15 années a permis de réduire les effets des précipitations extrêmes. Malgré une certaine stabilité des précipitations annuelles d'une année à l'autre, il est constaté une tendance à la diminution des pluies annuelles à partir des années 1990. Celle-ci est peu perceptible au début puis elle est très importante à la fin du siècle.

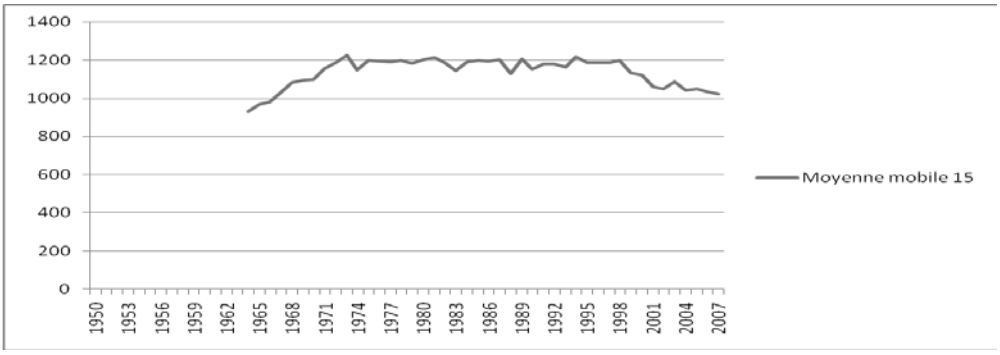

Fig. 3 Moyenne Mobile

3.4 Classification de la sècheresse dans l'extrême Nord de Madagascar

La méthodologie utilisée pour catégoriser les types de sècheresse fondée sur l'expression de l'indice pluviométrique en pourcentage a permis de classer l'état de la sècheresse pendant la période étudiée.

Tableau 2. ***Classement de la sècheresse***

Intensité de la sècheresse	Année très sèche	Année sèche	Année de Sècheresse modérée	Année normale	Année humide	Année très humide
nbre d'année	2	14	21	8	4	9
%	3.45	24.14	36.21	13.79	6.90	15.52

Le tableau 2 montre que durant la période d'étude, il a été observé deux années très sèches (1956 et 2001), quatorze années sèches et vingt et une années de sècheresse modérée. Ainsi, malgré une prédominance de la sècheresse à 63.8% des années étudiées, il apparaît que plus de la moitié sont des années de sècheresse modérée (36.21%). L'analyse des résultats obtenus montre que la deuxième période de 1990-2007 est marquée par 13 années déficitaires dont 62% sont considérés comme d'une sècheresse modérée, 31% sont constitués d'années sèches et 7% représente les années très sèches. Les impacts de ces déficits sur le monde rural méritent d'être étudiés.

4. DIMINUTION DE LA PRODUCTION RIZICOLE ET MUTATION DES PRATIQUES CULTURALES

4.1. La diminution de la production agricole

Les déficits pluviométriques observés pendant la période 1990-2007 ont eu des répercussions non négligeables sur l'agriculture de la région. Celle-ci est basée sur la pratique de la riziculture pluviale et irriguée en saison sèche. Les enquêtes menées dans treize villages repartis de part et d'autre des versants de la Montage d'Ambre ont montré que les paysans qui s'adonnent à la riziculture perdent chaque année 35% de leur récolte du fait du manque d'eau. L'un des faits les plus marquants a été observé dans le terroir d'Antongombato, un des villages du versant ouest, lors de la saison culturale 2000-2001 où sur101 riziculteurs, un seul a pu obtenir de récolte (Hong-Wa , 2007).

D'après les statistiques officielles, une baisse significative de l'ordre de 29207 tonnes a été enregistrée entre la période sèche de 1997 à 2000. Ce qui équivaut à une baisse de production rizicole de l'ordre de 50.14%. La raison de cette baisse réside dans le fait que le riz de contre saison a été abandonné par la majorité des riziculteurs par manque d'eau. D'après le service du génie rural d'Antsiranana, si auparavant celui-ci a été pratiqué par 60% des paysans, actuellement il ne concerne plus que 15% des riziculteurs.

4.2. Vers une mutation des pratiques culturales dans la région de la Montagne d'Ambre

4.2.1. De la diminution des surfaces cultivées à la gestion de l'eau

Face à l'insuffisance de la précipitation, les paysans ont réduit leur surface cultivée de sorte que l'eau devient suffisante pour permettre l'irrigation de la parcelle. Cette mutation culturale a été visible pour les deux versants de la Montagne d'Ambre avec un taux de 8%. Mais face à la persistance de la sècheresse, un mode de gestion de l'eau fondée sur le principe d'une irrigation tournante a été observé. Cette méthode est appliquée par 20% des riziculteurs du versant ouest contre 77 % du versant est. Ce qui montre que le versant est, moins arrosé, est plus affecté par le phénomène de sècheresse.

3.2.2. L'introduction de nouvelles cultures dans les pratiques agricoles paysannes

Les difficultés de la pratique de la riziculture par le manque d'eau ont favorisé l'émergence et le développement des cultures secondaires dans les terroirs agricoles de la région de la Montagne d'Ambre. Pour le versant ouest, la population agricole s'est plus orientée vers les cultures pluviales et itinérantes. Quant au versant est, elle a opté plutôt pour la pratique des cultures de contre saison. Ces nouvelles formes de mise en valeur de l'espace observées sur les versants de la Montagne d'Ambre peuvent être interprétées comme une réaction des paysans face à la baisse de la précipitation dans la région. La figure n°4 montre les différents processus qui ont conduit la population de ces zones à adopter de nouvelles stratégies afin de continuer à mettre en valeur les terres.

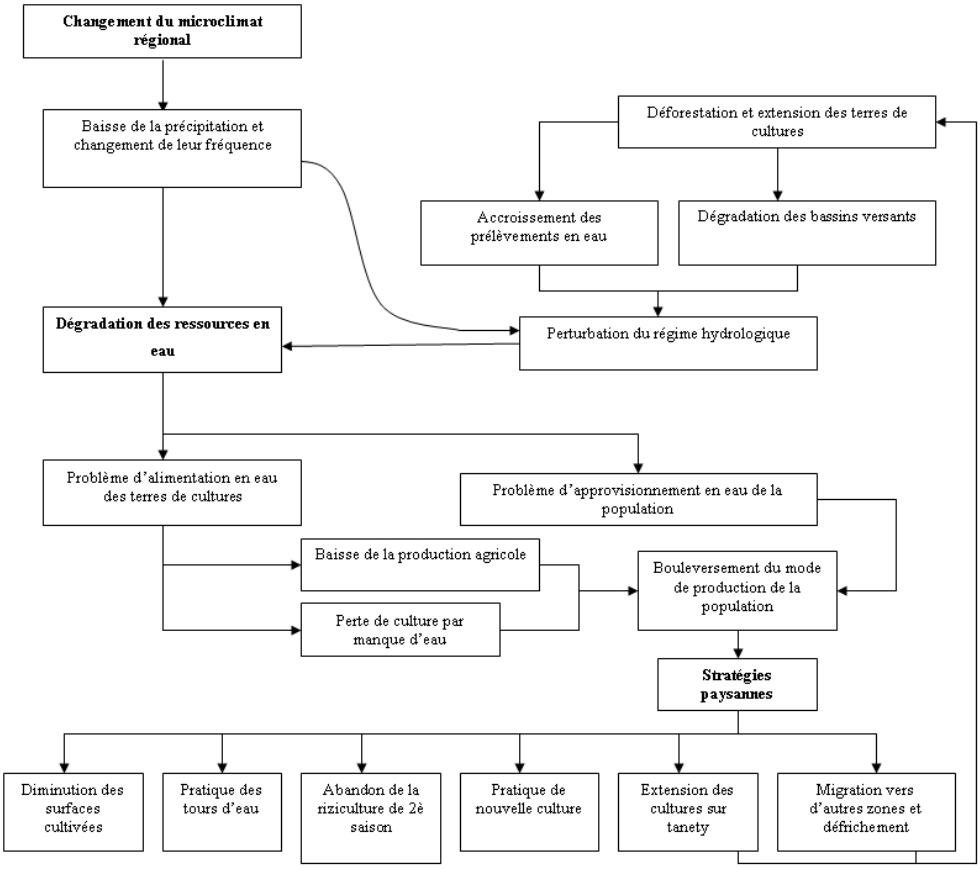

Fig. 4 Bilan des effets de l'assèchement du climat dans la Montagne d'Ambre

Dans ce schéma, le changement du climat régional, notamment la baisse de la précipitation influe sur les régimes hydrologiques des rivières. Ce qui a généré par la suite divers problèmes comme celui de l'alimentation en eau des terres de cultures. Les impacts de ces phénomènes sont nombreux : baisse de la production agricole, perte de culture par

manque d'eau qui ont entraîné le bouleversement du mode de vie et de production des paysans vivant dans les zones basses. En réponse à cette nouvelle situation, la population a adopté de nouvelles stratégies comme la diminution des surfaces cultivées en riz, la pratique des tours d'eau, l'abandon de la riziculture de deuxième saison et dans certains cas l'arrêt définitif de la culture du riz dans les terroirs. A l'instar de la riziculture, on assiste à la pratique de nouvelles cultures sur l'espace agricole des villages mais aussi au développement des cultures sur les collines qui nécessitent parfois la migration de certains paysans à la lisière des massifs forestiers de la Montagne d'Ambre. A l'heure actuelle, cette stratégie paysanne permet à la population de mieux réagir aux problèmes de manque d'eau mais elle implique d'autres difficultés auxquelles il faut faire face à l'avenir car les cultures pluviales débordent de leur espace et menacent les versants forestiers de la Montagne d'Ambre.

CONCLUSION

L'étude de la variabilité interannuelle des précipitations dans la région de la Montagne d'Ambe a montré l'alternance entre des périodes déficitaires et excédentaires avec une prédominance de la tendance sèche. Par leur fréquence et leur intensité, les années sèches ont des impacts sur les différentes pratiques agricoles, dont la lutte contre l'assèchement, constitue le fait majeur de cette tendance climatique.

BIBLIOGRAPHIE

Daoud K., Medjerab A., (1996) .*La tendance générale des pluies dans l'ouest Algérien*, Variabilité du Climat et Stratégie d'adaptation paysanne en Tunisie, vol VI, 81-105

Daoud K., Daoudi M., Abdellaoui A., (1996), *Fluctuation spatio-temporelle des précipitations sur le versant sud de l'atlas Blideen (Algérie*), Variabilité du Climat et Stratégie d'adaptation paysanne en Tunisie, vol VI, 107-113

Donque G., (1975), *Contribution géographique à l'étude du climat de Madagascar*, Laboratoire de géographie, Université de Tananarive, 475p.

Dufournet R., (1972), Régimes thermiques et pluviométriques à Madagascar, ORSTOM, *Madagascar Revue de Géographie*, 20, 26-91

Hong-Wa A., (2007), *La dégradation des ressources en eau dans l'extrême Nord malgache, le cas de la Montagne d'Ambre*. Mémoire de DEA, FLSH, Université d'Antananarivo, 95p.

Meddi H. Meddi. M., (2007), *Variabilité spatiale et temporelle des précipitations du Nord-Ouest de l'Algérie*, Geographia Technica, 2, 49-55

Pagney P., (1996), *Contribution a l'étude de la variabilité des pluies sur le Maghreb septentrional*, Variabilité du Climat et Stratégie d'adaptation paysanne en Tunisie, vol VI, 41-64

Randrianarison J., (1991), *Les cyclones et l'homme à Madagascar*, Université de Paris Sorbonne (Paris IV), Thèse de Doctorat d'état, 583p.

Rossi G., (1976), *L'extrême Nord de Madagascar (Tome I et II)*, Aix en Provence, thèse de Doctorat, 439p.

THE INFLUENCE OF SWALES ON THE SPATIAL VARIABILITY OF SOIL PROPERTIES IN SOUTHERN LOUISIANA, U.S.A

S. Johnson[1], D. Weindorf[1], M. Selim[1], N. Bakr[1], Y. Zhu[1]

ABSTRACT:
Soil physicochemical properties vary among different landscapes and elevations. The spatial variability of soil properties in a 1.66 ha pasture exhibiting artificial swales was evaluated near Bayou Wikoff, Louisiana to identify relationships between particle size (clay %), organic carbon (OC %), and soil reaction (pH), with elevation. High density sampling was conducted in the field, geo-located via global positioning system (GPS), and subjected to physicochemical lab analysis. Results showed high clay % (μ = 27.95%), high OC % (μ = 2.38%), and strongly acidic soils (μ = 5.15). Results were spatially georeferenced and interpolated across the landscape with the ArcGIS spatial analyst tool. Three interpolation methods (spline, inverse-distance weighting [IDW], and regression kriging) were evaluated to determine values between sampled points. Spline interpolation showed strong relationships between elevation and OC %, pH, and clay %; all linked to swale location. The regression kriging also produced acceptable results and provided a good estimate of soil properties between sampled points. This method is more applicable to small datasets and is directly weighted on adjacent points, versus the entire dataset. For sampled points, significant correlation coefficients ($p < 0.05$) were found between elevation and clay % ($r = -.61$), pH ($r = -.32$), and OC % ($r = -.64$). All three measured soil properties were inversely proportional to elevation as it decreased towards the bayou. Best management practices should focus on swale lows to reduce total suspended solids (colloidal clay) as means of improving water quality entering nearby bayous.
Keywords: *Spatial variability, regression kriging, spline, interpolation*

1. INTRODUCTION

The spatial variability of soil properties has profound impacts on effective land management. Vegetative productivity is often tied to nutrient concentrations within the soil and develops a continuum across the landscape in response to natural pedogenesis. However, anthropogenic alterations such as drainage swales, tillage, and terracing can markedly affect the spatial distribution of soil properties (*Blanco-Canqui et al., 2004; Cambardella et al., 1994; Saldana et al., 1998; Stein et al., 1989*).

Several predictive modeling tools are available for describing soil spatial variability. Among them, regression kriging, inverse distance weighting (IDW), and spline analysis are commonly used to describe soil variability (*Kravchenko and Bullock, 1999; Chaplot et al., 2006; Gaston et al., 2001; Haws et al., 2004; Liu et al., 2006; Mueller, et al., 2004; Robinson and Metternicht, 2005*). Regression kriging is a geostatistical interpolation method based upon a principal of spatial autocorrelation; where the direction and distance from known points govern the prediction of values at unknown points (*Karydas et al., 2009*). Inverse distance weighting is a technique whereby the values at unknown locations are inversely related to their distance from locations with established data (*Isaaks and Srivastava, 1989*). Spline interpolation is a polynomial smoothing technique used to minimize sharp bends in continuous data (*ESRI, 2009*).

[1] *LSU AgCenter, 307 MB Sturgis Hall, Baton Rouge, LA, 70803, USA*

Numerous studies have proven the utility of kriging to evaluate soil spatial variability. Kriging interpolation requires a large datasets to be collected for valid results (*Jung et al., 2006*). *Webster and Oliver (1992)* proposed that 50 to 100 data points are required for the construction of a reliable variogram to support kriging interpolation. *Kravchenko (2003*) compared kriging to IDW with 256 samples obtained from a grid with 30 m spacings. This research concluded that kriging was as accurate as IDW only when large datasets are used. *Zhang et al. (2007)* used kriging to evaluate soil organic matter, total N, total P, and total K in tilled soils of northeast China. They concluded that geostatistical kriging was sufficiently accurate to evaluate the spatial variability of most soil nutrients. In southeastern Louisiana, *Sigua and Hudnall (2008)* evaluated the spatial variability of 40 composite soil samples. They found significant spatial dependence for the physicochemical parameters evaluated, and identified lateral (east-west) and vertical (north-south) morphological patterns. *Needelman et al. (2001)* concluded that kriging provides considerably better nutrient distribution models when there is a strong auto-correlation of nutrients on a studied field in east-central Pennsylvania.

Spline and IDW interpolations are other statistical analysis used to obtain undetermined values. *Price et al. (2000)* found that when predicting climate variables, spline interpolations produce more statistically accurate results. They also found that spline interpolations generate smoother, more accurate boundaries, even when the source provides limited data. However, spline techniques often predict values that can exceed the actual minimum and maximum of measured values, which is not always desirable for measuring soil properties (*Karydas et al., 2009*). *Anderson et al. (2005)* chose IDW interpolations because unknown values would be influenced by the nearest points rather than the entire dataset. *Leenaers et al. (1990)* concluded that IDW produced more accurate results than any other interpolation method when mapping Zn concentrations on soil samples in the Netherlands. *Conversely, Kravchenko (2003)* found that IDW has a statistical disadvantage over the kriging method. Ultimately, *Price et al. (2000)* found that both IDW and spline methods have the potential to produce accurate estimation of unknown data. *Largueche (2006)* determined that kriging was more appropriate for classical statistics because the method incorporates spatial correlation for the entire dataset. *Kravchenko and Bullock (1999)* found that correlation coefficients were higher with kriging interpolation than IDW when studying soil properties. For this study, spline and regression kriging methods are focused because they provide more accurate results for larger datasets.

In southern Louisiana, catenas of soil pedogenesis are difficult to distinguish given minimal elevation relief. In many areas, elevation differences are only a few meters per kilometer. However, variation in soil properties does exist and is often associated with bayous and rivers (*Weil, 2003*). Large river systems (Mississippi, Atchafalaya, Red, and Sabine) have deposited alluvial sediment across southern Louisiana resulting in great heterogeneity of soil properties.

In addition to natural soil variability, the introduction of drainage swales, furrows, or terraces has the potential to produce even greater spatial variability of soil properties for a given field. This has implications on land management and water quality. Surface runoff containing fertilizer, sediment, pesticides, and fecal coliforms has the potential to threaten water quality (*LDEQ, 2009*). To avert potential impacts caused by swale/furrow installation, a thorough understanding of their impact upon natural soil variability is required. The goals of this study were to: 1) select a site representative of common swale/furrow installation practices in southern Louisiana, 2) collect high density, georeferenced soil samples from the site and conduct physicochemical lab analyses, 3)

produce high resolution maps of soil variability via regression kriging and spline interpolation, and 4) determine the impact of swales upon soil spatial variability.

MATERIALS AND METHODS

General site description

St. Landry Parish is located in south-central Louisiana (30° 24' N; 92° 09' W). Climate of the area is moist subtropical, with mean annual precipitation and mean annual temperature of ~1360 mm and ~19.6°C, respectively (Soil Survey Staff, 1986). Soil temperature regimes are thermic and moisture regimes are locally udic or aquic (Soil Survey Staff, 2009a). Elevation of the parish ranges from 2 to 23 m above sea level (Soil Survey Staff, 1986). Soils range from very strongly acidic (pH = 4.5) to slightly alkaline (pH = 8.4) and often have a silty or loamy texture, with increasing clay throughout the profile. Soils in the eastern section of St. Landry Parish are alluvially deposited by the Atchafalaya and Mississippi rivers, and also by the Red River distributaries. Soil orders found in St. Landry Parish include Alfisols, Mollisols, Ultisols, Vertisols, and Entisols (Soil Survey Staff, 1986).

For this study, 104 surface soil samples (0-4 cm) were collected from a 1.66 ha field adjacent to Jessie Richard Rd. The field is 165 m to the east of Bayou Wikoff (Plaquemine Brule Watershed, Mermentau River Basin) (LSU ATLAS, 2009). Soil mapping units at the sampling site include: Jeanerette series [JeA] (0-1% slope, fine-silty, mixed, superactive, thermic Typic Argiaquolls), Frost series [FoA] (0-1% slope, fine-silty, mixed, active, thermic Typic Glossaqualfs), and Patoutville series [PaA] (0-1% slope, fine-silty, mixed, superactive, thermic Aeric Epiaqualfs)(Soil Survey Staff, 2009a). The extents of the JeA, FoA, and PaA mapping units across the sampling site are ~43%, ~39%, and ~18%, respectively (Soil Survey Staff, 2009b). A modified grid sampling scheme (10.5 x 8 m) (0.0084 ha) was utilized to facilitate sample collection. Iqbal et al. (2005) determined that areas with <400 m between samples are required for effectively analyzing physicochemical variability in Mississippi delta soils. Samples were collected in May 2009, georeferenced using a Garmin e-Trex global positioning system receiver (Garmin International, Olathe, KS), sealed in plastic bags, and transported to the lab for analysis.

Laboratory analysis

Standard soil physicochemical analyses were conducted at the LSU AgCenter in Baton Rouge, LA. Samples were oven dried at 30°C and ground to pass a 2 mm sieve. Particle size analysis was conducted using a modified hydrometer method with 24 h and 40 s, clay and sand determinations, respectively (Gee and Bauder, 1986). Loss on ignition organic matter (LOI_{OM}) was conducted at 550°C for 4 h following Nelson and Sommers (1996). Using the organic matter quantities, OC % was calculated using Ranney's (1969) conversion [equ. 1]:

$$\text{organic matter, \%} = .35 + 1.80 \times \text{\% organic C} \quad [1]$$

Soil pH was determined on saturated pastes according to the Soil Survey Staff (2004). Pastes were allowed to equilibrate for 24 h, and then quantified using an Orion 2 Star pH meter (Thermo Scientific, Waltham, MA). Mehlich III extractable elements were obtained (Soil Survey Staff, 2004) and quantified using a Ciros model inductively coupled plasma atomic emission spectrometer (Spectro Analytical Instruments, Marlboro, MA).

Digital analysis (datasets, classic, geostatistics)

Orthoimagery and digital elevation models (DEMs) were obtained from the Soil Survey Staff (2009c). Point data from handheld GPS units was uploaded into ArcGIS 9.2 (ESRI, 2009) and georeferenced to lab data. Contour maps were developed using spatial analyst tools for 1 and 2 m intervals. Classical statistics and geo-statistics were developed using Excel (Microsoft, 2007) and evaluated at the 95% confidence level. Accuracy assessment was performed using a 20% validation sample subset with and without elevation as a dependant factor. Due to the high correlation of elevation with the measured properties, it is essential to integrate the elevation when creating interpolation maps. First, the predictive equation using regression methods for the entire dataset between the elevation and the soil property was obtained. Next, the predicted values and residuals (actual value - predicted value) were calculated based on the established regression equation, for the entire study area. The actual values (non-regression) and residual values (regression) were then interpolated using regression kriging and spline methods. For validation, the extracted residual values were added to the aforementioned predicted values to check the accuracy of the interpolated method. Finally, interpolated residual and predicted values were combined to produce spatial distribution maps.

RESULTS AND DISCUSSION

Lab Results

A basic statistical summary of the lab results is presented in **Table 1**. Clay % ranged from 21 to 41%, with a mean of 27.83%. Most soil textures were silt loam, confirming soil mapping unit data for the JeA, FoA, and PaA soils (Soil Survey Staff, 2009a). Soil pH values ranged from extremely acidic (4.22) to slightly acidic (6.53) with a strongly acidic mean (5.15). Organic C % ranged from 0.4374 to 5.1762%, with a mean of 2.3805%. This large variability could be due to sampling error. A correlation table (**Table 2**) is provided to show the effects of elevation on the measured soil properties. There are high correlations between the elevation and evaluated soil properties. The elevation is inversely proportional to all soil factors analyzed; as the elevation increases, each measured property decreases in value. For example, in the swales (lower elevation), the pH, OC %, and clay % values are higher. Furthermore, the north and western portions of the pasture are lower-lying and have higher concentrations of clay and organic carbon with lower pH values, compared to the more elevated southern and eastern parts of the pasture.

Table 1. ***Statistical analysis of data from a studied field in St. Landry Parish, LA.***

Procedure	Minimum	Maximum	Mean	σ
Clay %	21	41	27.83	4.44
pH	4.22	6.53	5.15	0.43
OC %	0.44	5.18	2.38	0.91
Elevation	13.28	13.74	13.54	.095

n = 104

Table 2. ***Correlation table for 95% confidence interval (p > .05) of data from a studied field in St. Landry Parish, LA.***

	Clay %	OC %	pH
Clay %	1		
OC %	0.663	1	
pH	0.420	0.399	1
Elevation	-0.610	-0.635	-0.320

The explanation for increasing clay % in swales must be considered. Pedon descriptions provided by the United States Department of Agriculture – Natural Resource Conservation Service (USDA-NRCS) show that soils in this area often have increasing clay throughout the profile expressed as argillic horizons (*Soil Survey Staff, 2009a*). How is one to say that the source of clay is not from a slicing of the original ground? This option can certainly exist. However, another option is that the clay increases as it moves across the surface into the swale as colloidal clay travels in suspension with water seeking elevational relief. There is a high correlation from lab data between clays and OC %. This correlation implies that the soil in the lower swales is not from a subsurface layer. Soil sublayers in this area of study tend to have a higher clay % and lower OC %, however we found high clay % in conjunction with high OC %. Clay and humus (from the organic matter) are both colloidal, collecting nutrients and water molecules. Due to their charged surface properties, both clay and humus act as a bridge between soil particles facilitating aggregation (*Brady and Weil, 2004*). Rainwater is likely carrying the clay and organics to lower elevations where it pools in low-lying swales.

Digital Analysis

Lab analyses were uploaded and interpolated in ArcGIS. For accurate interpolation results, this study required an incorporation of elevation data (regression). Without spatially considering the elevation, the 20% validation results show weak significance between the actual values versus regression kriging or spline interpolated values, where R^2 values were .253 and .019, respectively (**Fig. 1**).

Once the regression was integrated, the correlation improved for both regression kriging and spline methods, with R^2 values of 0.454 and 0.305, respectively (**Fig. 1**). **Fig. 2a** illustrates a regression kriging interpolation, using elevation integration with clay % (*ESRI, 2009*). **Fig. 2b** represents a regression spline interpolation with clay % and elevation factors. **Fig. 2a** confirms the relationship between higher swale elevation and clay %.

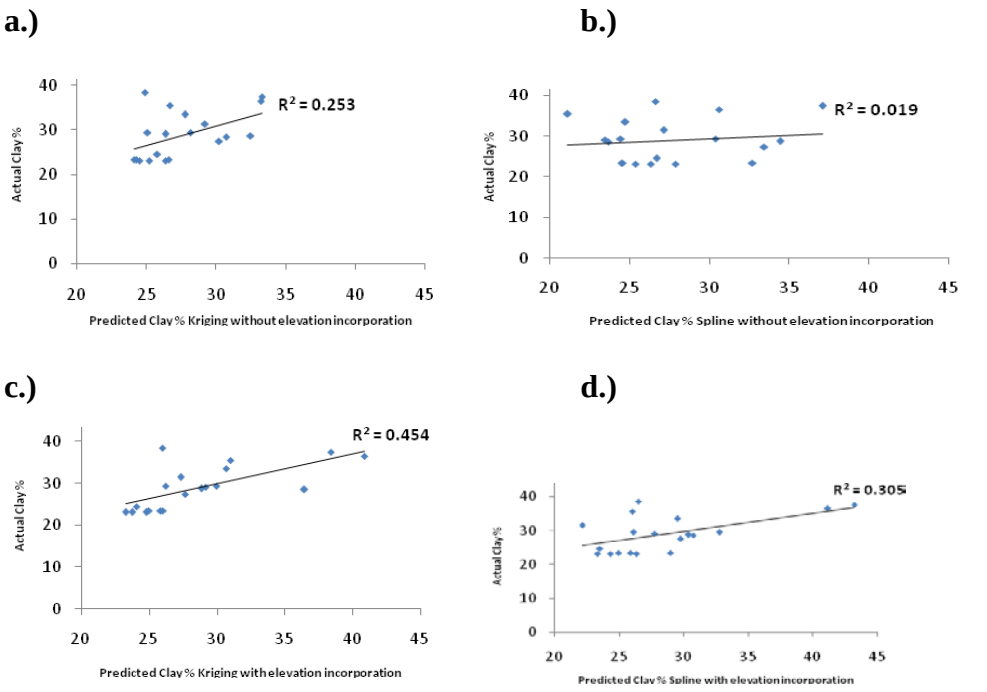

Fig. 1 a.) Correlation graph for non regression kriging of clay % for a studied field in St. Landry Parish, LA, USA.;b.) Correlation graph for non-regression spline of clay % for a studied field in St. Landry Parish, LA, USA.; c.) Correlation graph for regression kriging of clay % for a studied field in St. Landry Parish, LA, USA.; d.) Correlation graph for regression spline clay % for a studied field in St. Landry Parish, LA, USA.

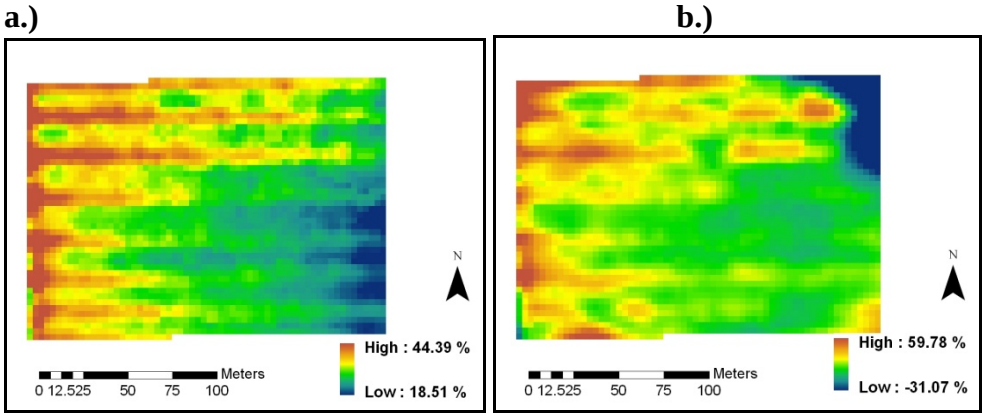

Fig. 2 a.) Regression kriging interpolation of clay % for a studied field in St. Landry Parish, LA, USA. b.) Regression spline interpolation of clay % for a studied field in St. Landry Parish, LA, USA.

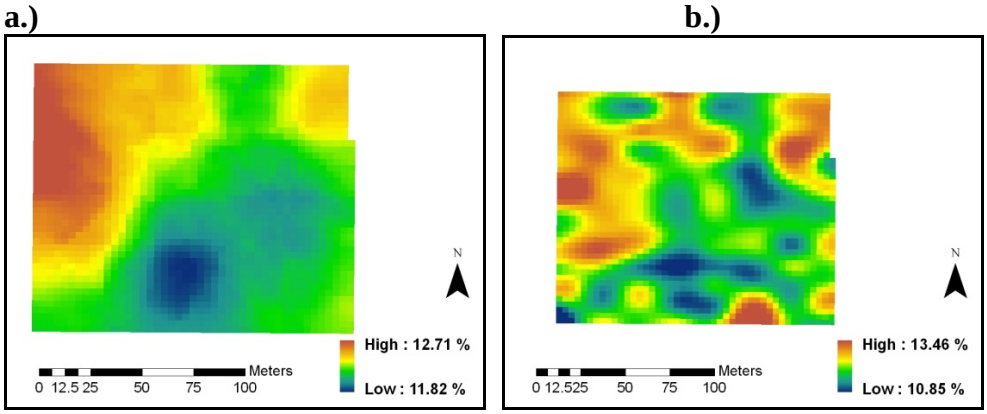

Fig. 3 a.) Regression kriging interpolation of OC % for a studied field in St. Landry Parish, LA, USA. b.) Regression spline interpolation of OC % for a studied field in St. Landry Parish, LA. USA.

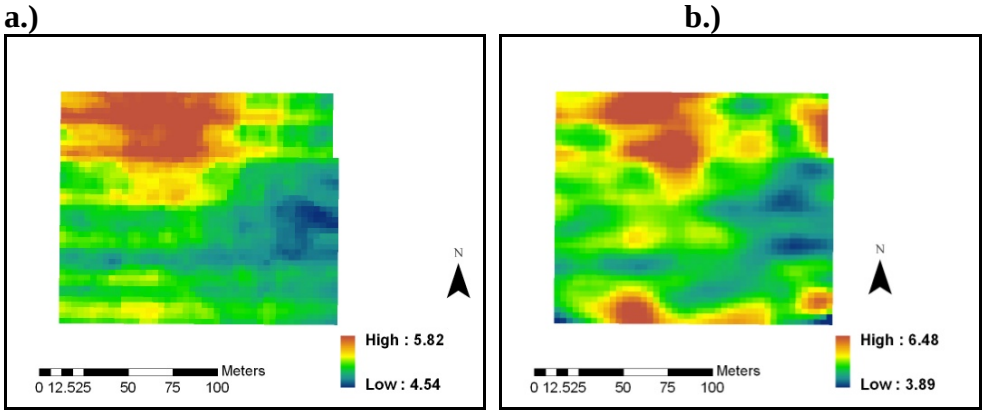

Fig. 4 a.) Regression kriging interpolation of pH for a studied field in St. Landry Parish, LA, USA. b.) Regression spline interpolation of pH for a studied field in St. Landry Parish, LA, USA.

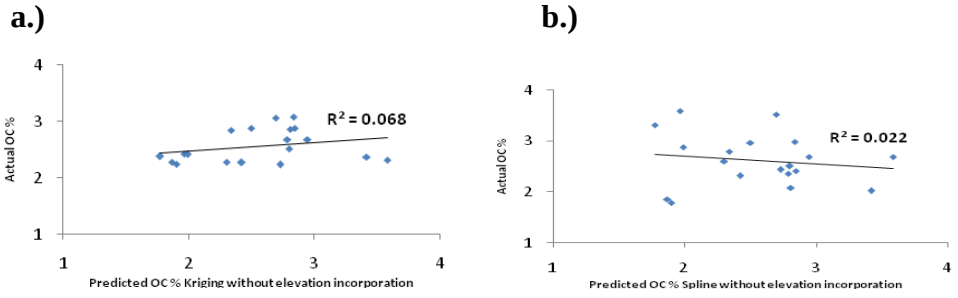

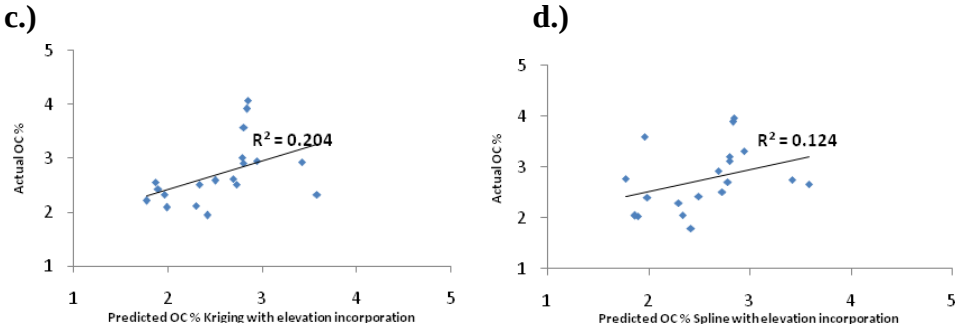

Fig. 5 a.) Correlation graph for non regression kriging of OC % for a studied field in St. Landry Parish, LA, USA.; b.) Correlation graph for non-regression spline of OC % for a studied field in St. Landry Parish, LA, USA.; c.) Correlation graph for regression kriging of OC % for a studied field in St. Landry Parish, LA, USA.; d.) Correlation graph for regression spline OC % for a studied field in St. Landry Parish, LA, USA.

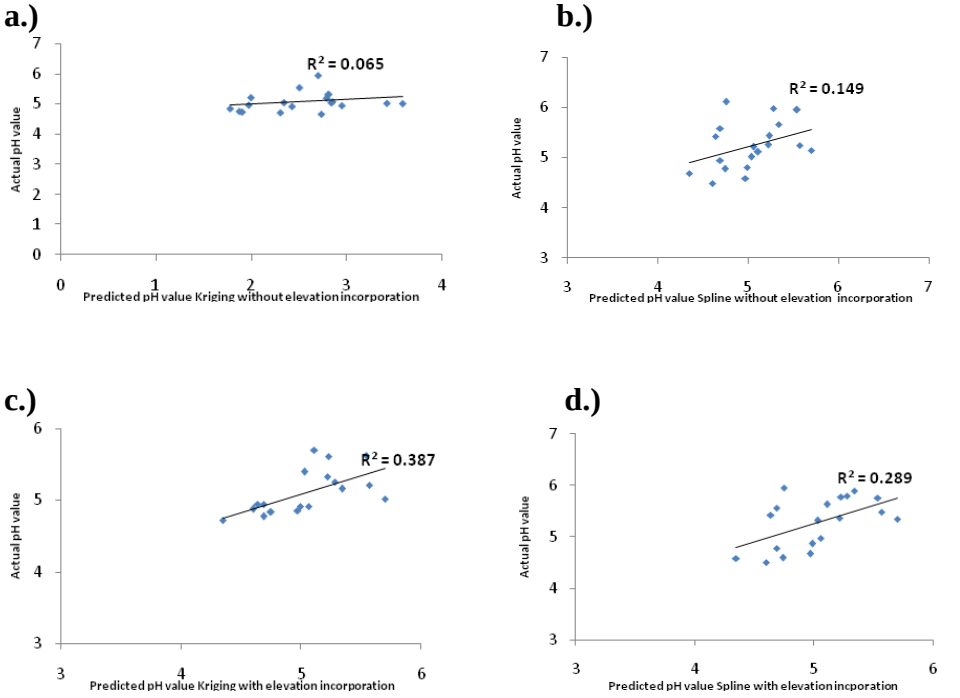

Fig. 6 a.) Correlation graph for non regression kriging of pH values for a studied field in St. Landry Parish, LA, USA.; b.) Correlation graph for non-regression spline of pH values for a studied field in St. Landry Parish, LA, USA.; c.) Correlation graph for regression kriging of pH values for a studied field in St. Landry Parish, LA, USA.; d.) Correlation graph for regression spline pH values for a studied field in St. Landry Parish, LA, USA.

Ultimately, for this research, regression kriging is preferred. Regression kriging produced more statistically significant results than spline interpolation (**Fig. 2a and 2b**). Regression kriging produced applicable estimates of clay (%) across the studied field while spline interpolation overestimated clay % in some areas (**Fig. 2a and 2b**). Similar trends exist for OC % and pH values for the regression kriging method (**Fig. 3-6**). Based on the statistical evaluation and regression kriging, it is evident that the swale formations do impact the spatial distribution the soil properties.

CONCLUSION

Sediment loading is a major concern for water quality, especially in Louisiana. Monitoring runoff is an essential part of improving water quality. The swales on this pasture are for monitoring water distribution along the field, however they are allowing for the pooling of water in the lower elevations (swales). High amounts of clays and organic matter are collected in swale lows and being transported into local bayous, causing sediment loading and thus, reductions in surface water quality. By determining the spatial variability of soil properties, better management practices can facilitate soil conservation on-site. A significant correlation was found between soil properties and swale formations. Kriging regression incorporates the elevation effect and provides a more accurate estimation of the distribution of soil properties, in comparison to a spline or non-regression interpretations. Best management practices should target swales as an ideal location for soil conservation efforts. This will result in long-term improvements in surface water quality through a reduction in sediment bonding.

REFERENCES

Anderson, C.J., W.J. Mitsch, and R.W. Nairn. (2005), *Temporal and spatial development of surface soil conditions at two created riverine marshes.* J. Environ. Qual. 34:2072-2081.

Blanco-Canqui, H., C.J. Gantzer, S.H. Anderson, and E.E. Alberts. (2004), *Grass barriers for reduced concentrated flow induced soil and nutrient loss.* Soil Sci. Soc. Am. J. 68:1963-1972.

Brady, N.C., and R.R. Weil. (2004), *Elements of the nature and properties of soils*: Second Edition. Pearson Education, Inc. New Jersey.

Cambardella, C.A., T.B. Moorman, J.M. Novak, T.B. Parkin, D.L. Karlen, R.F. Turco, and A.E. Konopka. (1994) *Field-scale variability of soil properties in central Iowa soils.* Soil Sci. Soc. Am. J. 58:1501-1511.

Chaplot, V., F. Darvoux, H. Bourennane, S. Leguedois, N. Silvera, and K. Phachomphon. (2006), *Accuracy of interpolation techniques for the derivation of digital elevation models in relation to landform types and data density*. Geoderma. 77:126-141.

ESRI. (2009), *Surface creation and analysis*. ArcGIS 9.2. The Redlands, CA.

Gaston, L.A., M.A. Locke, R.M. Zablotowicz, and K.N. Reddy. (2001), *Spatial variability of soil properties and weed populations in the Mississippi delta*. Soil Sci. Soc. Am. J. 65:449-459.

Gee, G.W. and J.W. Bauder. (1986), *Particle size analysis*. *In* Bigham, J.M. (ed.) Methods of soil analysis: Part 1 – physical and mineralogical methods. SSSA-ASA. Madison, WI.

Haws, N.W., B. Liu, C.W. Boast, P.S.C. Rao, E.J. Kladivko, and D.P. Franzmeier, (2004), Spatial *variability and measurement scale of infiltration rate on an agricultural landscape.* Soil Sci. Soc. Am. J. 68:1818-1826.

Iqbal, J., J.A. Thomasson, J.N. Jenkins, P.R. Owens, and F.D. Whisler. (2005). *Spatial variability analysis of soil physical properties of alluvial soils.* Soil Sci. Soc. Am. J. 69:1338-1350.

Isaaks, E.H. and R.M. Srivastava. (1989). *Applied geostatistics*. Oxford University Press, New York.

Jung, W.K., N.R. Kitchen, K.A. Sudduth, and S.H. Anderson. (2006). *Spatial characteristics of claypan soil properties in an agricultural field.* Soil Sci. Soc. Am. J. 70:1387-1397.

Karydas, C.G., I.Z. Gitas, E. Koutsogiannaki, N. Lydakis-Simantiris, and G.N. Silleos. (2009). *Evaluation of spatial interpolation techniques for mapping agricultural topsoil properties in Crete.* European Association of Remote Sensing Laboratories eProceedings. 8:26-39.

Kravchenko, A.N. and D.G. Bullock. (1999). *A comparative study of interpolation methods for mapping soil properties.* Agron. J. 91:393-400.

Kravchenko, A.N.(2003). *Influence of spatial structure on accuracy of interpolation methods.* Soil Sci. Soc. Am. J. 67:1564-1571.

Largueche, F.Z.B. (2006). *Estimating soil contamination with kriging interpolation method*. Am. J of Appl. Sci. 3:1894-1898.

LDEQ. (2009),. *Louisiana TMDL process information* – 303d water quality assessment [online]. Louisiana Department of Environmental Quality. Available at http://www.deq.louisiana.gov/portal/tabid/130/Default.aspx. Louisiana DEQ. Verified 15 Sept. 2009.

Leenaers, H., J.P. Okx, and P.A. Burrough. (1990), Comparison of spatial prediction methods for mapping floodplain soil pollution. Catena. 17:535-550.

Liu, T.L., K.W. Juang, and D.Y. Lee. (2006). *Interpolation soil properties using kriging combined with categorical information soil maps.* Soil Sci. Soc. Am. J. 70:1200-1209.

LSU ATLAS. (2009). *Basin subsegment 2004* map [online]. Louisiana State University. Available at http://atlas.lsu.edu/. LSU Cadgis Research Center. Verified 9 Sept. 2009.

Microsoft. (2007). *Statistical analysis. Microsoft Excel 2003*. Redmond, WA.

Mueller, T.G., N.B. Pusuluri, K.K. Mathias, P.L. Cornelius, R.I. Barnhisel, and S.A. Shearer. (2004), *Map quality for ordinary kriging and inverse distance weighted interpolation*. Soil Sci. Soc. Am. J. 68:2042-2047.

Needelman, B.A., W.J. Gburek, A.N. Sharpley, and G.W. Petersen. (2001), *Environmental management of soil phosphorus: Modeling spatial variability in small fields.* Soil Sci. Soc. Am. J. 65:1516-1522.

Nelson, D.W. and L.E. Sommers. (1996). Total *carbon, organic carbon, and organic matter*. *In* Bigham, J.M. (ed.) Methods of soil analysis: Part 3 – chemical methods. SSSA-ASA. Madison, WI.

Price, D.T., D.W. McKenney, I.A. Nalder, M.F. Hutchinson, and J.L. Kesteven. (2000). *A comparison of two statistical methods for spatial interpolation of Canadian monthly mean climate data*. Agri. and Forest Meteor. 101:81-94.

Ranney, R.W. (1969), *An organic carbon-organic matter conversion equation for Pennsylvania surface soils.* Soil Sci. Soc. Am. J. 52:965-969.

Robinson, T.P. and G. Metternicht. (2005), *Testing the performance of spatial interpolation techniques for mapping soil properties.* Computers and Elect. in Ag. 50:97-108.

Saldana, A., A. Stein, and J.A. Zinck. (1998), *Spatial variability of soil properties at different scales within three terraces of the Henares River (Spain)*. Catena. 33:139-153.

Sigua, G.C. and W.H. Hudnall. (2008), *Kriging analysis of soil properties, implication to landscape management and productivity improvement.* J. Soils Sed. 8:193-202.

Soil Survey Staff. (1986), *Soil survey of St. Landry parish, Louisiana*. USDA-NRCS. US Gov. Print. Off. Washington, DC.

Soil Survey Staff. (2004), *Soil survey laboratory methods manual version 4.0*. USDA-NRCS. US Gov. Print. Off. Washington, DC.

Soil Survey Staff. (2009a), *Official soil series descriptions [online]*. USDA-NRCS. Available at http://ortho.ftw.nrcs.usda.gov/cgi-bin/osd/osdname.cgi. Verified 4 Sept. 2009.

Soil Survey Staff. (2009b), *Web soil survey data* – St. Landry parish, LA [online]. USDA-NRCS. Available at http://websoilsurvey.nrcs.usda.gov/app/HomePage.htm. Verified 30 Sept. 2009.

Soil Survey Staff. (2009c), *Orthoimagery and DEM data for St. Landry Parish* via Geospatial Gateway [online]. USDA-NRCS. Available at http://datagateway.nrcs.usda.gov/. Verified 02 Oct. 2009.

Stein, A., J. Bouma, M.A. Mulders, and M.H.W. Weterings. (1989), *Using co-kriging in variability tudies to predict physical land qualities of level river terrace*. Catena. 2:385-402.

Weil, R. (2003), *Getting to know a catena: a field exercise for introductory soil science.* J. Nat. Resour. Life Sci. Educ. 32:1-4.

Webster, R., and Oliver, M.A. (1992), *Sample adequately to estimate variograms of soil properties*. J. Soil Sci., 43:177-192.

Zhang, X.Y., Y.Y. Sui, X.D. Zhang, K. Meng, and S.J. Herbert. (2007), *Spatial variability of nutrient properties in black soil of Northeast China.* Pedosphere. 17:19-29.

MOBILIZATION AND MANAGEMENT OF THE WATER RESOURCES IN THE NORTH-EAST OF ALGERIA

N. Khérici[1], H. Bousnoubra[1], E.F. Derradji[1], A. Maoui[1]

ABSTRACT:
With regard to the constant increase in the requirements out of water for the area for the Algerian North-East (Skikda, Annaba, El Tarf, Guelma and Souk Ahras), related on the increase in the population, the socio-economic development and the establishment of industries, the chronic water deficit is difficult to fill. It is asked to begin the deepened research in the policy of the water, based on the evaluation of the surface and underground water resources and justified by the installation of a new more reliable and more effective strategy of stock management. To this end, it is proposed to study the situation of the water resources in the Algerian North-East and its evolution in time by sector of use. By considering in a joint way, pressures dependent on the offer and the request of water (quantitative criterion), and while preserving objectives to limit degradations of the resources (qualitative criterion), thus we try to optimize the allowance between the various uses and to study the withdrawals carried out on a durable level on the ecological and economic plans. In order to answer the concerns of the hour and the current context, this work relating to the problems of water resources, their evaluation and their management, falls under the development and the improvement of the assessment offers–request of North–East Algeria.
After detailed evaluation, a negative assessment results from this with resource needs, highlighting a critical situation and recording a deficit worrying with short and long-term. Thus the current reserves will not be any more a solution for the increasing requirements of water, which require the installation of an urgent policy of integrated water management.

Key words: *subsoil waters resources, surface waters, assessment, equipment, needs, offers, potential hydrous, renewable reserves, management, evaluation.*

1. INTRODUCTION

Water is a major socio-economic factor in development; see same ecological concerns in the world. The need for managing it according to the essential uses is necessary for each country. The shortage of water and its degradation worry more and more the population in countries of the whole world. According to FAO (2000), the drinking water world demand will double every 20 years and as pollution threatens the supply of surface water, groundwater resource becomes increasingly scarce.

To meet the concerns of the time, the current context and the problems of water resources, their assessment and management, this work is part of the development and improvement of supply-demand balance of Eastern Algeria.

[1] *Geology Laboratory. University of Annaba. BP N ° 12. El Hajar. 23200. Annaba. Algeria*

2. DESCRIPTION OF THE AREA OF STUDY

2.1 Location

The study area is located in the north-east of Algeria; it includes 5 wilayas (Provinces) spread over an area of 16285 km ², covering the north (from west to east Skikda, Annaba and El Tarf) and south (Guelma and Souk Ahras) of the area. Naturally, it is limited to the north by the Mediterranean Sea, south by the Tell Atlas, to the east by the borders between Algeria-Tunisia and to the West by the crystalline formations of Jijel (**Fig. 1**).

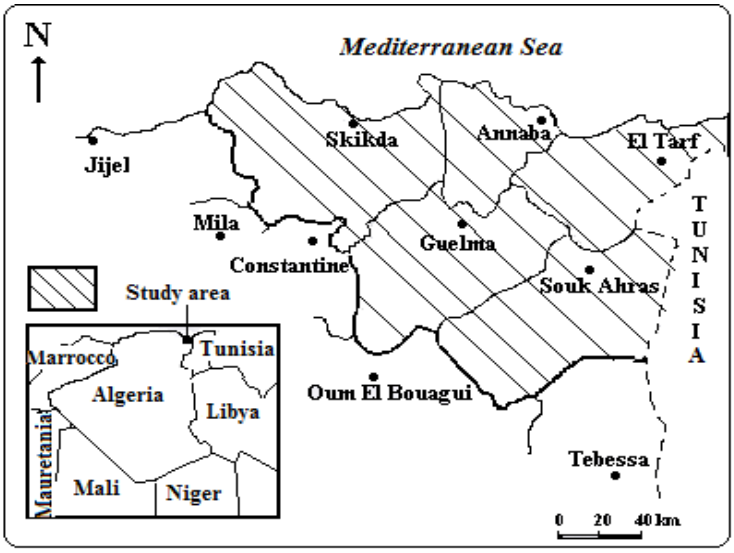

Fig. 1 Map of location of study area

The study of the evolution of rain takes part in the potential role of surface waters to the filling of dams. It also contributes to the renewal of surface water and groundwater (*Meddi, 2003*).

Thus the region can distinguish two main rainfall zones:

- A coastal strip where the water does not exceed the 700mm/yr on the plains, but recorded more than 1000mm in the hills (Bougaroun Cape, Cape Rosa...).
- An area within which the rainfall is relatively low, which recorded an average of between 600 and 400 mm/yr (Guelma and Souk Ahras).

2.2 Hydrographic network

The drainage is especially pronounced in the northern part (**Fig. 2**). The hydrologic analysis is a platform for better understanding the behaviour of hydrologic basins. Among the basins and sub-watersheds located in the region (*Ghachi, 1982; Kherici, 1993; Benrbah, 2006; Bounab, 2007; Bousnoubra 2002*), one quotes:

- Those of the littoral formed by Mafragh wadi, Kébir East wadi, Kébir West wadi, Safsaf wadi and finally the Guebli wadi.

- Those inside at the North, the Seybouse wadi or more in the South the Médjerda wadi and Mellègue wadi.

The **Table 1** shows the annual inputs and the drained surface area of the main wadis of the region.

Table 1 ***Annual throughput and area of the drained surface of the principal wadis of the region***

Wadi	Drainage area (km²)	Flow (Mm^3/year)
Kébir Est	680	295
Bounamoussa	575	127
Guebli	202	49
Safsaf	1165	150
Kébir Ouest	1169	282
Bouhamdane	1194	96
Cherf	1104	107
Mellah	550	151
Seybouse	6071	359
Medjerda	1377	202
Mellègue	1440	80

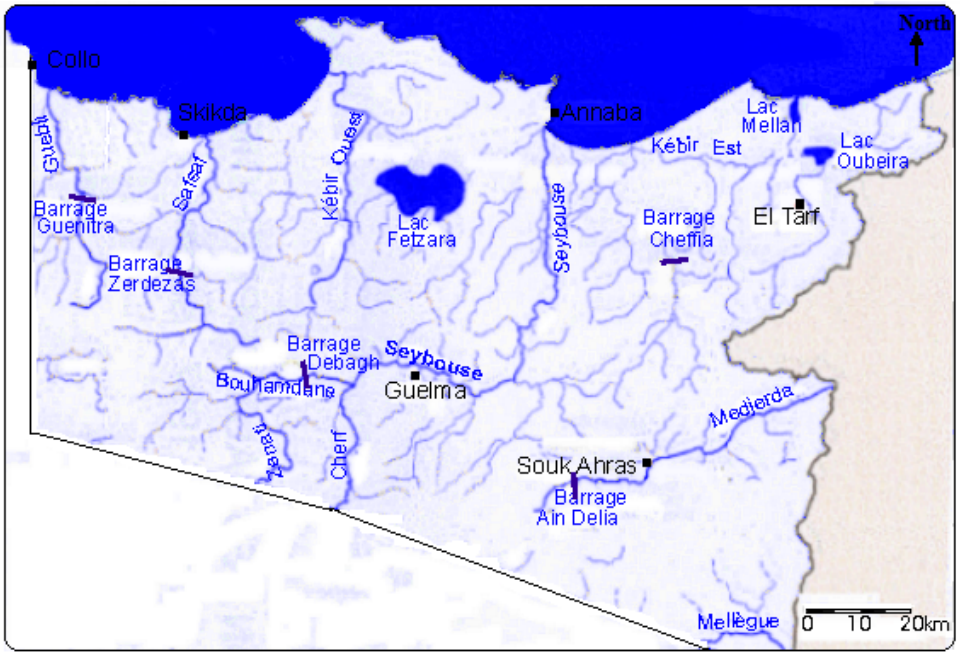

Fig. 2 Map of the hydrographic network of the principal wadis of North East Algeria***n***

2.3 Nature of aquifers and their formation

Geological, geophysical and hydrogeological investigations confirm the existence of several types of aquifers (**Fig.3**):

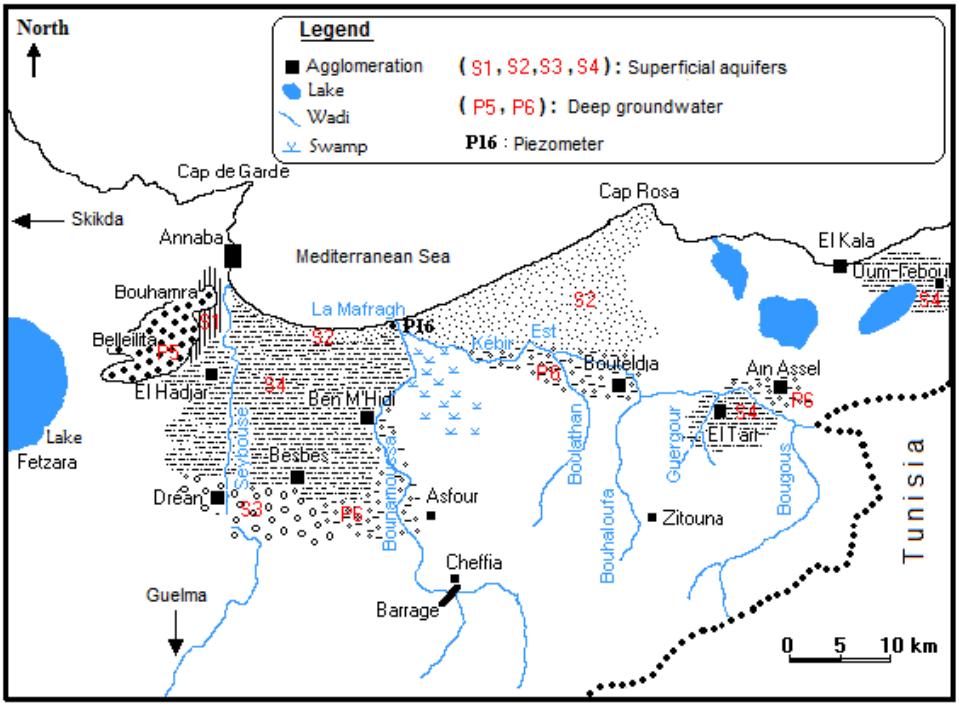

Fig.3 Location of the principal waters resources in the study region

- The surface aquifers contained in sedimentary formations with an interstice permeability of Plio-Quaternary (dune of Guerbes, Les Salines and Bouteldja). They have a relatively large spatial extension, although their thickness is sometimes low.
- The alluvial layers which sometimes become free captives and constitute a particular type of aquifers, formed by large spreading sand and gravel wadis (aquifer of Collo, Safsaf, Bouchegouf). These layers provide 60% of groundwater collected in the region, in particular because of the ease of access and their excellent flow. They are the privileged place of exchanges between the wadis and large unconfined aquifers.
- The deep aquifers, contrary to the homogeneous superficial aquifers, represent a hydrogeologic anisotropic medium with heterogeneous permeability They are located in fissured limestone and sometimes thermal (Guelma, SoukAhras).. These layers contain rather important reserves which remain difficult to quantify because of the complexity of the fissured medium

3. METHODOLOGY

Partial studies were collected on the levels of the administrative services (town halls, daïras, wilayas) and specialized national agencies (university, ANAT, ANRH, EPEA, DHW, ABH… etc). For the majority, specific and not integrated in an economic and social development plan of the country, were supplemented by displacements on grounds and personal investigations. They allowed the acquisition of an abundant documentation admitting a synthetic vision accompanied by regional figures. Simple statistical methods allowed a confrontation between offers and demand of water in relation with the socio-economic development at short and long-term.

4. RESULTS

4.1 Evaluation of the surface water resources

In spite of relatively high runoff volumes (more than 1800 m3/year), only a quantity of limited water is mobilized (**Table 2, Fig.4**) giving 382 Mm3/ year. This hydrous potential is therefore limited to water dams and used for the drinking water supply, the irrigation and industry.

4.2 Evaluation of the underground water resources

The underground water resources of the whole area (**Table 2, Fig.4**) add up a volume of approximately 192 Mm^3 of which the most important reserves are in the aquifers of Annaba -El Tarf. In sum, the volume of surface water available is approximately 382 Mm^3, of which 60% are from the coast (132 Mm^3 of Skikda and 100 Mm^3 in the region of Annaba), accounting for the 2/3 of the total water resources (574.68 Mm^3). However this water is exposed to the pollution whose treatment is expensive and sometimes non-existent.

Tableau 2. ***Resources mobilized in surface water and groundwater in the north-east of Algeria***

Area	Annual surface water potential hydrous (Mm^3)	Annual underground water potential (Mm^3)	Total Volume (Mm^3)
Annaba-Tarf	100	83	183
Skikda	132	48	180
Guelma	68.79	33.62	102.41
Souk Ahras	82	27.27	109.27
Total	382.79	191.89	574.68

As for the groundwater, the chemical quality is better, but they represent only 1/3 of total volume (191.89 Mm^3) of which 43% belongs to the aquifer of Annaba-El Tarf.

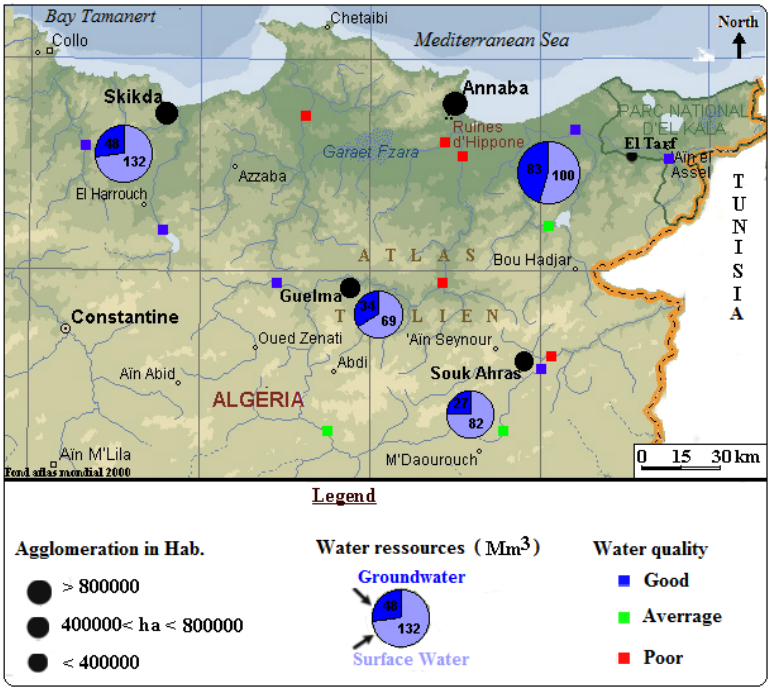

Fig. 4 Resources and quality of surface water and groundwater of North East Algeria

5. ASSESSMENT AND PERSPECTIVE

5.1 Evaluation of the assessment resources needs

The projected volume of water used by the three sectors (AEP, AEA, AEI), in time made it possible to confront the produced volume and that consumed by these sectors' users (**Table 3, Fig. 5**).

Tableau 3. ***Evolution according to the time of the global needs of North East Algeria***

Sector / Year	*AEP(Mm^3/year) 150 l/j/hab	*AEA(Mm^3/year) 5000 m^3/ha/year	*AEI (Mm^3/year)	Volume total (Mm^3/year)
1987	109.47	**185.63**	**39.07**	**326.87**
1990	116.00	**281.27**	**39.07**	**431.93**
1995	127.75	**302.54**	**39.07**	**471.00**
2000	140.64	**330.22**	**39.07**	**519.29**
2005	154.70	**361.05**	**64.76**	**600.39**
2010	170.40	**390.48**	**71.24**	**664.88**
2015	187.70	**415.08**	**78.97**	**730.73**
2020	206.74	**436.26**	**86.86**	**799.17**
2025	227.74	**466.04**	**89.91**	**878.27**

**AEP (drinking water),*AEA (agricultural water supply),*AEI (industrial water supply)*

Currently produced volumes do not exceed 216 Mm^3/year, but according to the needs (**Fig. 5**), which rise at 519.29 Mm^3/year, the demand cannot be satisfied. If one draws from all the movable resources in particular surface waters and ground water, one observes that the situation would become alarming with course term. Existing resources calculated add up a volume in surface water and groundwater out of 574.68 Mm3/yr, but the demands for water (all sectors confused users) in the year 2005 are 600.39 Mm3/an, largely exceeding the offer; in the medium term a deficit still relatively more increased will be generated by the strong water demand, from where the requirement rises for a rational exploitation of the resources with all investments needed.

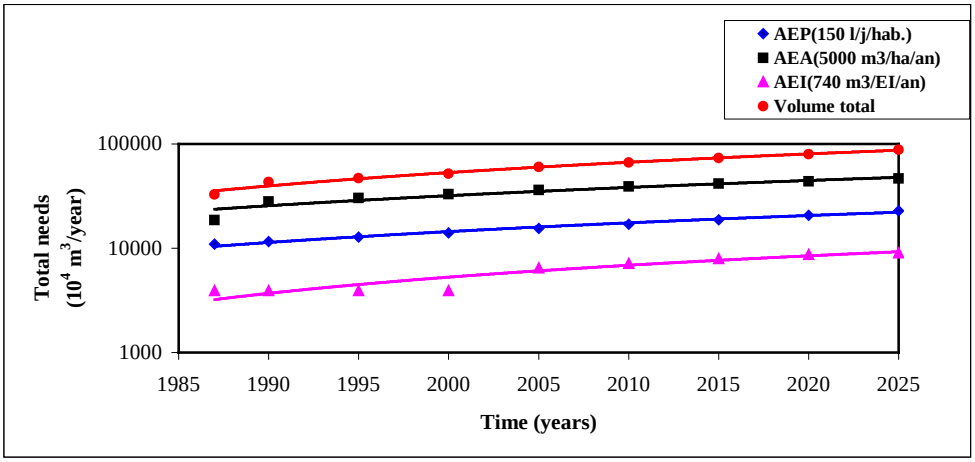

Fig. 5 Evolution according to the time of the global needs of North East Algeria

6. CONCLUSION

It is in the sector of the water supply for irrigation where the proportion of the demands for water remains the strongest, it represents more than 60% of the total water demand, or the current offer is not satisfied. The water consumption of the area in all important sectors is currently superior to renewable quantities. The hydrous deficit rises regularly. In addition, the prospects for exploitation of new conventional resources are limited, even inexistent in certain cases. The water resources and more particularly the groundwater are still lightly taken into account in policy planning: no collecting is made because of the protection object intended to limit the negative impact of human activities on water quality.

REFERENCES

Benrabah S. (2006). *Current status of water resources in the wilaya of Skikda (summary trial): results-management-perspective.* Mémoire de Magister. Univ.Annaba. 147p.

Bounab S. (2007). *Current status of water resources in the wilaya of Annaba, El Tarf (summary trial): results-management-perspective.* Mémoire de Magister. Univ.Annaba.160p.

Bousnoubra, H. (2002). *Water resources in regions of Skikda, Annaba, El Tarf, Guelma, Souk-Ahras (north-eastern Algeria) .- Evaluation and Management Perspective .- vulnerability and protection.* Thesis PhD. Annaba. Algérie.159 p.

Council of Europe (2000). *Insufficient water resources and agriculture*; Report of the Committee on Agriculture, Rural Development and Food .26 p.

Detay, Mr. D'Arras, D., Suzane P. (1992). *Management of water resources in western Paris region.* The White Coal. International Review of water. Volume 4, pp295-308.

Ghachi, A. (1986). *Use of water resources in Algeria: the basin Seybouse*. Edition of the OPU. Algiers. No. 2-2-1910. 508p.

Kherici, N. Messadi, D. (1992). *Importance of groundwater resources of the dunes of North Africa*. Mediterranean Geology Review, Volume XIX, No. 2, 69-76.

Mébarki, A. (1984). *Water resources and development in Algeria: the basin Rhumel*. Edition OPU. Algiers. No. 1212-09-84. 302p.

Meddi M., Hubert P. (2003). *Impact of change in rainfall on the water resources of north-western Algeria.* International conference on hydrology of the Mediterranean and semi-arid regions, Montpellier, No. 278, pp. 229-235pp.

National Agency for Planning (ANAT). (1996.2000). *Arrangement of Provinces of Annaba and El Tarf.* Unpublished reports.

.

INVESTIGATIONS DENDROCLIMATOLOGIQUES DU SAPIN DE CEPHALONIE EN GRÈCE CENTRALE

M. A. Papadopoulos[1]

ABSTRACT: Dendroclimatic investigation of fir trees in Cephalonie, Central Greece
In this study four tree-ring widths mean (site) chronologies as well as one of their local chronology, were analyzed, according to climatic factors. The tree-ring data cover a period of 185 years (1820-2004) and resulted from the analysis of 78 wood carrots taken from 40 dominant Greek fir (Abies cephalonica) trees in Central Greece. Of the climatic data, monthly precipitations and mean monthly temperatures were used for a time period of 33 years (1972-2004). Mean sensitivity of the raw tree-rings data (SM: 0,12 -0,25) revealed the existence of a relatively strong climatic signal in tree-rings succession. Based on the Principal Components Analysis of the 4 site chronologies of the indices, the climate is responsible for a 47, 6 % of the total variance of the tree-rings width. Tree-ring to climate relationships, calculated on the level of the local chronology over the period 1972-2004, show a positive influence of June precipitations and September temperatures on tree-ring widths, and a negative one with November precipitations of the previous to tree-ring formation year.

Key-words: *dendrochronology, dendroclimatology, tree-ring, response function, Abies cephalonica.*

RÉSUMÉ:
Dans cette étude, nous analysons quatre chronologies moyennes (stationnelles) des épaisseurs des cernes du sapin de Céphalonie (Abies cephalonica) en Grèce Centrale et la résultante chronologie locale, en fonctions des facteurs climatiques. Les données des épaisseurs de cernes couvrent une période de 185 ans (1820-2004) et proviennent de l'analyse de 78 carottes de bois, prélevées de 40 arbres dominants. Les données climatiques concernent les précipitations mensuelles et les températures moyennes mensuelles d'une période de 33 ans (1972-2004). La sensibilité moyenne des données brutes des cernes (SM : 0,12 -0,25) montre l'existence d'un signal climatique assez fort dans la succession des cernes. L'Analyse en Composantes Principales (ACP) de 4 chronologies stationnelles des indices montre que le climat traduit le 47,6% de la variance totale des cernes. Les relations cerne-climat, calculées au niveau de la chronologie locale, sur la période 1972-2004, montrent une action positive des précipitations du Juin et des températures du Septembre et une action négative des précipitations du Novembre sur l'épaisseur de cerne.

Mots clés: *dendrochronologie, dendroclimatologie, cerne, fonction de réponse, Abies cephalonica.*

1. INTRODUCTION

Le sapin de Cephalonie (Abies cephalonica) est une espèce endémique de la végétation qrecque, qui forme des forêts pures du Péloponnèse jusque en Grèce Centrale (mont Tymfristos) et des forêts mélangées avec Abies borisii regis plus septentrionales jusqu' au mont Olympe et Athos (*Athanasiadis, 1986*). Ces dernières décennies, les forêts du sapin en Grèce connaissent des problèmes de dépérissement (*Markalas, 1992; Tsopelas et al., 2001*). Ces problèmes rencontrés en Grèce (*Tsopelas et al., 2001; Raftoyannis et al., 2008*) mais

[1] *Institut Technologique d'Education de Lamia, Département Forestier et d'Aménagement d'Environnement naturel, 361 00 Karpenissi, Grèce. E-mail: ampapadopoulos@teilam.gr*

également dans d'autre pays Européens (*Becker, 1989; Webster et al., 1996*) ont été attribuées aux facteurs climatiques et en particulier à la sécheresse.

Le dépérissement des forêts et d'une manière plus générale, les modifications des écosystèmes forestiers liées au changement climatiques font le sujets de plusieurs études (Bert, 1993; Ciesla et Donaubauer, 1994; Brofas et Economidou, 1994 ; Aussenac, 2002). Dans cette optique, la dendroécologie, branche de la dendrochronologie (Kaenen et Schweingruber, 1995), peut être utilisée pour analyser l'impact du climat en observant les variations des cernes des arbres (*Fritts et Swetnam, 1988; Schweingruber, 1996*).

Le sapin a fait l'objet d'études dendroécologiques en Europe (*Becker et Levy, 1988; Tessier et al., 1990; Bert et Becker, 1990; Manetti and Cutini, 2006*). En Grèce, des études concernant le sapin de Cephalonie ont été réalisées par Heliotis et al. (1988) et Papadopoulos (1998). Ces études examinent principalement le rôle des facteurs du milieu et de la pollution atmosphérique sur la croissance radiale du sapin. Dans cette étude on examine la variation interannuelle de l'épaisseur des cernes en fonction des facteurs climatiques.

2. MATERIEL ET METHODES

La région d'étude se trouve en Grèce Centrale, à Karpenissi, 200 kilomètres au nord d'Athènes et elle est composée de 4 sites de forêts de sapins de Cephalonie (**Fig. 1, Tab. 1**). Pour la station de Agios Nikolaos (alt. 1120 m ; période 1973-2005), les précipitations moyennes annuelles sont de 1402mm, la température moyenne annuelle est de 9,9 oC, la température moyenne minimale du mois le plus froid est de –1,5 oC et la température moyenne maximales du mois le plus chaud est de 25,2 oC. La période de sécheresse estival suivant le diagramme ombrothermique de Bangouls et Gaussen dure de mi-juin au début Septembre.

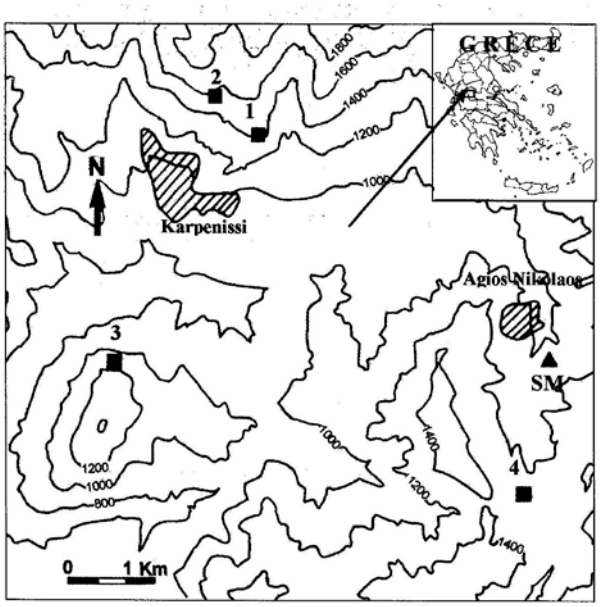

Fig. 1 Carte de localisation des populations du Sapin de Cephalonie (1-4) et de la station météorologique de Agios Nikolaos (SM).

Table 1. ***Cordonnées géographiques et nombres des arbres et des carottes prélevées par site.***

Sites	**1**	**2**	**3**	**4**
Latitude	38°55´27´´	38°55´33´´	38°53´22´´	38°51´59´´
Longitude	21°48´35´´	21°48´32´´	21°46´43´´	21°51´49´´
Altitude (m)	1480	1520	1080	1260
Arbres (Carottes) prélevées	13 (26)	7 (14)	10 (18)	10 (20)

Pour chaque site, sur une superficie forestière de 0,1-0,2 ha, des prélèvements par carottages (échantillons cylindriques du bois) sont réalisés sur 7-13 arbres dominants. Au niveau de chaque arbre, 1 ou 2 carottes à environ 1,30 m au dessus du sol (pour un total de 14-26 carottes pour chaque site) sont réalisées avec la tarière de Pressler, (Tab. 1). La préparation des carottes, puis l´interdatation des cernes, qui permet d'attribuer à chaque cerne l'année exacte de sa mise en place, sont effectuées conformément aux procédures classiques de la dendrochronologie (*Stokes et Smiley, 1968; Fritts, 1976; Schweingruber, 1988, 1996*). L'épaisseur des cernes est ensuite mesurée au 1/100 de millimètre, à l'aide du système d'analyse d'image Windendro (*Régant, 2007*). A chaque carotte est donc attribuée une série chronologique de mesures que l'on appelle chronologie élémentaire. Les données des chronologies élémentaires ont été transformées en indices de croissance par filtrage (calcul *d'une courbe lissée), puis par standardisation (rapport de la valeur mesurée à la valeur correspondante de la courbe théorique ajustée aux données) (Fritts*, 1976; Cook et al., 1989). Ensuite, à chaque site a été construit une chronologie moyenne (stationnelle) par le total des chronologies élémentaires indicées du site et puis une chronologie locale par la moyenne de 4 chronologies stationnelles.

Pour chaque site et au niveau des chronologies élémentaires des données brutes, un paramètre classique en dendrochronologie, la Sensibilité Moyenne (*Fritts, 1976*) a été calculé. Ensuite, les années à cerne mince ou épais ont été calculées, à l'aide d'une Analyse en Composantes Principales (*Guiot, 1990*), appliqué sur la matrice de 4 chronologies stationnelles des indices pour la période 1820-2004. Le CP1 permet la classification des cernes suivant leurs épaisseur. Des valeurs positives élevées sur le premier axe représentent des années caractéristiques à cerne épaisse, des valeurs négatives élevées représentent des années caractéristiques à cerne mince. Enfin, les relations cerne-climat ont été calculées sur la période 1972-2004, entre la chronologie locale et 24 régresseurs climatiques (précipitations mensuelles et températures moyennes mensuelles). Suivant la pratique utilisée dans la région Méditerranéenne (*Serre, 1985*), chaque paramètre climatique est construit sur une période de douze mois, s'étendant du mois d'Octobre de l'année qui précède la formation du cerne au mois de Septembre de l'année de son élaboration. Les données climatiques proviennent de la station météorologique de Agios Nikolaos (Karpenissi) qui fait partie du réseau de l'Institut Forestier d'Athènes. La méthode utilisée est celle des Fonctions de Réponse (*Fritts, 1976*), calculées à l'aide du programme PPPBase (*Guiot et Goeury, 1996*). Le calcul fait appel à une régression orthogonalisée, Bootstrap (Guiot, 1991).

3. RÉSULTATS ET DISCUSSION

Le coefficient de Sensibilité Moyenne (SM) de 4 chronologies stationnelles des données brutes varie de 0,12 à 0,25, avec une valeur moyenne 0,17 (Fig. 2). Ces valeurs de (SM) sont comparables à celles qui ont été calculées pour d'autres conifères en Grèce et qui poussent dans la même zone de végétation que le sapin de Cephalonie (Papadopoulos, *1995*).

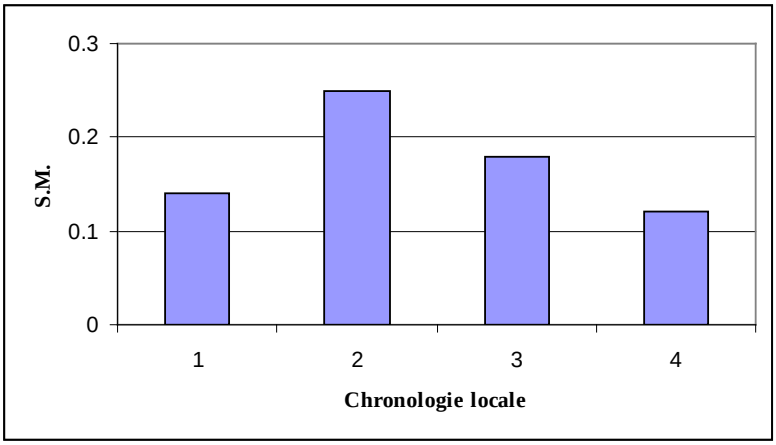

Fig. 2 Sensibilité moyenne de 4 chronologies stationnelles des données brutes.

L'ACP montre que le premier axe principal traduit 47,6 % de la variance totale (**Tab. 2**). Ce pourcentage représente la variation interannuelle commune des épaisseurs des cernes qui traduit, d'une manière quantitative, l'action des facteurs climatiques sur la croissance radiale du sapin de Cephalonie en Grèce Centrale. Les autres axes principaux traduisent l'action d'autres facteurs du milieu ou de la structure des populations du sapin, qui ne font pas l'objet dans cette étude.

Tableau 2. ***Valeurs des Composantes Principales 1-4***

.P.	aleur ropre		roduit umulé
	,903	7,6	.903
	,877	1,9	.669
	,838	1,0	.399
	,382	,5	,534

La présentation des valeurs de la première Composante Principal (Fig. 3) permet de visualiser les cernes minces (valeurs négatives) et les cernes épais (valeurs positives) du sapin pour la période 1820-2004. Parmi eux les plus caractéristiques sont:

- cernes minces: 1824, 1845, 1861, 1890, 1907, 1908, 1969, 1978, 1997, 2000,
- cernes épais: 1827, 1858, 1885, 1900, 1905, 1930, 1959, 1960, 1975, 1999.

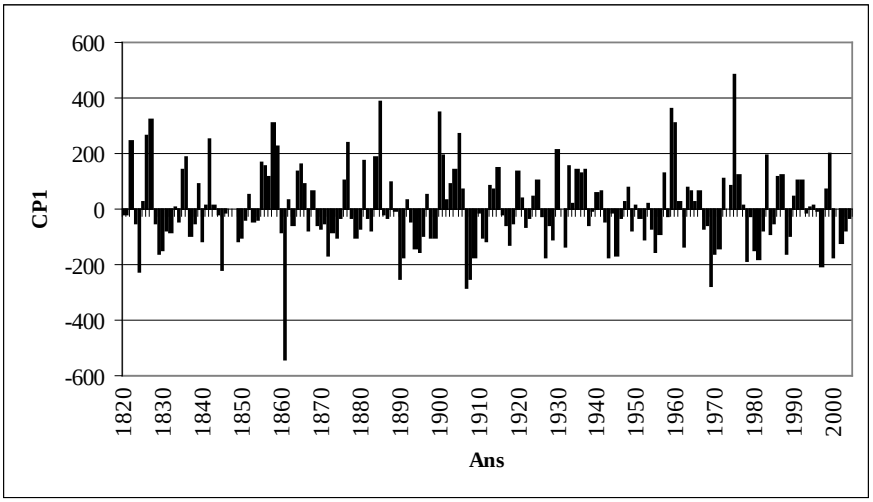

Fig. 3 Diagramme des valeurs du PC1 de l'ACP de 4 chronologies stationnelles des indices. Valeurs positives: cerne mince, valeur négative: cerne épais.

Les résultats, obtenus pour la chronologie locale, sont présentés dans la figure 4. L'épaisseur des cernes est négativement corrélée à 90% avec les précipitations de novembre qui précède la formation de cernes et positivement à 95% avec les précipitations de juin de l'année de formation des cernes. En ce qui concerne les températures, l'épaisseur des cernes est positivement corrélée à 90% avec les températures de septembre de l'année de formation de cerne. Durant la période estivale on note des relations inverses avec les températures, mais à un niveau inférieur à 90%.

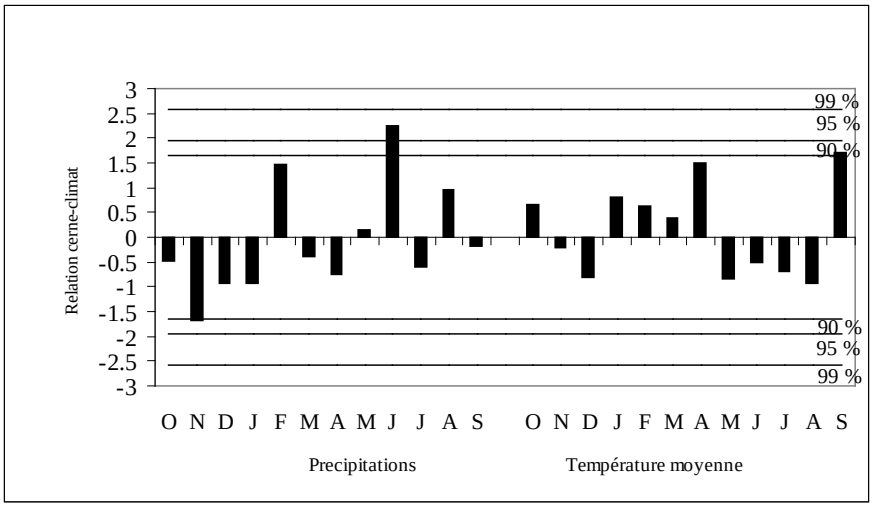

Fig. 4 Profil des fonctions de réponse de la chronologie locale des indices d'épaisseur des cernes du Sapin de Céphalonie en Grèce Centrale avec les précipitations mensuelles et les températures moyennes mensuelles pour la période 1972-2004. La ligne horizontale représente le seuil de signification.

L'action négative des précipitations de novembre s'explique probablement par les problèmes phytopathologiques qui peuvent affecter les arbres, si les hivers sont très pluvieux. Par contre, l'action positive des précipitations de juin peut s'expliquer par la demande en eaux des arbres pour la réalisation des processus physiologiques et de l'activité cambiale qui commence durant la période fin mai début juin. Des relations similaires avec les précipitations estivales ont été observées pour le sapin en France (Serre *et al*., 1988; Rolland, 1993). Les relations positives des températures de septembre traduisent l'impact de ce facteur sur le comportement thermique qui doit être favorable pour la continuation de la croissance radiale dans cette haute altitude.

En examinant les précipitations de Juin, qui ont la signification statistique la plus importante parmi les résultas obtenus, on constate qui il y a une tendance de diminution des pluies durant les dernières décennies, ce qui pose des questions sur le rôle des précipitations de ce mois sur la diminution de la croissance des cerne et la mortalité des sapins.

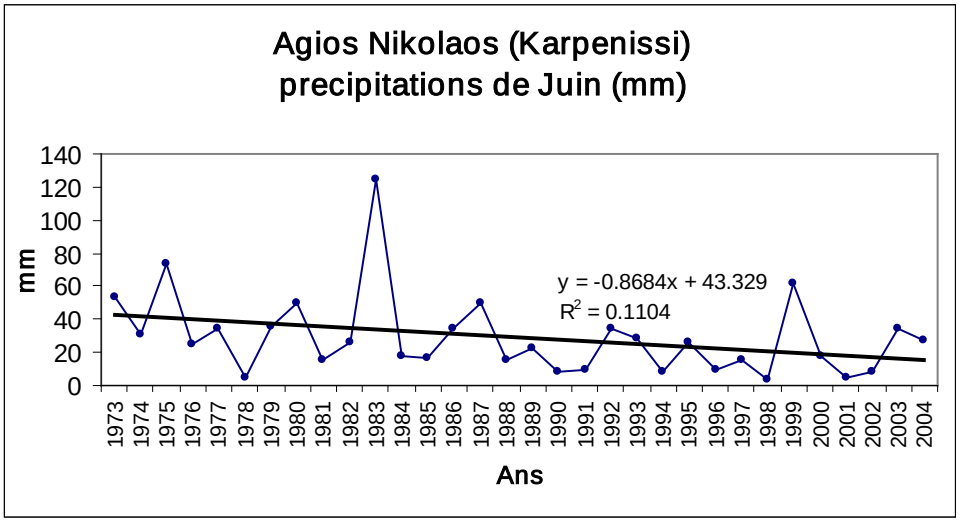

Fig. 5 Précipitation du Juin de la station de Agios Nikolaos sur la période 1973-2004.

CONCLUSIONS

Le sapin de Cephalonie est une espèce sensible aux variations interannuelles des paramètres pluviothermiques. L'analyse des relations cernes-climat permet de décoder le signal climatique qui englobe les épaisseurs de cernes de cette espèce en Grèce Centrale. Cette information peut servir pour construire un modèle de croissance radiale de l'espèce dans la région d'étude. Ceci est utile pour interpréter, en liaison avec les résultas d'autres études sur la croissance et la phytopathologie du sapin, le phénomène du dépérissement des forets de sapin en Grèce.

BIBLIOGRAPHIE

Aussenac G., (2002), E*cology and ecophysiology of circum-Mediterranean firs in the context of climate change*. Annals of Forest Sciences, 59, 823-832.

Athanasiadis N., (1986), *Botanique forestière, (arbres et arbustes des forêts de Grèce), Tome II*, Giahoudis-Giapoulis (eds), Thessaloniki: 309p.

Becker M., Levy G., (1988), *A propos du dépérissement des forêts: climat, sylviculture et vitalité de la sapinière Vosgienne*. Rev. For. Fr, 40, 5, 345-358.

Becker M., (1989), *The role of climate on present and past vitality of silver fir forest in the Vosges Mountains of northeastern France*. Canadian Journal of Forest Research 19, 1110-1117.

Bert G.D., (1993), *Impact of ecological factors, climatic stresses and pollution on growth and health of silver fir (Abies alba Mill.) in the Jura mountains: An ecological and dendrochronological study*. Acta Oecologia 14, 229-246.

Bert G.D., Becker M., (1990), *Vitalité actuelle et passée du sapin (Abies alba Mill.) dans le Jura. Etude dendroécologique*. Ann. Sci For. 47, 395-412.

Brofas G., Economidou E., (1994), *Le dépérissement du Sapin du Mont Parnasse. Le rôle des conditions climatiques et écologiques.* Ecologia Medirerranea, 20, 1-8.

Ciesla W.M., Donaubauer E., (1994), Decline and dieback of trees and forests. A global overview. *Food and Agricultural Organization of the U.N., FAO Forestry Paper, 120 p.*

Cook E., Briffa K., Shiyatov S., Mazepa V., (1989) *Tree-ring standardization and growth-trend estimation. In: Methods of dendrochronology. Applications in the environmental sciences*. Cook and Kairiukstis (eds*)*, Kluwer Acad. Pub., International Institute for Applied Systems Analysis, 104-123

Fritts H.C., (1976) *Tree-rings and climate.* Academic Press, London, 567p.

Fritts H.C., Swetnam T.W., (1988) *Dendroecology: a tool for evaluating variations in past and present forest environments.* Advances in Ecological Research, 53 p.

Guiot J., (1990) *Methods and programs of statistics for paleoclimatology and paleoecology. Quantification des changements climatiques: Méthodes et programmes, Monographie N^{o} 1*. INSU, PNEDC, 253 p.

Guiot J., (1991) *The bootstrapped response function*. Research report. Tree-ring Bull. 51, 39-41.

Guiot J, Goeury C., (1996) *PPPBase, a software for statistical analysis of paleoecological and paleoclimatological data*. Dendrochronologia 14, 295-300.

Heliotis F., Karandinos M., Whiton J., (1988) *Air pollution and the decline of the fir forest in Parnis National Park*, Near Athens, Greece. Environmental Pollution 54, 29-40.

Kaennel M., Schweingruber F. H., (1995) *Multilingual glossary of dendrochronology. Terms and definitions in English, German, French, Spanish, Italian, Portuguese, and Russian*. WSL/ FNP, Haupt, 467p.

Manetti M.C., Cutini A., (2006) *Tree-ring growth of silver fir (Abies alba Mill.) in two stands under different silvicultural systems in central Italy*. Dendrochronologia 23, 145-150.

Markalas S., (1992) *Site and stand factors related to mortality rate in a fir forest after a combined incidence of drought and insect attack.* Forest Ecology and Management 47, 367-374.

Papadopoulos A.M., (1995) *Dendrochronologie – dendroclimatologie des espèces conifères en Grèce*. In: Elliniki Dasologiki Etairia (Eds), Proc. 7^{o} Congés Forestier: Exploitation de ressources forestières, 625-632. (In Greek).

Papadopoulos A.M., (1998) *Etudes des relations dendroecologiques du sapin au Mont Tymfristos In: Elliniki Dasologiki Etairia* (Eds), Proc. 8^{o} Congés Forestier: Problèmes de la sylviculture, 218-226. (In Greek).

Raftoyannis Y., Spanos I., Radoglou K., (2008) *The decline of Greek fir (Abies cephalonica Loudon): Relationships with root condition.* Plant Biosystems 142, (2), 386-390.

Régant (2007), *Windendro (2008a), For Tree-Ring Analysis*. Régent Instruments Inc, Québec Canada, 132p.

Rolland Ch., (1993), *Tree-ring and climate relationships for Abies alba in the internal Alps*. Tree-Ring Bulletin, **53**, 1-11.

Schweingruber F. H., (1996), *Tree Rings and Environment. Dendroecology*. Birmensdorf, Swiss Federal Insitute for Forest, Snow and Landscape Research. Haupt. 609p.

Schweingruber F. H., (1988) *Tree rings basics and applications of dendrochronology*. Kluwer Academic Publishers. 276p.

Serre-Bachet F., (1985), *La dendrochronologie dans le bassin méditerranéen*. Dendrochronologia **3**, 77-92.

Serre-Bachet F., Tessier L., Loris K., (1988), *Mise en place et signification du cerne.* In: Hackens T., Munaut A.V. and Till C. (eds). Wood and archaeology. Pact 22, I. 1, 13-23.

Stokes M.A., Smiley T.L., (1968), *An introduction to tree ring dating*, University of Chicago Press, Chicago.

Tessier L., Serre-Bachet F., Guiot J., (1990), *Pollution fluorée et croissance radiale des conifères en Maurienne (Savoie, France)*. Ann. Sci. For. 47, 309-323.

Tsopelas P., Angelopoulos A., Economou A., Voulala M., Xanthopoulou E., (2001), *Monitoring crown defoliation and tree mortality in the fir forest of Mount Parnis, Greece*. In: Radoglou, K. (Eds.), Proceedings of the International Conference on Forest Research, "*A challenge for an integrated European approach*", Thessaloniki. NAGREF, Forest Research Institute, Thessaloniki, 253-258.

Webster R, Rigling A., Walthert L., (1996), *An analysis of crown condition of Picea, Fagus and Abies in relation to environment in Switzerland.* Forestry 69**,** 347-355.

AN ANASTOMOSED SECTION OF THE CRIŞUL REPEDE RIVER IN THE OLD MILITARY SURVEY MAPS

Judit Petrovszki[1]

ABSTRACT

In this paper the planform of the Crişul Repede (Sebes-Körös) River is analyzed. Downstream of Oradea, along the present Romanian-Hungarian border, a surprising feature is found on the pre-regulation maps. A part of the river has anastomosed pattern albeit the all other section on the Great Hungarian plain is meandering. The natural evolution of this river section is followed in the sheets of the First and the Second Military Surveys, between 1783 and 1859. Some changes on the maps are because of the errors of the surveys but surprisingly a lot of them can be verified even the modern maps. The river regulation was done between the Second and Third Surveys, so these latter sheets from the 1880s shows both the last natural and the planned regulated forms of the river.

Keywords: *river dynamics, river planform, Great Hungarian Plain, Crişul Repede River, anastomosed planform, Romania, Hungary*

1. INTRODUCTION

The Crişul Repede (Sebes-Körös) River takes its rise in Izvorul Crişului, in the nortern Apuseni Mts. It flows through the eastern part of the Great Hungarian Plain (GHP) and joins to the Fehér- and Fekete-Körös (Crişul Alb and Crişul Negru). This estuary produces the Hármas-Körös ('triple Körös') River that joins to the Tisza at Csongrád.

The total catchment area of the Criș/Körös River system (Barcău/ Berettyó, Crişul Repede/Sebes-Körös, Crişul Negru/Fekete-Körös and the Crişul Alb/Fehér-Körös) is cca. 28000 km^2. The 47 %, 13000 km^2, of it is in Hungary, and 53 %, 15000 km^2, is in Romania. The average water discharge of the Sebes-Körös is 38 m^3s^{-1}. During the river controls, the originally 162 km long river became shorter, with 23 cutoffs its length was reduced to 86 km.

The rivers, by their pattern, can be divided into 6 groups: straight, meandering, braided, anastomosing, wandering and anabranching pattern (**Table 1**; *Leopold & Wolman, 1957; Schumm, 1963; Rust, 1978; Miall, 1996)*. The Körös River System belongs to the meandering pattern, but along a few kilometers, the pattern is anastomosing (see **Figs. 1 &** 2). This section was the Romanian side along the present Hungarian-Romanian border, between Toboliu (Romania) and Berekböszörmény (Hungary). After the river controls, the new channel is almost straight, so we can not see this character afterwards.

Meandering rivers, by self-organizing their structure, can maintain the channel slope (*Stølum, 1996*). So the varying vertical movements change the river structure and sometimes the river pattern, too (*Ouchi, 1985*).

[1] *Department of Geophysics and Space Science Eötvös University H-1117, Pázmány Péter sétány 1/c, Budapest, Hungary geojudit@gmail.com*

Table 1. ***The patterns of the alluvial rivers by their geometric parameters***
(Br: the braiding index, the numbers of pool-riffle pairs per thalweg wavelength, Brice, 1964;
S: sinuosity; Rust, 1978; Miall, 1996; Timár, 2003)

Br / S	Br<1	1<Br<3	Br>3
S<1,5	straight	anabranching	braided
S>1,5	meandering	wandering	anastomosing

The anastomosing planform is considerably different: its multichannel character is opposite to the single-channel nature of a meandering river. The divided channels of the anastomosing rivers themselves are meandering. This planform type appears at very low river energy, such as in coastal or inland deltas. Here, in an extremely flat part of the GHP, the energy of the river is low, producing this exceptional anastomosing pattern. A sudsiding zone, which has a connection with the Sárrét Plain farther west in Hungary, can be supposed along this very river section. In this paper, I provide how this river section varied during the last few centuries, in the maps of the Military Surveys of the Habsburg Empire.

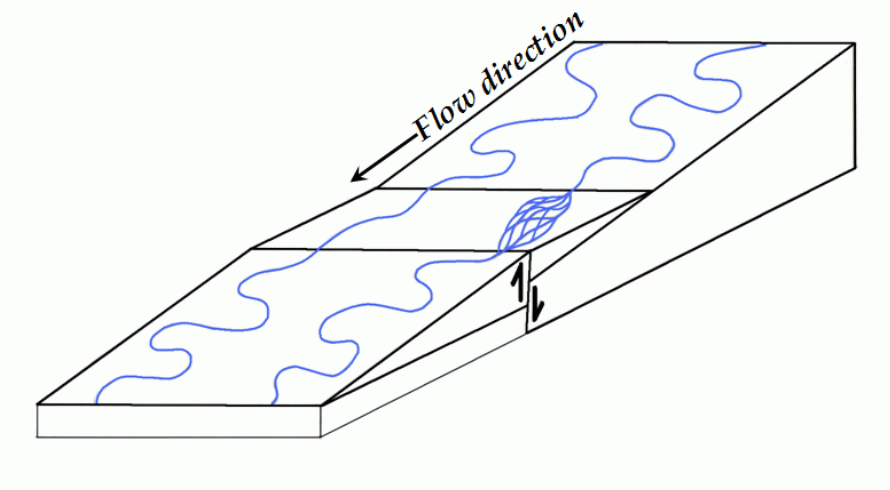

Fig. 1 Response of the meandering river to a zone of active tectonism (Petrovszki & Timár, in press). If the vertical movements of the surface provides a very low angle slope, the sinuosity falls or, in extreme cases, the planform changes to anastomosing. This change is identified at the Crişul Repede River, downstream of Oradea

2. THE HABSBURG MILITARY SURVEYS AND THEIR RECTIFICATION

The First Military Survey

At the end of the years 1760, Maria Terézia ordered a military survey for the whole area of the Habsburg Empire. The Hungarian sheets were issued between 1783-86 (Paldis, 1919; Borbély & Nagy, 1932; Kretschmer et al., 2004; Jankó, 2007). The scale of these maps is 1:28,800 (1 Viennese inch in the map equals to 400 Viennese fathoms in the field). There was no triangulation network behind it (Strenk, 1992), instead of that, field measuring tables were used for the survey. They were generally placed to an elevated point of the field. Positions of these humps are reliable in the sheets.

There are four terrain types indicated in these sheets: agricultural fields, meadows, forests and marshlands. The military maps were made primarily for infantry use, so where a marshland was also a forest, the marshland was drawn as it had more military importance. There are a lot of parish church in the former Monarchy, which were build during the reign of Emperor Joseph II, simultaneously to the First Military surveys, so they are not found in the sheets.

The georeference of the First Survey, however, can be defined by quadratic formulas (Arcanum, 2006) for any zone of the Empire. These formulas provide a general accuracy of one kilometer with extreme errors of even four kilometers. The individual sheets can be rectified by these formulas and after their usage, by just a few or just one ground control point(s; Timár et al., 2007).

The Second Military Survey

The Second Military Survey of the Habsburg Empire was made between 1806 and 1869, in the area of the historical Hungary from 1819 to1869, with some interruption (Jankó, 2001; 2007). The surveying got to the area of the Körös River System, about the same time of the controls of the main rivers, around 1857-61. During the measuring, they draw the natural, uncontrolled channels, but they also signed the planned cutoffs.

The projection of the survey can be interpreted as Cassini projection in GIS environment (Timár, 2004). The Empire was divided into 14 zones with 8 independent projection centers (Timár et al., 2006). In the historical Hungary the projection center was the Viennese Stephansdom, the size of the sections is 24*16 inches. The scale of the maps is 1:28,800, similarly to the First Survey (Hofstätter, 1989). Because of the large mapped area, the distortions are high at the margins. The estimated accuracy of the maps is 50-100 meters, slightly higher at the borders far from the projection center. Rectification can be done by defining just the four corners of the sheets (Veverka & Čechurová, 2003; Timár et al., 2006).

Both the maps of the First (**Fig. 2**) and Second Military Surveys (**Fig. 3**) shows anastomosing river planform near Toboliu at Crişul Repede River, before the water control measures.

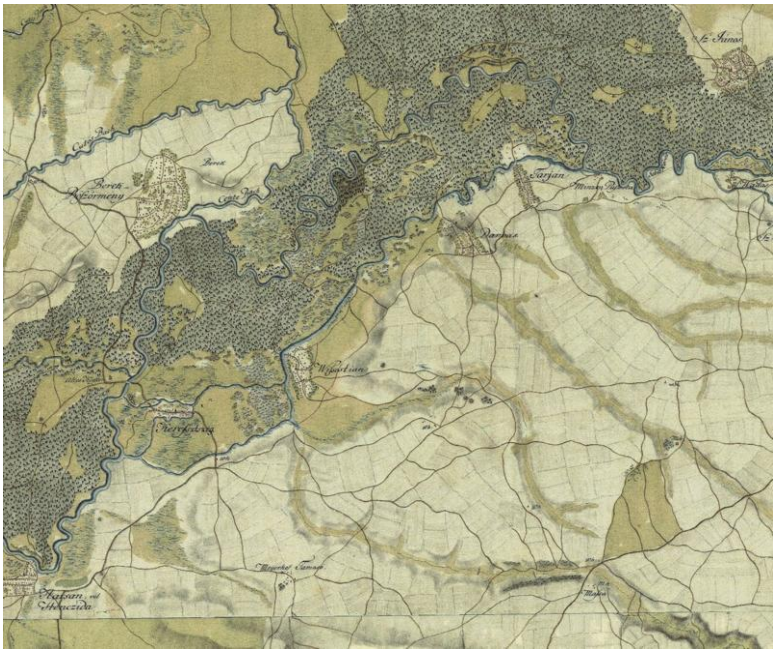

Fig. 2 The anastomosed part of the Crişul Repede downstream of Oradea, near Toboliu (Wifsestian in old maps) in the sheets of the First Military Survey (1783-86).

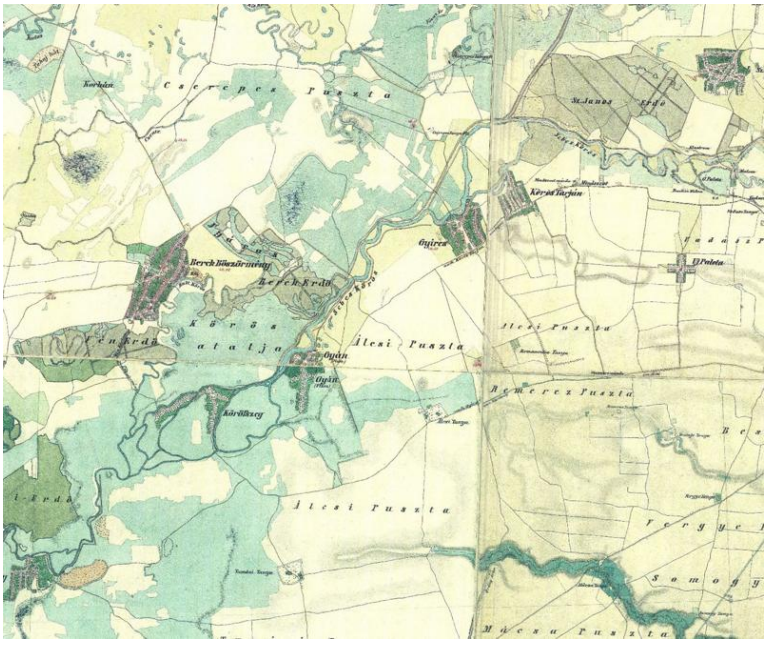

Fig. 3 The anastomosed part pf the Crişul Repede downstream of Oradea, near Toboliu (Gyán in old maps) in the sheets of the Second Military Survey (around 1860).

The Third Military Survey

This survey was made in the 1880s. The survey has a triangulation base but it was not adjusted (Timár & Molnár, 2008). Indeed, the coordinates in the sheets can be interpreted as astronomical ones, and the accuracy of the rectification is 200 meters (Molnár & Timár, 2009). Color sections, with the scale of 1:25000, were also drawn but later they were lost for the most part of Hungary, only their black-and-white copies remained. The map used in this paper had a scale of 1:75,000 (Biszak et al., 2007; **Fig. 4**). Rectification is based on projection grid lines of the Budapest-centered Stereographic grid (Timár et al., 2003).

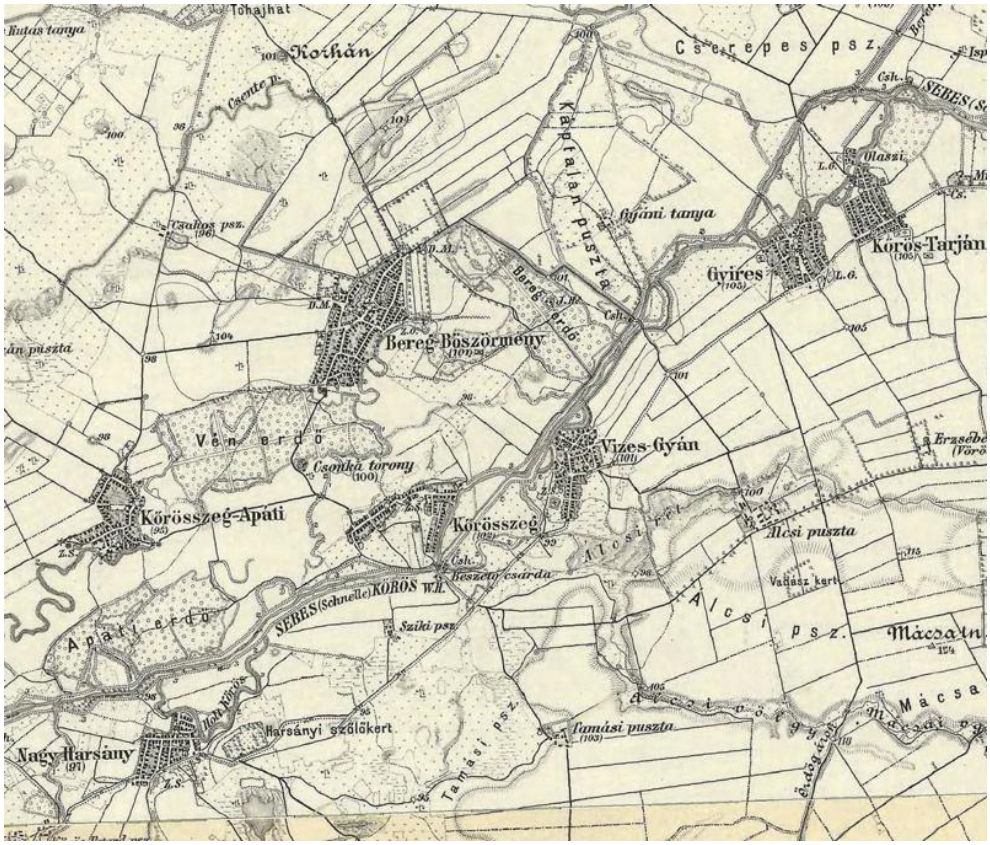

Fig. 4 The river section shown in Figs. 1 & 2 is shown as partly regulated in the Third Military Survey map

The anastomosing part of the river on the maps, made in different years

The anastomosing river section was digitized on the maps of the Second Military Survey (Petrovszki, 2008). We can overlay the digitized pattern on the maps of the First Military Survey to see, that the character of the river is about the same on the two maps, but the channels are in different places. This was, because the river was not controlled and it is the last natural change of the river that was fortunately mapped (**Fig. 5**).

Another interesting point on these maps, is the location of some settlements. Most of them are in the similar positions in the maps, but during the first survey Berekböszörmény mapped about 2 km north from its present position. In the newer maps, the position of this settlement is identical to the modern location. The surprising position of Berekböszörmény in the First Survey can be a result of some measuring mistake, or maybe the village moved to a different place, when the river changed its bed. It is not unique in the Pannonian Basin (Pišút & Timár, 2007). By the time of the Third Survey, the river was controlled, so we cannot see the anastomosing pattern, and even the meanders were rather eliminated. In the Landsat ETM satelite image from 2000, we can still see the mark of the ancient anastomosing channels (**Fig.** 6).

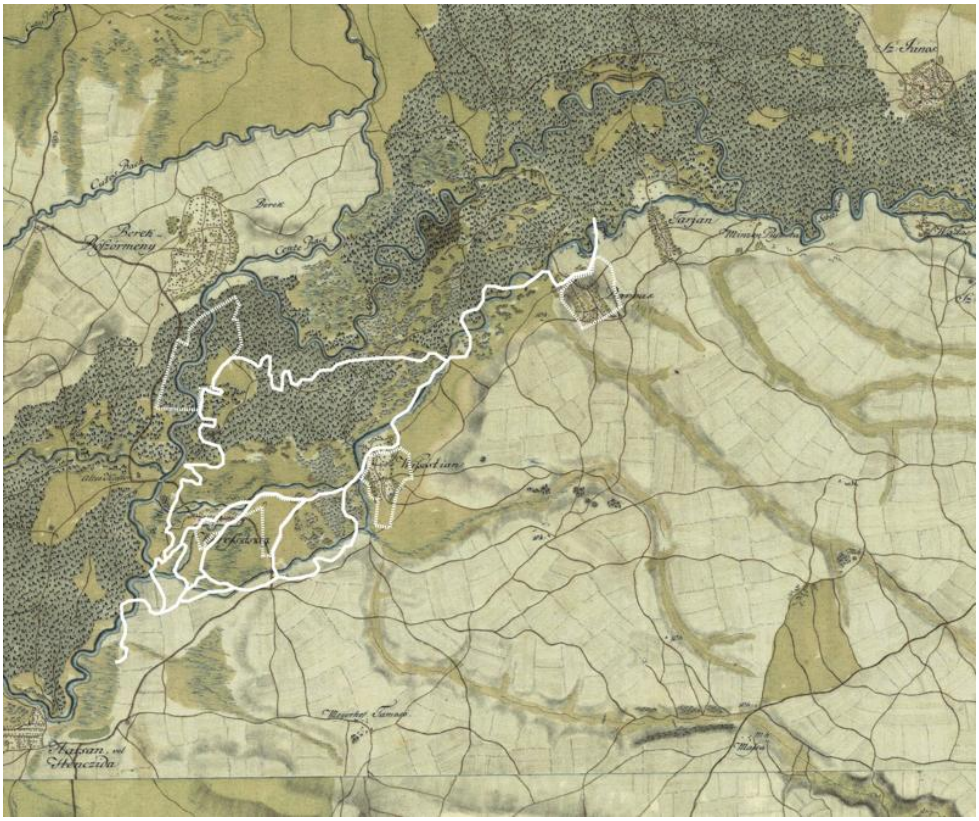

Fig. 5 Channel pattern of the Second Military Survey (continuous white lines) printed over the First Survey sheets. Positions of the settlements, according to the Second Survey, are indicated by dotted line. Note the change in position of Berekböszörmény (east of the river).

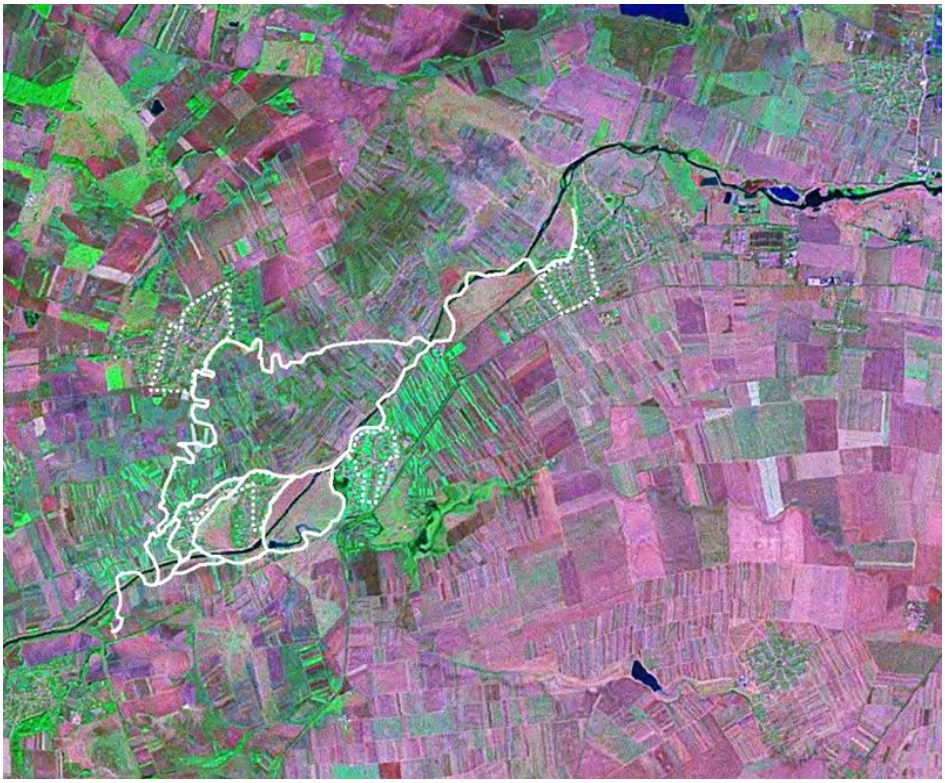

Fig. 6 Channel pattern of the Second Military Survey (continuous white lines) printed over the Landsat ETM satellite image

SUMMARY

The section of the Crişul Repede River between Toboliu and Berekböszörmény was mapped as an anastomosing river both in the First and Second Military Surveys. The location of the river branches are in somewhat different position, perhaps because of mapping errors but it is also possible that it was the real shape of the channel.

It can be stated that the maps of the Second Military Survey are real: the marks and traces of ancient channelbeds can be identified in the satelite images. Moreover, the old channel traces are in the same position where the channels were measured in the mid-19th century. The position of the straight, controlled channel, shown in the Third Survey is also verified by the satellite images. The difference between the maps and the satelite images stays under the maximal error of the map rectification.

REFERENCES

Arcanum (2006): *Digitized maps of the Habsburg Empire – The First Military Survey*. DVD-issue, Arcanum Database Ltd., Budapest.

Biszak, S., Timár, G., Molnár, G., Jankó, A. (2007): *Digitized maps of the Habsburg Empire - The third military survey*, Österrechisch-Ungarische Monarchie, 1869-1887, 1:75000. DVD-issue, Arcanum Database Ltd., Budapest.

Borbély A., Nagy J. (1932): *Magyarország I. katonai felvétele II. József korában*. Térképészeti Közlöny 2: 1-2. issue.

Brice, J. C. (1964): *Channel patterns and terraces of the Loup Rivers in Nebraska*. *USGS Prof. Paper*, 422B.

Hofstätter, E. (1989): *Beiträge zur Geschichte der österreichischen Landesaufnahmen*, I. Teil, Bundesamt für Eich- und Vermessungwesen, Wien, 196 p.

Jankó, A. (2001): *A második katonai felmérés*. Hadtörténeti Közlemények 114: 103-129.

Jankó, A. (2007): *Magyarország katonai felmérései, 1763-1950*. Argumentum, Budapest, 196 p.

Kretschmer, I., Dörflinger, J., Wawrik, F. (2004): *Österreichische Kartographie*. Wiener Schiften zur Geographie und Kartographie – Band 15. Institut für Geographie und Regionalforschung der Universität Wien, Wien, 318 p.

Leopold, L. B., Wolman, M. G. (1957): *River channel patterns; braided, mean-dering and straight*. USGS Prof. Paper 282B: 1-73.

Miall, A.D. (1996): *The geology of fluvial deposits.* Springer, Berlin, 522 p.

Molnár, G., Timár, G. (2009): *Mosaicking of the 1:75,000 sheets of the Third Military Survey of the Habsburg Empire.* Acta Geod. et Geophys. Hung. 44(1), in press.

Ouchi, S.(1985) *Response of alluvial rivers to slow active tectonic movement*. Geol. Soc. Am. Bull. 96: 504-515.

Schumm, S.A.(1963): *A tentative classification of alluvial river channels*. US Geol. Surv. Circ. V477.

Paldus, J. (1919): *Die militärischen Aufnahmen im Bereiche der Habsburgischen Länder aus der Zeit Kaiser Josephs II.* Akademie der Wissenschaften in Wien. Philosophisch-historische Klasse Denkschriften, 63. Band, 2. Abhandlung, Universitäts-Buchhändler, Buchhändler der Akademie der Wissenschaften in Wien.

Petrovszki, J. (2008): A *Körös-vízrendszer morfometriai vizsgálata neotektonikai következtetésekkel*. MSc. Thesis, Eötvös University, Budapest, 41 p.

Pišút, P., Timár, G. (2007): *A csallóközi (Žitný ostrov) Duna-szakasz folyódinamikai változásai a középkortól napjainkig.* In: Kázmér, M. (ed.): Környezettörténet – Az utóbbi 500 év környezeti eseményei történeti és természettudományi források tükrében. Hantken Kiadó, Budapest, pp. 59-74.

Rust, B.R. (1978): *A classification of alluvial channel systems.* In: Miall, A. D. (ed.): Fluvial Sedimentology. Canadian Soc. Petrol. Geol. Mem. **5**: 187-198.

Strenk, T. (1985): *The stucture of maps covering Hungary from the first military topographic survey*. Ann. Univ. Sci. Bud. de Roland Eötvös Nom. Sect. Geophys. et Meteor., Tom. I.-II.: 360-372.

Stølum, H.-H. (1996): *River meandering as a self-organization process.* Science 271: 1710-1713.

Timár G. (2003): *Geológiai folyamatok hatása a Tisza alföldi szakaszának medermorfológiájára*. Ph.D. Thesis, Dept. of Geophysics, ELTE, Budapest, 135 p.

Timár, G. (2004): *GIS integration of the second military survey sections – a solution valid on the territory of Slovakia and Hungary*. Kartografické listy 12: 119-126.

Timár, G., Molnár, G. (2008): *A harmadik katonai felmérés térképeinek georeferálása.* Geodézia és Kartográfia 60(1-2): 23-27.

Timár, G., Molnár, G., Márta, G. (2003): *A budapesti sztereografikus, ill. a régi magyarországi hengervetületek és geodéziai dátumaik paraméterezése a térinformatikai gyakorlat számára.* Geodézia és Kartográfia **55**(3): 16-21.

Timár G., Molnár G., Székely B., Biszak S., Varga J., Jankó A. (2006): *Digitized maps of the Habsburg Empire* – The map sheets of the second military survey and their georeferenced version. Arcanum, Budapest, 59 p.

Timár, G., Biszak, S., Molnár, G., Székely, B., Imecs, Z., Jankó, A. (2007): *Digitized maps of the Habsburg Empire – First and Second Military Survey, Grossfürstenthum Siebenbürgen.* DVD-issue, Arcanum Database Ltd., Budapest.

Veverka, B., Čechurová, M. (2003): *Georeferencování map II. a III. vojenského mapování.* Kartografické listy 11: 103-113.

A MODELLING APPROACH USING THE GEOGRAPHIC INFORMATION SYSTEMS FOR DECISION MAKING IN THE WATER SECTOR

M. H. Sellami[1], I. Trabelsi[1]

ABSTRACT:
In this work we are putting forward a general method based on geographical information system in order to make the right decision at moment for all the fields of water sector by responding to the following requests: To foresee for what time the existing resources and water networks could satisfy all consumers categories and which solutions of rehabilitation we can put in at time. To propose a new schemes of water networks for the consumers not yet connected or for those whose the existing network could not assume their water need in the future. To make an interface permitting the link between all databases, information layers, thematic maps, equations and models propounded in order to exploit them when preparing guides for future sustainable development and every time we are asked to make a rapid decision. A first application of this model has been done for SILIANA region. The results are satisfying.

Keywords *information layers and thematic maps; geographical position; water resources; adduction/distribution networks; water consumers; rehabilitation scenario and model.*

1. INTRODUCTION

At the world level, for a national scale (country) and within a regional resolution (locality and district) the durable development is a key word considered by the experts of all the disciplines as a core around which must revolve their projects. Those projects that concern generally three larges axis: agricultural, industrial and services need the water as engine for their working. As technology in all fields becomes more and more sophisticated it is being considered as necessity for the development actions in the different sectors. Which has induced a dramatically increase in water consumption. Added to the problems caused by the climatic change, the amount of potable water available suffered a dangerous diminution [5, 8, 9, 10, 15, 16, 20, 21, 24, 28, 29, 31]. The circuit of the available water starts from the resources, generally ground water or surface water, passes through the adduction and distribution networks to arrive finally at the level of consumption [14, 24, 28]. The questions we must ask at the beginning are how to manage the water available? in what level, when and how we must intervene first in order to assume the water needed for all categories of consumers while avoiding the water wasting? which methodology to follow and systems to develop that can serve as data basis and supports for decisions making?. Many studies exist in the bibliography trying to respond to those questions, but , generally they treat by region and by consumer category every part alone (resource or adduction/distribution or consumption) [1, 2, 3, 5, 12, 21, 30, 31, 33]. We can't found a general method or model, that if applied to any region (respectively category of consumer) or to all regions (respectively all consumers categories) at the same time, could answers

[1] *Unité Rayonnement Thermique Département de Physique Faculté des Sciences de Tunis2092 Ecole Supérieur des Ingénieurs de l'équipement Rural de Medjez El bab, 9070, Medjez El bab* Mh.sellami@planet.tn

those questions instantaneously for all levels. In this study we will present a global model, using the geographical information system, could help to make the appropriate decision, at any time, for all levels of the water network, in any region and for any consumer category. A first application of this model to SILIANA (a region in the Western - North of Tunisia) will be introduced.

2. MATERIALS AND METHODS

We will put in at this part, the different steps to follow, the mathematical equations/models and the necessary materials that can be used to control, to monitor and to evaluate, by geographical position, the actual and future situation of water circuit: water availability at the resources level, the state of the adduction/distribution networks, the consumer requirements (agricultural sector, industrial sector, service sector).

2.1 Equations for geographical position

The determination of a geographic position of any point (M) means to express its coordinates in the spherical references[3, 23, 28, 30]. Those coordinates are, generally, noted (r, θ, φ) where r is the altitude, θ is the longitude and φ is the latitude (**Fig. 1**). If we note by (m) the horizontal projection of (M), we can write r = OM, θ = angle <Oz, OM >, φ = angle <Ox, Om>. With (O, Ox, Oy, Oz) are the axes of an orthonormal reference and O the origin of the reference. We can then express the projected coordinates of (M) as follow $x = r \sin\theta \cos\varphi$, $y = r \sin\theta \sin\varphi$, $z = r \cos\theta$.

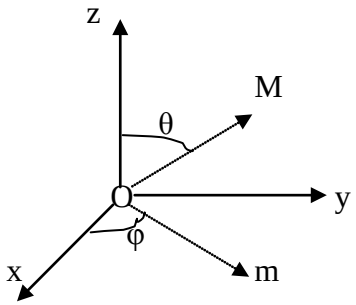

Fig. 1 Basic schema for geographic referencing

2.2 Equation and models for the resources level

Generally there is two classes of resources: the surface resources and the ground water resources. The amount of water available is generally linked to climatic conditions: precipitation, temperature, evaporation. The prediction of resources efficiencies can be done easily for any region by applying this reasoning: After limiting the different surface lakes, all waterways, the different water sheets (water table and deep water sheet) in every region, we consider every one of them as a closed system for which we apply the balance equation. This later is presented as the equilibrium between the inflow, out flow, income and lost of water for every system defined. It can be written in global form as follow [28]:

$$\Delta V_w = V_{i,w} + (P + Q_{l,in}) - (Q_e + Q_{l,out})$$

- where:
ΔV_w - variation of water volume in the defined system
$V_{i,w}$ - initial water volume in the defined system
P - precipitation
$Q_{l,in}$ - the lateral inflow for the defined system from all the directions
Q_e - water lost by evaporation from the defined system
$Q_{l,out}$ - the lateral outflow for the defined system from all the directions

So then we can formulate the fictive water debit at a determined time for the defined system by:

$$Q_f = \frac{\Delta V_w}{\Delta t}$$

- where:
Q_f - fictitious water flux
ΔV_w - variation of water volume in the defined system for the desired period
Δt - variation of time in the defined system for the desired period

The determination of every term in the balance equation depends on the climatic conditions, soil structure, soil occupation and the geologic characteristics in the region studied. We can measure them directly by using the necessary apparatus and methods (piezometric and geological mapping, hydrological measurements, meteorological measurements). We can also estimate them by applying empirical formulas or models for water transfer in the atmosphere and in the soil (weather forecasting models, general circulation models, hydrologic models, biosphere and evaporation estimating). They are based on the resolution of the following general equation of water and mass transfer [28, :

$$\frac{\partial \overline{q}}{\partial t} + \overline{u}\frac{\partial \overline{q}}{\partial x} + \overline{v}\frac{\partial \overline{q}}{\partial y} + \overline{w}\frac{\partial \overline{q}}{\partial z} = -\left[\frac{\partial}{\partial x}\left(\overline{u' q'}\right) + \frac{\partial}{\partial y}\left(\overline{v' q'}\right) + \frac{\partial}{\partial z}\left(\overline{w' q'}\right)\right] + k_v \nabla^2 \overline{q}$$

- where:
$\overline{q}$: mean variation of water mass or water flux ;
$\overline{u}$; $\overline{v}$, $\overline{w}$: mean value of the water mass velocity in the respectively directions ox, oy and oz
q': turbulent fluctuation of water mass
u', v', w': turbulent fluctuation of the water mass velocity
$\frac{\partial}{\partial t}$:partial variation on behalf of the time
$\frac{\partial}{\partial x}$, $\frac{\partial}{\partial y}$, $\frac{\partial}{\partial z}$: partial variation in the space in the three directions ox, oy and oz
k_v: the molecular diffusivity in the medium of the defined system

2.2.1. The surfaces resources

They are formed from the hydrographical networks (rivers), natural lakes, barrages lakes', natural water sources. Their localisations is possible by establishing numerical maps and land numerical models using the precedent equations, land altimetry measures, thematic maps and aerial photos (satellite and planes). The amount of water available is generally linked to climatic conditions: precipitation, temperature, evaporation. We must limit the fluvial network (length and capacity of the primary line water, secondary line water, tertiary line water…) and we have to determine the capacities of the existing lakes (geographical localisation, extent and water height). This is done by direct measurement with the necessary apparatus, by using the thematic maps and by applying the above equations.

2.2.2. The ground water and table water resources

They are considered, generally, as non-renewable resources. They don't depend on climatic parameters but they are sustained our days to an overexploitation. Determining the amount of water that exists, for how time it can assume our needs and the possibility of their artificial recharges are questions that we can model. So we must make a geological sweeping, a piezometric scanning and mapping and we have to make many forages for testing and controlling the existing sheets and to discover if possible the new ones. Then by using thematic maps and models for underground hydraulic we can elaborate equations for water sheet folding, expanse, height and volume. By utilising the statistical studies, land use plan, agricultural maps, economic plans, directing plans for development by region we can propose mathematically relationships for the evolution of water consumption by sector and by region. We can then determine the life duration of the ground water and the amount of water to add when thinking to their recharge.

2.3 Equations and models for the adduction/distribution water networks level

The adduction/distribution networks are defined as the course that the water flow follows from the source to the consumer. Our days, in rural or urban zones, to assume the water needed at time and to avoid its loss in route there is tendency to conduct the water by special canalisations (pipes, conduits), hydraulic accessories and apparatus (pump, tanks, treatment stations, floodgates, bends, diaphragm). The differentiation between adduction and distribution is arbitrary. It depends on the sector to supply with water and is only to facilitate the conception of the network when making hydraulic studies. Generally, the adduction part is that from the sources to the tank or to the series of tanks for water storage and treatment. The distribution is that from the tanks to the consumer: fields and plants for agricultural sector, houses for potable sector (service sector) and factories for the industrial sector. Calculating a water network signifies determining the length of pipes, their diameters, nature or material of fabrication, number of conduits sections', types and number of hydraulic accessories, their capacities (surface, volume, power, energy…) and finally the cost. There is many mathematical relations ships, formulas and models that are used to make the hydraulic calculus. They are based on the energy balance between the initial point of the network (resource) to the end point of the network (entrance to the consumer property). This energetic balance is formulated by the theorem of Bernoulli expressed as follow:

$$H_{initial} = H_{final} + J_{initial\text{-}final}$$

- where:

$H_{initial}$ - the energy at the initial point of network

H_{final} - the energy at the final point of the network

$J_{initial\text{-}final}$ - the total lost of energy between the initial point and the final point of the network

Generally, between the initial and final points of a water line, and because of topographical problems, we have to consider many particular points where there is change of slope, change of direction and/or obstacles. They are called knots. The distance between two successive particular points (knots) defined the length of a pipe section. If we note A and B the two successive knots, we can, by applying the Bernoulli theorem to the pipe section AB, write:

$$H_A = H_B + J_{A\text{-}B}$$

$$H_A = z_A + P_A + J_A$$

$$H_B = z_B + P_B + J_B$$

- where:

H_A, H_B: are the energy at, respectively, point A and point B

z_A, z_B: are the altitudes of, respectively, point A and point B

$J_{A\text{-}B}$: is the total lost of energy in the pipe section AB

J_A, J_B: are the singulars lost of energy due to contact with hydraulic accessory at, respectively, the points A and B

P_A, P_B: are the pressures at ,respectively, point A and point B

The total lost of energy $J_{A\text{-}B}$, is defined as the sum of the singular energy lost (J_A and J_B) and the linear energy lost between A and B ($j_{A\text{-}B}$). For every hydraulic accessory in the network corresponds a particular singular energy lost (floodgates, bends, diaphragm…). While for the linear energy lost there is many empirical formulas. They express generally the linear energy lost by the water inside the pipes as function of the diameter, the water flow, the conduit roughness and the nature of fabrication material. We can give here as example the following [14, 24]:

Blasius formula: $j = 7.77\ 10^{-4}\ Q^{1.75}\ D^{4.75}$

Scimemi formula: $Q = 48.8\ D^{2.68}\ j^{0.56}$

Bresse formula : $D = 0.32\ Q^{0.4}\ j^{-0.2} + 0.005$

Where Q is the debit (m^3/s), j is the linear lost of energy (m/m), D is the pipe diameters (m). So we have to know the altitude of the particular points (from topographical measurements and level curves maps) and the pressure needed to assume the distribution of water to all the consumers which must be superior to the highest manometeric level at the streamside. By applying the Bernoulli theorem for every pipe section we can deduce all the needed parameters for the hydraulic network conception. I must signal here that there is many models and soft wares that can be used and that they are established from the precedent reasoning and formulas[1, 12, 14, 24, 33].

2.4 Equations and models for the consumer level

In the conception of a hydraulic network, we must begin by defining the consumers. This means calculating the amount of water they need and the minimum pressure permitting to lead water to the consumer at the highest manometeric level now and in the future.

As said above, there are three categories of consumers depending on their activities: agricultural activities, industrial activities and services activities.

2.4.1. For the agricultural activities

The amount of water to lead is that needed by the plants in the field and by field in the region for all vegetal speculations that exist. There is many models permitting to estimate the water needed by plants as function of the physiological characteristics of every specie (leaf area index, sap flow, stomatal resistance), soils types (texture, structure, permeability, porosit), climatic parameters (solar radiation, temperature, precipitation, evaporation, transpiration, heat) and the economical and demographic evolution by region. Their use is possible and it depends on the precision asked. We present here a simple and general formula permitting to calculate the amount of water needed by plants in the field [7, 14, 24, 34] :

$$Q = K_c * \ ETP$$

- where:

Q : amount of water needed

K_c: cultural coefficient that depends on the types of plants and soils

ETP: potential evapotranspiration

For the water needed by plants in the future, it can be evaluated as function of demographic evolution, the sort of tolerant vegetation to install as food, the type of industrial culture to implant, the evolution of the agro-alimentary industry and the climatic change. So we must know the economical and political orientations for the durable development by region and we have to utilize the agricultural maps, land-use plan, the data basis for vegetations characteristics, the gene banks, climatic data basis, models for plants transpiration, biosphere models, circulation and climatic models [24-28]

2.4.2. For the industrial activities

The amount of water needed depend on the type of product and the different process used inside the industry. So we must do multi audit studies to evaluate the real need. We can give here some examples of water needed by sort of industry: for the textile industry (cotton tissue) we need 4500 l/kg, for dairy industry we need 10 l/l milk, for the paper industry we need 222 – 330 m/t, for the sugar industry we need 3000 l /t.

For the future, the water needed is evaluated as function of the orientation of the durable development axis by region, census studies, economic plan, the technology evolution and the market demand. We can intervene here to advice about what industry to install in what region after studying the water circuits.

2.4.3. For the service activities

The amount of water needed here is that to consume as potable water. It depend on the number of residents by region, their requirement in comfort, their evolution in the future.

We have to use the census studies and the statistical models to evaluate the change in the future. They are generally based on the following equations [14, 28, 33]:

- For the demographic evolution we have:

$$P_y = P_{y0} (1 + \tau)^{y - y_0}$$

- where:

P_y: is the population number for the year (y)

P_{y0} : is the population number for the reference year (y_0)

τ: is the population evolution rate

- For the consumption evolution we have:

$$C_y = C_{y-1} (1 + \Gamma)^n$$

- where:

C_y : is the water consumption for the year (y)

C_{y-1}: is the water consumption for the year (y-1)

n: number of years for which we estimate the consumption

Γ : consumption evolution rate

2.5. Representation of data on numerical support

We will identify here the data processing support to use in order to make the link between data bases, maps, models and equations established and to show the results in graphics or tables formats and files. So we can evaluate the actual situation, take decision and intervene at moment. Also, we can foresee the future state for the resources, networks and consumers, propose the adequate scenarios for management, rehabilitation and development. After propounding the necessaries equations, mathematical models, software and maps to use, we can organize the data we dispose in the form of a data conceptual model, data logical model data physical model and land numerical model. The GIS tools' to utilize are:

- ENVI 4.2: The environment for visualizing image to elaborate the land numerical model
- ArcView GIS 3.2 to digitalize the information layers from maps, to organise the data tables and to make the link with mathematical models and software of calculus
- Power AMC Designor 6.0 for data arrangement
- Epanet 2.0 for hydraulic calculus and pressure verification
- Hydrogen as interface of link with hydraulic calculus
- 3D Analyst and Spatial Analyst for spatial and 3 D analysis and representation

The same reasoning and the same tools were used for the region of SILIANA as we will present later.

3. APPLICATION OF THE MODELLING APPROACH TO THE REGION OF SILIANA

3.1. Model conception

Depending on the quantity of items and data basis we dispose (input), the thematic maps/plans to realise (output) are those representing the different information layers needed in decision making (proposing a solution scenario).

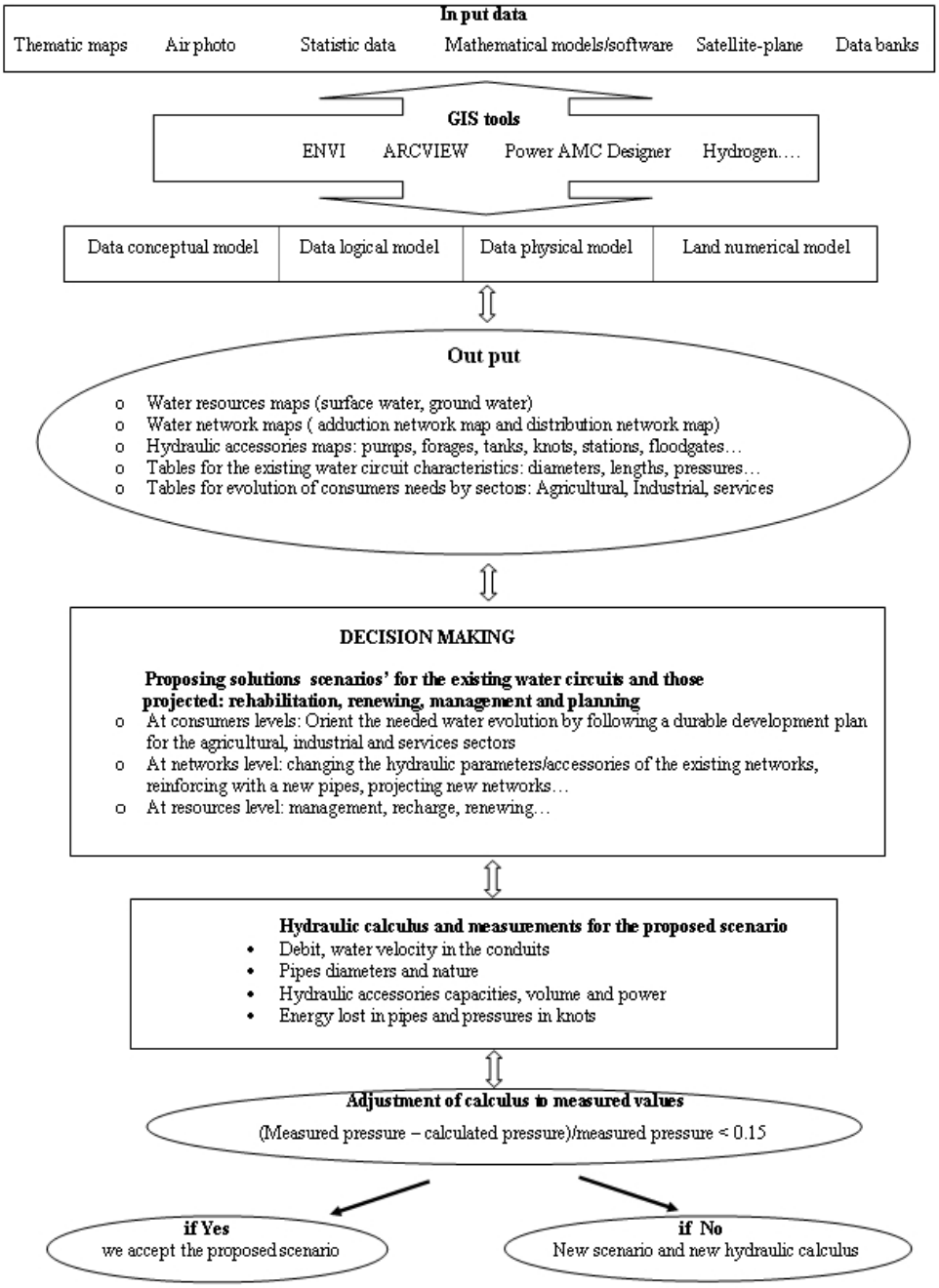

Fig. 2 A block diagram for the modelling methodology

We list here the following: geologic maps, hydrographic network maps (primer, secondary, tertiary rivers), topographic maps for the land numerical model, soil type maps, land use maps, lakes and table water maps, grounds waters maps, adduction and distribution network maps, hydraulic accessories maps, knots maps. After, we have to make the hydraulic calculus for the proposed scenario in order to accept or refuse it. **Fig. 2** proposes the schematic representation of the modelling methodology.

A first application of the model has been done to the region of SILIANA in the West-North of Tunisia. The purpose is to model the geographic and hydraulic potable water circuit for SILIANA region. At the beginning we have identified, limited and evaluated the water resources available (surfaces resources, ground water resources, artificial resources). After, by using the necessaries equations, mathematical models and software, we have diagnosed the different adduction/distribution networks that exist and calculated their hydraulic parameters: the lengths of pipes, diameters, pressures and debit at different positions, types and capacities of hydraulic accessories, risk of conduits corrosions and filling, risks of pipe damage and water leak. Experimental verification of calculus have been done by measurement of pressure and water flow at different positions (GPS, pressure captors, debit captors). Finally we have distinguished all types of water consumers in the region, calculated their water needs and determined those connected to the water network and those who are not yet connected.

3.2. Results and discussions

By using the GIS tools and the brut data we dispose, we have established the multi-layers information map'. It is presented in **fig.** 3. It comports the following items: Topographic layer (level curves), hydrographic networks layer (first, secondary and tertiary river lines), geologic layer, forages for ground water resources layer, adduction network layer, hydraulic accessories layers. After using the necessary calculus and the existing databases we have numerated the actual water distribution network. It is shown in figure 4. From figure 3 and figure 4 we can deduce the next results:

- Geographical situation:

The zone studied is referenced by these coordinates: Longitude 2° 27' 33"; Latitude: 71° 18' 16", Altitude: 400 and 460 mNGT

Table 1. ***Characteristics of the water resources***

Forages	Altitude (mNGT)	Static level (mTN)	Debit (l/s)
Ramlia	438	-17.1	16
Siliana II Bis	457	-19	26
SI 14	438.62	-25	20
Elguabel	449.4	-20	25

- Water resources:

Because the flow in the rivers networks is irregular, the region is supplied by water only from ground water sheet via 4 forages. Here with their characteristics (**Table 1**):

- Adduction and distribution water networks:

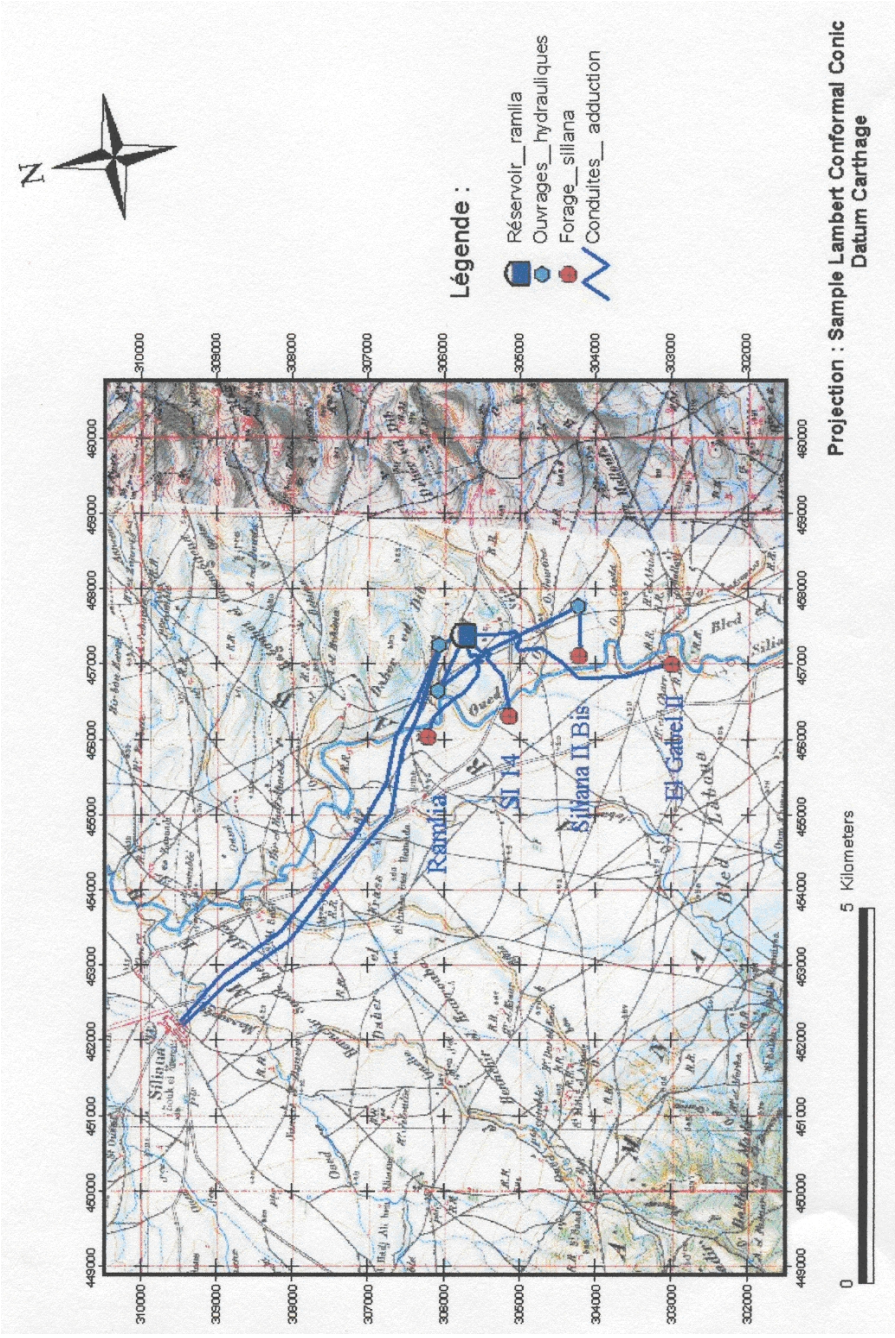

Fig. 3 A thematic maps representing the superposition of the following information layers: topographic maps, geologic map, rivers network map, adduction network map, hydraulic accessories map, water resources map (forages)

We have verified the hydraulic calculus for the existing adduction/distribution networks and we have measured at different points of the network the pressures, debits and conduits diameters for the adjustment. **Table 2** offers the main features:

Table 2. ***Characteristics of the adduction/distribution networks***

	Sections number	Nature	Mean diameter	Total mean length
Adduction network	7	AC, PE, Fonte	200 – 315 mm	25189 m
Distribution network	718	AC, PE, PVC	80 – 250 mm	248038 m

From **fig. 4**, we remark that there is five pressure levels in the network: less than 20 m, between 20 and 40 m, between 40 and 50 and more than 60m. But for the majority of knots, the pressure is between 20 and 40 m which is a threshold fixed by the Tunisian National Society of Water Distribution for each subscriber. The singular knots for which we have recorded a feeble pressures are between 10 and 20 m and those for which we have registered high pressures are not too distant from 50 m and for both the problem is due to the subscriber altitude. So there is no real problems of pressure actually (year 2007).

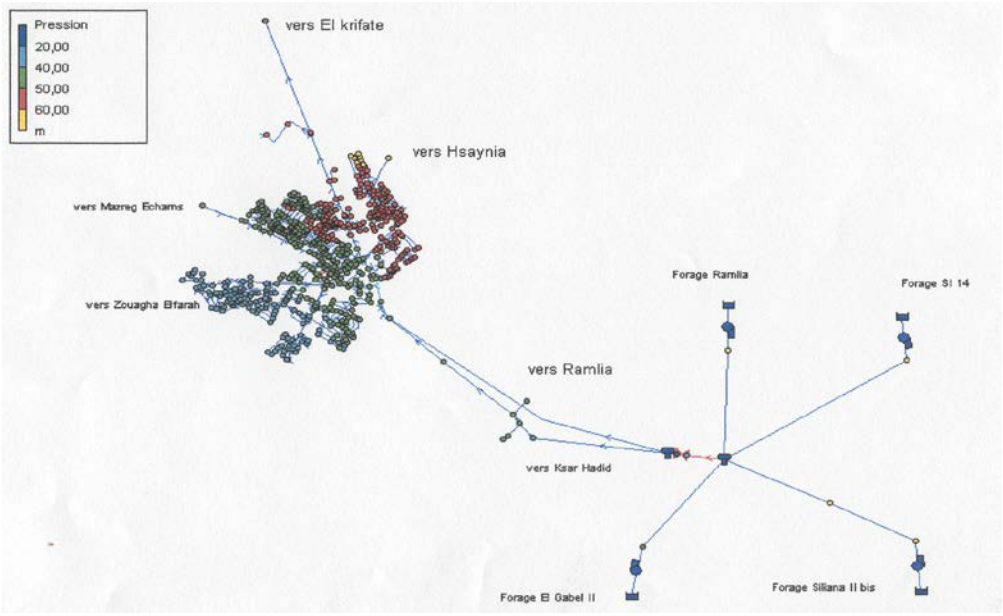

Fig. 4 ***Modelling of pressure in the adduction/distribution networks for the year 2007***

- For the consumer:

We have evaluated the amount of water needed by the consumers actually and in the future, those who are connected and those who are not yet connected. The principal results

for the evolution of the daily volume for consumption and resources from 2006 to 2030 are propounded in **table 3**.

Table 3. ***Evolution of the daily water volume for the consumptions and resources***

year	2006	2010	2015	2020	2025	2030
Water needed	3964 m^3/day	4401 m^3/day	5022 m^3/day	5738 m^3/day	6563 m^3/day	7515m^3/day
Resources	7517 m^3/day	7517 m^3/day	7517 m^3/day	7517 m^3/day	7517 m^3/day	7517m^3/day

We can say that the existing resources assume the needed water until the year 2030. So we must think to a new resource or to a technical solution like recharging the existing resources or installing a new storage tank.

Fig. 5 shows the calculated prevention of the pressure and the energy lost for the year 2030 in the adduction and distribution networks. We notice a high pressures (much more than 50 m) and an important lost of energy (more than 3 m/km) in the pipes of the high zone. We can suggest here many scenarios of rehabilitation. After hydraulic modelling, we have proposed to replace many conduits sections by others with a diameter varying between 400 and 500 mm. The new pressure and energy lost repartitions for the year 2030 appears in figure 6. For all the pipes, we notice a net amelioration for the pressure (between 20 and 50 m) and for the energy lost (between 1 and 2 m/km). The same reasoning and simulation could be effectuated for different paces of time (daily, monthly, yearly…) in order to take the appropriate decision at time.

4. CONCLUSION

In this work we have presented a general modelling approach to manage a water circuit. It permits to test, evaluate and monitor both the actual and future situations of the water resources, the adduction/distribution network pipes and the consumers water need. It offers the means and tools to take momentarily the appropriate decision about the adequate solution and scenario for management, rehabilitation, renewal and projection. It provides an interface to connect mathematical models and software to thematic maps and data basis. The out puts of this approach could be easily analysed, interpreted and brought up to date and the making decision process could be ran for a moment. A first application of this model has been done for the potable water circuit of SILIANA region in the West-North of Tunisia. After exploiting the disposed data basis and thematic maps and by applying the mathematical models established, we have diagnosed the actual water circuit till the year 2007, we have estimated the yearly evolution of water volume for both resources and consumers and we have calculated the pressure repartition in all the knots of the adduction/distribution network until the year 2030. We have realised that the resources could not satisfy the consumers after 2030 and that we will have pressures insufficiencies in many zones of the network. We have proposed a scenario of rehabilitation, we have calculated the new hydraulic parameters of the network propounded and we have prescribed the correspondent map. We notice a net amelioration. A work for applying and ameliorating this approach was started. We will try to use new and more precise models for estimating the water needed and its evolution for the agricultural, industrial and services

sectors. For that matter, we will apply the approach to other regions for which we dispose the adequate data [1, 12, 28, 30, 31].

ACKNOWLEDGEMENTS: The authors would like to thank all the members (Director and Technicians) of the National Society for Water Exploitation and Distribution of Tunisia for their collaboration.

REFERENCES

Allani W. (2008), *Etude du plan Directeur du réseau d'alimentation en eau potable du complexe Gaafour* , Thesis for Studies End supervised by M.H.Sellami, E.S.I.E.R ,Medjez El Bab, Tunisia. 128 pages.

Andrew J. Tyre, Brigitte Tenhumberg and C. Michael Bull. (2006), *Identifying landscape scale patterns from individual scale processes*. Ecological Modelling, Volume 199, Issue 4, pp..442 – 450.

Annequin R. and Boutigny J. (1978), *Sciences Physiques. Mécanique I*» 4ème Edition, Librairie Vuibert, 128 pages.

Austin, M. (2007), *Species distribution models and ecological theory: A critical assessment and some possible new approaches*. Ecological Modelling, Volume 200, Issue 1-2, pp. 1 – 19.

Baroudi I., Lehlou A.A., Bayoumi A. (2006), *"Managing water demand policies, practices and lessons from the Middle East and North Africa forums"* Arab Scientific Publishers, Arabic version 98 pages.

Battaglia M. and Sands P., (1997), *Modelling site productivity of Eucalyptus globules in response to climatic and site factors.* A.J.P.P. 24, pp. 831-850. Berbigier.P, Bonnefond .JM., (1995. Measurement and modelling of radiation transmission within a stand of maritime pine (Pinus pinaster Ait). Ann. Sci. For. 52, pp. 23-42.

Burose D., et al., (2002), *Atmospheric Modeling and Integration between Meteorology and Hydrology*. G.L.W.A. German Programme on Global Change in the Hydrological Cycle. Status Report, pp.111-115.

Callister W.D. (2001), *Science et Génie des Matériaux*, Modulo Editeur. 5ème édition. 781 pages.

10- Ciret C. and Henderson-Sellers A., (1997b), *Sensitivity of global vegetation models to present-day climate simulated by global climate models*. Global Biogeochemical Cycles., vol. 11, pp. 415-434.

Cowling SA, Field CB., (2003), *Environmental control of leaf area production: implications for vegetation and land-surface modeling.* Global Biogeochemical Cycles, 17, pp. 1–14.

Chron A., (2008), *Etude du réseau d'alimentation en eau potable du complexe Soliman : Diagnostic et perspectives d'amélioration*, Thesis for Studies End, E.S.I.E.R ,Medjez El Bab, Tunisia. 84 pages.

Dimitrios Schizas and George Stamou., (2007), *What ecosystems really are—Physicochemical or biological entities?*. Ecological Modelling, Volume 200, Issues 1-2, pp.. 178-182.

Ennabli N. (2001), *Les circuits Hydrauliques*, Edition Universitaire de la Tunisie, I.N.A.T., 51 Chapters, 700 pages.

Frank Ewert. (2004), *Modelling Plant Responses to Elevated CO2: How Important is Leaf Area Index?* Annals of Botany, vol. 93, pp. 619-627.

Gilles F. (1997), *L'agriculture dans la nouvelle économie mondiale,* Presses Universitaires de Farnce. 379 pages.

Graham D. Farquhar, Susanne von Caemmerer, and Joseph A. Berry., (2001), *Models of Photosynthesis*, Plant Physiol., Vol. 125, pp. 42-45

Granier A. and Loustau D., (1994), *Measuring and modelling the transpiration of a maritime pine canopy from sap-flow data*. Agricultural and Forest Meteorology. 71, 61-81.

Heike Lischke, Niklaus E. Zimmermann, Janine Bolliger, Sophie Rickebusch and Thomas J. Löffler. (2006), *Tree Mig: A forest-landscape model for simulating spatio-temporal patterns from stand to landscape scale.* Ecological Modelling, Volume 199, Issue 4, pp. 409 – 420.

Henderson-Sellers A., McGuffie K., Zhang L. and Gross C., (1995), *Sensitivity of global climate model simulations to increased stomata resistance and CO2 increases*. J. Clim. 8, pp. 1738-1756.

Joseph L. Eastman, Michael B. Coughenour and Roger A. Pielke, Sr., (2001), *The regional effects of CO2 and landscape change using a coupled plant and meteorological model*. Global Change Biology, Vol. 7, issue 7 page 797.

Monserud R. A., Tchebakova N.M. and Leemans R., (1993), *Global vegetation change predicted by the modified Budyko model*. Climatic Change. Vol. 25, pp. 59-83.

Omrane M.N. (2001), *The principal rules for maps establishment*, Centre d'Edition Universitaire de la Tunisie, Arabic version 238 pages.

Punmia B.C and Ashok J., (1998), *Enironmental Engineering 2. Waste Water Engineering*, Laximi Publications (P) LTD. 23 Chapters; 660 pages.

Sellami M.H. et Sifaoui M.S. (1999), *Modelling solar radiatif transfer inside the oasis : Experimental validation*, Journal of Quantitative Spectroscopie and Radiative Transfer, juin 1999, 63/1 pp 85-96.

Sellami M.H. et. Sifaoui M.S. (2003), *Estimating transpiration in an intercropping system: measuring sap flow inside the oasis*, Agricultural Water Management 59, 191-204

Sellami M.H. et Sifaoui M.S. (2008), *Modelling of heat and mass transfer inside a traditional oasis. Experimental validation*, International Journal of Ecological Modelling; 210, 144-154.

Sellami M.H., (2008), *A scientific guide for agricultural water management and biodiversity conservation inside the North African oasis*, Chapter In: Agricultural Water Management Research Trends. ISBN 978-1-60456-159-3. Editor: Magnus L. Sorensen © 2008 Nova Science Publishers.

Sellers P.J., Mintz Y., Sud Y.C. and Dalcher A., (1986), *A simple biosphere model (SiB) for use within general circulation models. Journal of the Atmospheric Sciences*, 43 (6), pp. 505-531.

Sithom H. (1999), *The personalities of Tunisian Geographical Regions*, Edition universitaire de la Tunisie. Arabic version, 333 pages.

Tantich J.R. (1989), *Water in Palestine. Political and economical geographic study*, Jamahiria Edition House, Arabic version, 304 pages.

Tournebize R. and Sinoquet H., (1995), *Light interception and partitioning in a shrub/grass mixture*, Agricultural and Forest Meteorology. 72, 277-294.

Trabelsi I. (2008), *Modélisation hydraulique et géographique du réseau d'eau potable de la ville de Siliana,* Thesis for Studies End, supervised by M.H.Sellami, E.S.I.E.R ,Medjez El Bab, Tunisia. 107 pages.

Varlet-Grancher C., Bonhomme R., Sinoquet H., (1993), *Crop structure and light microclimate. Characterization and applications*, Editions INRA, Paris. pp. 518.

UTILISATION DES SYSTEMES D'INFORMATION GEOGRAPHIQUE ET DU MODELE DRASTIC POUR L'EVALUATION DE LA VULNÉRABILITÉ DES EAUX SOUTERRAINES DANS LA PLAINE DE BERRECHID, MAROC

A. Aït Sliman[1], A. Fekri[2], N. Laftouhi[1], K. Taj-Eddine[1]

ABSTRACT: A GIS based drastic model for assessing groundwater vulnerability in shallow aquifer in berrechid area, Morocco. During the last years, groundwater quality has been deteriorated in many parts of Morocco due to agricultural expansion, solid waste disposal and industrialization. This study presents an assessment of the vulnerability of Berrechid aquifer. The study of vulnerability involves evaluating the sensitivity of the resource of any kind of polluting elements emerging from soil surface and focusing on the physical characteristics of the area in question. GIS and model DRASTIC was used to assess vulnerability. The results got show that the area studied consists of three categories of vulnerability, higher DRASTIC index appear in areas when water is shallow and in areas not protected by quaternary clays, namely north, north-west and south-east parts of regions studied. While areas with low vulnerability are located, where clay is thicker and water deeper.

Keywords: *Berrechid-Maroc ; Groundwater vulnerability ; DRASTIC model; GIS*

RESUME:
Au cours des dernières années, la qualité des eaux souterraines s'est détériorée dans de nombreuses régions du Maroc à la suite de l'expansion de l'agriculture, l'élimination des déchets solides et de l'industrialisation. Cette étude fait état de l'évaluation de la vulnérabilité de l'aquifère de Berrechid. L'étude de la vulnérabilité consiste à évaluer la sensibilité de la ressource à toute forme de polluant introduit à partir de la surface du sol en se basant sur les propriétés physiques du milieu. La méthode DRASTIC couplée à un SIG a été appliquée afin d'évaluer la vulnérabilité de ce système aquifère. Les résultats montrent que la zone d'étude se décline en trois classes de vulnérabilité, les indices DRASTIC les plus élevés apparaissent au niveau des zones de faible profondeur de la nappe et au niveau des zones non protégées par les argiles quaternaires, soit dans les parties nord, nord-ouest et sud-est de la région étudiée. Tandis que les zones moins vulnérables sont situées dans les secteurs où l'épaisseur d'argiles de recouvrement est importante et la nappe plus profonde.

Mots clés : *Plaine de Berrechid, Vulnérabilité des eaux souterraines, Model DRASTIC, SIG, Maroc.*

1. INTRODUCTION

Actuellement, le Maroc est soumis à de nombreuses tractations quant aux modes de production agricole et industrielle. Elles semblent avoir de multiples effets négatifs sur l'environnement et sur l'harmonie sociale au sein des milieux ruraux. Etant conscients de la problématique actuelle et souhaitant savoir quels pourraient être les outils permettant de

[1] *Université Cadi Ayyad, Faculté des Sciences Semlalia Département de Géologie, BP.2390 Marrakech Maroc.*
[2] *Université Hassan II Mohammedia, Faculté des sciences ben M'Sik, Casablanca Maroc*

gérer et de protéger les ressources en eaux souterraines à l'échelle régionale, nous avons cherché à étudier la vulnérabilité intrinsèque des eaux.

La cartographie permettant d'identifier la vulnérabilité des eaux souterraines à la contamination correspond à un type de carte hydrogéologique spécialisée répondant à un besoin particulier et visant un public varié. Ce sont des cartes schématiques réalisées dans le but d'aider la prise de décision pour l'aménagement du territoire. Elles peuvent combler des besoins d'inventaire et guider les organismes de réglementation pour assurer une gestion globale de l'ensemble de la ressource en eau souterraine d'un territoire. Les intervenants dans le secteur de l'eau et leurs partenaires peuvent donc les utiliser pour se donner les moyens de mieux comprendre les dynamiques écologiques et par conséquent d'assurer la protection des nappes phréatiques (*Aller et al., 1987*).

L'objectif principal de cette étude est l'évaluation de la vulnérabilité de l'aquifère en utilisant le modèle DRASTIC (Aller et al., 1987) et la combinaison des données des calques hydrogéologiques dans le SIG (Depth of water, net Recharge, Aquifer media, Soil media, Topography, Impact of vadose zone and hydraulic Conductivity.)

2. CONTEXTE D'EVALUATION : PLAINE DE BERRECHID

Cette étude s'inscrit dans le cadre du projet PAGER/Settat, qui vise parmi ses activités la caractérisation régionale du système aquifère de la plaine de Berrechid couvrant une superficie de 1500 km2. Le terrain est caractérisé par un relief généralement plat, limité au Sud et au Sud Est par le plateau de Settat, à l'Est et au Nord Est par l'oued Mellah, à l'Ouest et au Nord Ouest par les affleurements Primaires et au Nord par la nappe de la Chaouia Côtière (**Fig. 1**).

Les formations du secteur d'étude sont principalement d'origine sédimentaire, d'âge Quaternaire et Plio-quaternaire et occupent toute la plaine. Ces formations reposent en discordance sur les formations sédimentaires du Crétacé et du Permo-Trias et sur les schistes Primaires. L'aquifère est constitué (ABHBC, 2003) principalement de formations de grés dunaires et calcaires lumachélliques, l'épaisseur varie de 0 m aux périphériques Est et Ouest à 40 m au centre. La recharge de l'aquifère se fait principalement dans ces zones marginales. Ces dépôts sont recouverts par endroit par des argiles dont l'épaisseur peut atteindre environ 50 m; argiles qui

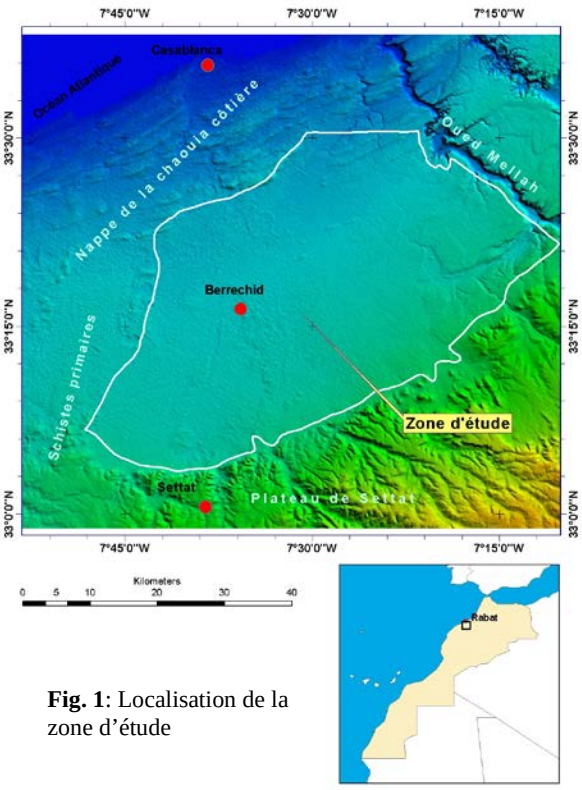

Fig. 1: Localisation de la zone d'étude

forment les plus importantes accumulations de dépôts quaternaires offrant une protection naturelle à l'aquifères pliocène.

Les zones où l'épaisseur de sédiments est plus faible (moins de 5 m) ou les secteurs où les dépôts quaternaires sont surtout formés de sables constitueraient des zones plus vulnérables à l'infiltration de polluants. C'est dans ce contexte qu'une étude de vulnérabilité s'avère intéressante pour savoir dans quelle mesure les zones à plus forte vulnérabilité constituent un danger pour la ressource en eau souterraine.

3. DONNEES ET METHODOLOGIE

Il n'existe pas de méthode absolue d'évaluation de la vulnérabilité des nappes d'eau souterraine, mais plusieurs méthodes d'estimation de la sensibilité des aquifères à la pollution ont été mises au point (*Murat et al., 2000*). Dans le cadre de la présente étude, la méthode DRASTIC a été choisie pour évaluer la vulnérabilité des eaux souterraines (*Aller et al., 1987*).

La méthode DRASTIC est une approche empirique et repose sur les hypothèses suivantes : le territoire d'application couvre plus de 0,4 km^2, le contaminant se propage dans le milieu à partir de la surface du sol par infiltration des précipitations et le type de contaminant n'intervient pas sur le degré de vulnérabilité. La méthode est basée sur l'évaluation de sept paramètres : profondeur de la nappe (D), recharge (R), type d'aquifère (A), type de sol (S), topographie (T), impact de la zone vadose (I) et conductivité hydraulique (C). Pour chaque paramètre, la plage de valeurs possibles est subdivisée en différents intervalles et une cote est attribuée à chacun d'eux. Un indice de vulnérabilité ($I_{DRASTIC}$) est alors calculé en additionnant la contribution des sept paramètres, pondérée selon l'importance de chacun de ces paramètres dans l'évaluation de la vulnérabilité, à l'aide de l'équation :

$$\mathbf{I_{DRASTIC} = DwDr + RwRr + AwAr + SwSr + TwTr + IwIr + CwCr}$$

- *avec :*
w et *r* désignent respectivement le poids et la valeur de l'intervalle (cote) attribués à chaque paramètre.

Tableau 1. Les données utilisées pour l'élaboration des sept calques des paramètres DRASIC

no.	Type de données	Sources	Format	Date	Carte de sortie
1	Données des forages (niveau statique)	Enquête de terrain	Table	2009	Profondeur de l'eau (D)
2	Pluie efficace	ABHBC	Table	1972-2003	Recharge (R)
3	Données des forages (lithologie)	ABHBC	Table	1956-2003	Aquifère (A)
4	Carte du sol	Ministère de l'Agriculture	carte	1996	Sol (S)
5	Topographie	ftp://e0srp01u.ecs.**nasa**.gov	Raster	2005	Pente (T)
6	Données des forages (lithologie)	ABHBC	Table	1956-2003	Zone non saturée (I)
7	perméabilité	ABHBC	Table	2003	Conductivité hydraulique (C)

Aux fins d'interprétation, les valeurs possibles de l'indice DRASTIC sont subdivisées en huit intervalles ou classes (**Tableau 1**).Toutes les données pertinentes à la vulnérabilité des eaux souterraines ont été rassemblées, y compris, par exemple, la topographie, la géologie, l'utilisation du sol, hydrologie, hydrogéologie et les précipitations. Le logiciel ArcGIS® a été utilisé pour compiler les données géospatiales, pour calculer les indices drastiques, et pour générer la carte de vulnérabilité.

La qualité des cartes de vulnérabilité dépend, entre autres, des données et du traitement auquel elles ont été soumises. Ainsi, un examen minutieux des données doit être effectué afin de mettre en évidence l'information disponible et sa qualité. Dans le cas de la présente étude, l'intégration des résultats des enquêtes du terrain effectuées pendant l'hiver 2009 a complété la connaissance du territoire qu'avait permise la compilation des données existantes. Les jeux de données disponibles sont de types ponctuel, vectoriel et matriciel (**Tableau 1**). Aux fins d'application des méthodes d'évaluation de la vulnérabilité, le but du traitement des données est la transformation des données de types ponctuel et vectoriel en données matricielles ainsi que l'uniformisation du format des données matricielles.

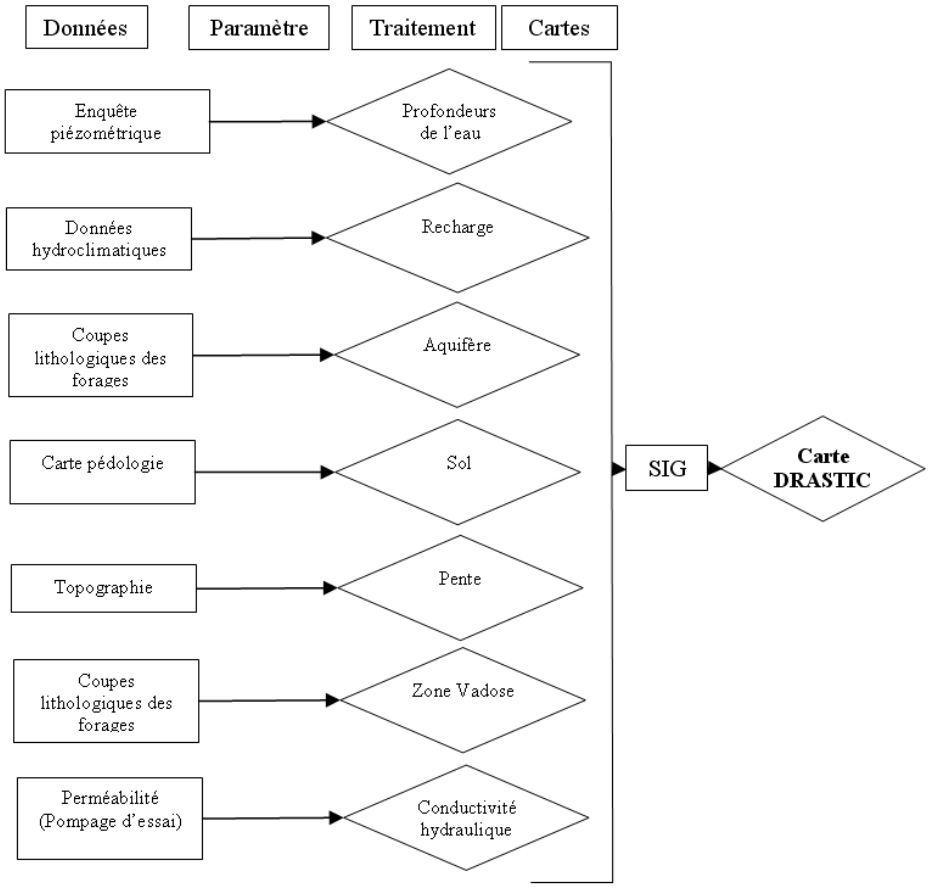

Fig. 2 Procédure d'élaboration de la carte de vulnérabilité selon la méthode DRASTIC

Pour atteindre ces objectifs, toutes les données disponibles et utiles pour évaluer la vulnérabilité ont été intégrées dans une *geodatabse* crée dans l'environnement ArcCatalog de ArcGis. Ces données vont subir par la suite une série de traitements permettant l'acquisition des cartes matricielles et paramétriques.

Le Model Builder d'Arctoolbox permet d'appliquer et de combiner l'ensemble des fonctions d'ArcGIS et de ses extensions. Les modèles de géotraitement ainsi créés sont une source d'économie et d'efficacité grâce à l'automatisation et au partage des processus.

4. ANALYSE DE SENSIBILITÉ

La Méthode DRASTIC utilise dans l'élaboration de la carte de vulnérabilité sept paramètres**.** Certains scientifiques affirment que la vulnérabilité des eaux souterraines peut être élaborée sans faire appel à tous ces paramètres (Barber *et al.*, 1993; Merchant, 1994). D'autres (Napolitano and Fabbri, 1996) sont allés dans le sens que les poids et les notes utilisées dans le modèle sont subjectives et qu'il n'y a pas de raison de ne pas douter de l'exactitude de l'indice de vulnérabilité ainsi élaboré, surtout en absence de preuve expérimentale. Afin de lever tous ces doutes, l'analyse de sensibilité du modèle a été effectuée.

Dans un premier temps les paramètres du model seront examinés en terme d'interdépendance et de variabilité (Babiker *et al.*, 2005; Rosen, 1994). Deux tests de sensibilité ont été effectués : « the map removal sensitivity analysis » introduit par Lodwick *et al.* (1990) et « the single parameter sensitivity analysis » introduit par Napolitano and Fabbri (1996).

Le 1er test permet d'identifier la sensibilité de la carte de vulnérabilité, en supprimant un ou plusieurs calques de la carte, il est calculé par l'équation suivante :

$$S = (|V/N-V'/n|/V)*100$$

- Avec :
S est la sensibilité mesurée exprimée en termes d'indice de variation.
V est l'indice de vulnérabilité DRASTIC non perturbé
V' est l'indice de vulnérabilité perturbé
N et n est le nombre de calques utilisés dans le calcul des indices.

Le test de « the single parameter sensitivity analysis » a été élaboré dans l'objectif d'évaluer l'impact des paramètres DRASTIC sur l'indice de vulnérabilité. Il est basé sur la comparaison entre les poids effectifs attribués aux paramètres d'entrés avec les poids théoriques. Les poids effectifs sont calculés par l'équation suivante :

$$W = (PrPw/V)*100$$

-Avec :
W poids effectif d'un paramètre.
Pr et *Pw* sont les poids et la valeur de l'intervalle (cote) attribués à ce paramètre.
V est l'indice de vulnérabilité DRASTIC.

L'application de l'analyse de sensibilité nécessite une base de données bien structurée et un SIG capable de manipuler un très grand nombre de tables. Pour éviter d'analyser le grand nombre de pixels dans la zone d'étude (**38 227**), l'idée de la sous-zone unique

présentée par Napolitano et Fabbri (1996) a été utilisée. Elle est définie comme un ou plusieurs polygones avec une combinaison unique *Di Ri Ai Si Ti Ii* et *Ci* des pixels, avec *Di Ri Ai Si Ti Ii* et *Ci*, sont les notes des sept paramètres utilisés pour calculer l'indice de vulnérabilité, et $1 < i < 10$. La fonction « combine » de ArcGis 9 à été utilisée afin d'identifier les sous zones. La combinaison des différents calques a donné lieu à 67 sous zones dont seulement 52 seront prises en considération (> à 10 pixels) dans l'analyse statistique.

5. RESULTATS ET DISCUSSIONS

Paramètres DRASTIC et vulnérabilité de l'aquifère

Profondeur de la nappe. L'évaluation du paramètre profondeur de la nappe à été élaboré par l'interpolation des données sur le niveau de l'eau mesuré lors de l'enquête piézométrique effectuée dans le cadre de cette étude en février 2009. L'interpolation est effectuée par la méthode du Krigeage ordinaire. Une classification de chaque pixel est ensuite effectuée en fonction des systèmes de cotation de la méthode DRASTIC (Tableau 2). La carte de la profondeur de la nappe montre que ce paramètre décroît graduellement du SE vers le NW, et les bordures Nord West sont les zones les plus susceptibles d'être contaminées (**Fig. 3 a**)

Recharge. Les valeurs du paramètre «recharge» sont acquises par l'application des polygones de Thiessen sur les données des pluies efficaces, ces valeurs sont classées, pour chaque pixel, en fonction du système de cotation de la méthode DRASTIC (Tableau 2). La carte matricielle élaborée montre que la recharge représente une note DRASTIC homogène sur tout le territoire d'étude (**Fig. 3 b**).

Type d'aquifère. La couverture limoneuse, et les terres végétales, rendent plus difficile la reconnaissance géologique de l'aquifère de la zone d'étude, l'élaboration de la carte matricielle du type d'aquifère a été basée, essentiellement, sur l'interprétation et la corrélation ente plus 200 forages réalisés dans la région d'étude. Ces corrélations montrent que l'aquifère est formé essentiellement par des faciès sableux et alluvionnaires. Par conséquent, la zone saturée offrira un déplacement très important des polluants (**Fig. 3c**).

Type de Sol. La carte des types de sol de la zone étude a été élaborée par la digitalisation de la carte pédologique nationale, réalisée par le Ministère de l'Agriculture et de la Mise en Valeur Agricole. Le paramètre «type de sol» est obtenu en répertoriant les différents types de sol en fonction des classes pédologiques définies par la méthode DRASTIC (Tableau 2). La carte matricielle montre que le secteur d'étude, présente trois classes de textures, prédominées par la texture argileuse et limono sableuse (**Fig. 3d**).

Topographie. Pour le paramètre topographie, une carte matricielle du pourcentage de pente est réalisée à partir du model numérique de terrain SRTM (ftp://e0srp01u.ecs.nasa.gov) et les valeurs de pente qui sont attribuées aux pixels sont en fonction du système de cotation de la méthode DRASTIC (**Tableau 2**). La carte matricielle ainsi élaborée, monte la prédominance des pentes inférieures à 2° (**Fig. 3e**).

Impact de la zone vadose. Le processus d'évaluation du paramètre Impact de la zone vadose, est basé sur l'interprétation des coupes lithologique des forages. La corrélation montre que la zone non saturée est constituée essentiellement par les faciès argileux et par du sable et gravier avec des passages d'argile (**Tableau 2**). La carte matricielle élaborée selon le système de cotation DRASTIC, met en évidence, la répartition de la zone vadose,

selon deux classes. Les zones couvertes par les argiles, correspondant aux zones les plus protégées (**Fig. 3f**).

Conductivité hydraulique. La carte du paramètre conductivité hydraulique, est établie par l'exploitation directe des données des pompages d'essai, ces données sont complétées par les sorties du modèle mathématique réalisé déjà dans la région (ABHBC, 2004). Ces données sont transformées en carte matricielle par Krigeage. Une classification de chaque pixel est ensuite effectuée en fonction des systèmes de cotation de la méthode DRASTIC (**Tableau 2**). La carte matricielle ainsi élaborée mis en évidence des perméabilités importantes dans la zone axiale de l'aquifère (**Fig. 3 g**).

Tableau 2. ***Les paramètres du modèle DRASTIC***

1. Profondeur de l'eau				2. Recharge			
Ranges (m)	Note (Dr)	Indice (Dr)	Poids	Ranges (mm)	Note (Dr)	Indice (Dr)	Poids
4.5 – 9	7	35	5	0 - 50	1	4	4
9 -15	5	25					
15 – 23	3	15					
23 – 30	2	10					
> 30	1	5					

3. Aquifère				4. Sol			
Aquifère	Note (Dr)	Indice (Dr)	Poids	Soil	Note (Dr)	Indice (Dr)	Poids
Sable et gravier	8	24	3	Limons sableux	6	12	2
				Limons silteux	3	6	
				Argiles	1	2	

5. Pente				6. Impact de la zone vadose				7. Conductivité hydraulique			
Ranges (degré)	Note (Dr)	Indice (Dr)	Poids	Ranges	Ratings (Dr)	Index (Dr)	poids	Ranges	Note (Dr)	Indice (Dr)	Poids
0 - 2	10	10	1	Sable et gravier avec passage d'argile	6	30	5	> 9.5	10	30	3
2 - 6	9	9		Silt et argile	3	15		5 – 9.5	8	24	
6 - 12	5	5						3.3 - 5	6	18	
								1.5-3.3	4	12	

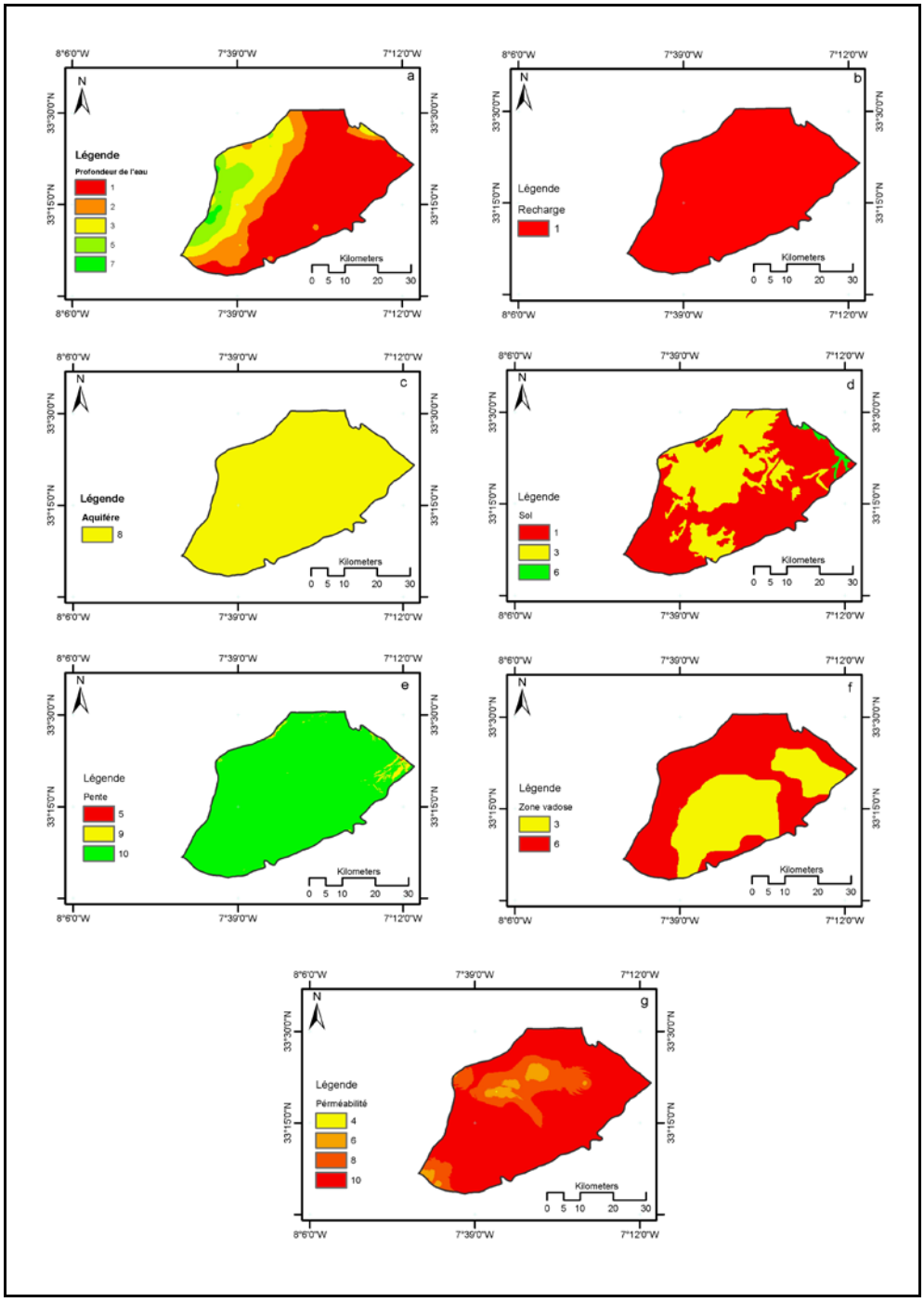

Fig. 3 Cartes utilisées pour l'élaboration de la carte de vulnérabilité

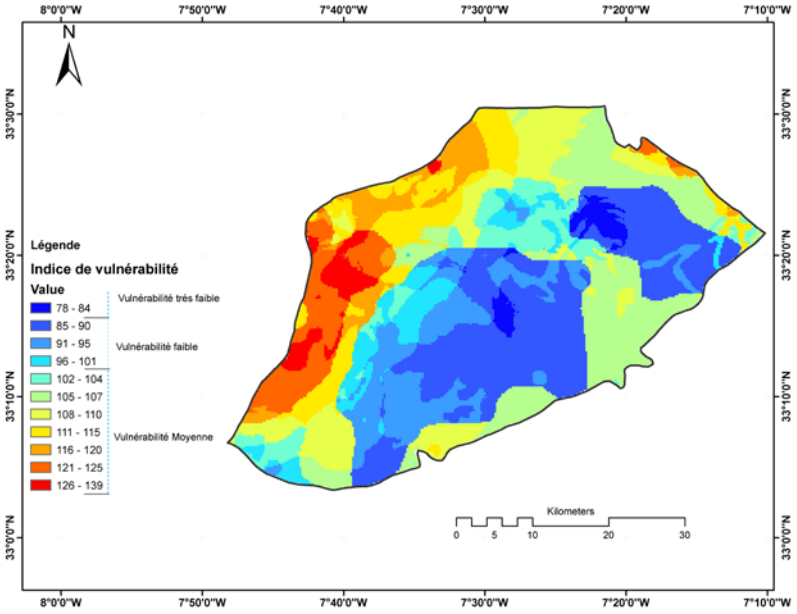

Fig. 4 Carte de vulnérabilité de la plaine de Berrechid (Modèle DRASTIC)

Sensibilité du modèle DRASTIC

Le tableau 3 illustre les données statistiques sommaires des sept paramètres utilisés pour calculer l'indice DRASTIC dans la plaine de Berrechid. L'analyse des moyennes montre que le plus grand risque de contamination des eaux souterraines de la plaine de Berrechid est favorisé par les paramètres « aquifère, Topographie et conductivité hydraulique » (dont les moyennes sont respectivement : 8, 9.98 et 9.47). Cependant le paramètre « zone non saturée » participe avec un risque modéré (moyenne est 4.76), et les paramètres profondeur de la nappe, sol et recharge favorise un risque faible (moyennes : 1.87, 1.09 et 1).

Le coefficient de variation montre que la grande contribution aux variations de l'indice de vulnérabilité est due au paramètre « Profondeur de la nappe » (CV : 70,59%). Les paramètres « Sol, zone non saturée et conductivité hydraulique » montrent une contribution moyenne (CV : 58,60%, 31,09% et 11,7%), Cependant la topographie, la recharge et l'aquifère représente une contribution à la variation de l'indice de vulnérabilité faible à nulle (CV : 1.6, 0 et 0).

Tableau 3. ***Les statistiques sommaires des paramètres DRASTIC***

	D	R	A	S	T	I	C
Min	1	1	8	1	5	3	4
Max	7	1	8	6	10	6	10
Moy	1,87	1	8	1,86	9,98	4,76	9,47
SD	1,32	0	0	1,09	0,16	1,48	1,048
CV	70,59%	0,00%	0,00%	58,60%	1,60%	31,09%	11,07%

Le test "Map removal sensitivity analysis"

Les résultats du test « Map removal sensitivity analysis », basé sur la suppression d'un ou plusieurs paramètres à la fois, sont représentés dans **les tableaux 4 et** 5. L'analyse statistique de l'indice de variation (mesure de sensibilité) est appliquée aux sous zones dont le nombre de pixels est supérieurs à 10 (52 sous zones). **Le tableau 4** illustre la variation de l'indice de vulnérabilité comme résultat d'élimination d'un seul paramètre DRASTIC. Il est clair que la suppression de l'un ou l'autre paramètre abouti à une grande variation de l'indice de vulnérabilité. Les paramètres « aquifère, topographie, zone non saturée et la conductivité hydraulique » sont considérés les plus responsables en terme de variation de l'indice (moyennes 11.01, 11.29, 10.51 et 11.11). La vulnérabilité semble être très sensible à la suppression du paramètre « topographie », bien que ce paramètre soit considéré théoriquement moins important (poids 1).

Dans le tableau 5, sont présentées les variations de l'indice de vulnérabilité dues à la suppression à la fois d'un ou de plusieurs paramètres. La suppression des calques était basée sur les résultats du test « Map removal sensitivity analysis » illustrés dans le tableau 4. Le calque ayant une faible influence sur la variation de l'indice de vulnérabilité est préférentiellement éliminé. La suppression de l'un ou l'autre paramètre ne montre aucune tendance dans les moyennes de l'indice de variation, ce qui signifie que tous les paramètres sont, sans exception, nécessaires pour le calcul de l'indice de vulnérabilité.

Tableau 4. ***Les statistiques du test « Map removal sensitivity analysis***

Paramètres enlevé	Variation index (%)		
	Min	Max	Moy
D	9	11	10,10
R	9	10	9,90
A	11	11	11,01
S	9	11	10,16
T	11	12	11,29
I	10	11	10,51
C	10	12	11,11

Tableau 5. ***Les statistiques du test « Map removal sensitivity analysis »***

Paramètres utilisés	Indice de Variation (%)		
	Moy	Min	Max
T, C, A, I, S and D	9,90	9,30	10,34
T, C, A, I and S	9,45	8,64	10,58
T, C, A and I	8,88	7,55	9,84
T, C and A	8,63	6,59	9,86
T and A	9,93	6,59	11,55
T	12,83	9,16	14,29

Le test "Single-parameter sensitivity analysis"

Après la mise en évidence de l'importance des sept paramètres dans le calcul de l'indice de vulnérabilité par le test **«Map removal sensitivity analysis»**, dans cette section l'objectif de l'application du test **«Single-parameter sensitivity analysis»**, est de compléter et confirmer les premiers résultats. Ce test consiste à faire une comparaison entre les poids théoriques et les poids effectifs des paramètres. Le tableau 6 représente les résultats du test, et montre que les paramètres « aquifère, topographie, zone non saturée et la conductivité hydraulique », sont les paramètres influençant beaucoup la vulnérabilité car leurs poids effectifs moyens (respectivement 38%, 47%, 23% et 41 %) sont supérieurs à leurs poids théoriques, sans négliger les autres paramètres surtout le paramètres « sol ».
Avec le test «Single-parameter sensitivity analysis», il est clair que les paramètres « aquifère, topographie, zone non saturée et la conductivité hydraulique » du modèle DRASTIC influencent beaucoup la vulnérabilité dans le secteur d'étude, raison de plus d'aller chercher d'autres informations de détails pour ces quatre facteurs.

Tableau 6. ***Les statistiques du test « Single-parameter sensitivity analysis »***

Paramètre	Poids théorique	poids théorique (%)	Poids effectif %		
			Moy	Min	Max
D	5	21,7%	11	4	26
R	4	17,4%	5	4	6
A	3	13,0%	38	30	38
S	2	8,7%	13	4	13
T	1	4,3%	47	35	64
I	5	21,7%	23	14	32
C	3	13,0%	41	26	56

CONCLUSION

Dans cette recherche, une tentative a été faite pour évaluer la vulnérabilité de l'aquifère de la plaine de Berrechid. Nous avons utilisé, pour cet objectif, le SIG moyennant la méthode DRASTIC. En effet, Le SIG a fourni un environnement efficace pour les analyses et une forte capacité de manipulation de grandes quantités de données spatiales.

Les sept paramètres du modèle ont été construits, classés et codés en utilisant l'outil SIG et ses fonctionnalités. L'indice de vulnérabilité, qui est défini comme étant une combinaison linéaire des facteurs, a été facilement calculée. Le SIG a fourni également des possibilités d'analyse de sensibilité de la carte de vulnérabilité ainsi élaborée.

La répartition spatiale des classes de vulnérabilité de la nappe de Berrechid *est globalement de faible à moyenne vulnérabilité*, les indices DRASTIC les plus élevés sont localisés essentiellement dans les zones NW de la ville de Berrechid. Ceci est expliqué par la faible profondeur du plan d'eau, la nature des formations lithologiques perméables relatives dans cette zone et les pentes faibles. Les zones à vulnérabilité très faible occupent les bordures NE et E de la zone d'étude. Cette faible vulnérabilité est due à l'éloignement

du plan d'eau, à la couverture argileuse formant une protection naturelle et à la faible perméabilité de l'aquifère.

L'analyses statistique et l'analyse de sensibilité ont mis en évidence, l'importance de tous les paramètres drastique dans l'élaboration du model finale de vulnérabilité du secteur d'étude, avec une prédominance et une influence des paramètres « aquifère, topographie, zone non saturée et conductivité hydraulique ».

Cette étude a produit un outil très précieux pour la gestion et l'aménagement, car il donne des indications complètes sur la vulnérabilité des eaux souterraines. Etant donné que la plaine de Berrechid dotée d'une importante zone industrielle, connaît aussi une forte activité agricole et est considérée la seule source d'eau pérenne de la région. Ainsi, il est dorénavant grand temps que les intervenants dans le secteur de l'eau (décideurs, utilisateurs, etc.), de l'environnement et les autorités locales, utilisent cette approche de la vulnérabilité comme outil d'aide à la décision, et réfléchissent sur des solutions et des aménagements favorisant une protection durable de cette ressource.

REMERCIEMENT

Cette étude s'inscrit dans le cadre du Projet PAGER/Settat (Province de Settat, Maroc), mené en partenariat entre la Coopération Italienne (Ambassade d'Italie au Maroc) et l'Université Cadi Ayyad de Marrakech (UCAM, Maroc). Nous remercions le projet PAGER qui a bien voulu mettre à notre disposition toutes les données et les moyens nécessaires à cette étude.

REFERENCES

Agence du Bassin Hydraulique du Chaouia Bouregureg, (2003), Rapport Etude de modélisation de la nappe de Berrechid, 49-72.

Aller, L., Bennet, T., Lehr, J. H., Petty, R. J., & Hacket, G. (1985). *DRASTIC: A standardized system for evaluating groundwater pollution using hydrological settings. Ada, OK, USA*: Prepared by the National water Well Association for the US EPA Of.ce of Research and Development.

Al-Adamat, R. A. N., Foster, I. D. L., & Baban, S. N. J. (2003). *Groundwater vulnerability and risk mapping for the Basaltic aquifer of the Azraq basin of Jordan using GIS, Remote sensing and DRASTIC*. Applied Geography, 23, 303–324.

Altine A., Gang C. (2008) A *GIS-based DRATIC model for assessing aquifer vulnerability to pollution in west Mitidja: Blida city, Algeria*. Research Journal of Applied 3 (7): 500–507.

Al-Hanbali, A., Kondoh, A. (2008). *Groundwater vulnerability assessment and evaluation of human activity impact (HAI) within the Dead Sea groundwater basin*, Jordan. Hydrogeology Journal. 499-510.

Amharref, M., Al. (2008). *Cartographie de la vulnérabilité à la pollution des eaux souterraines : Application à la plaine du Gharb (Maroc)*. Journal of Water Science. p. 185-199.

Anwar, M., Prem, C. C., & Rao, V. B. (2003). *Evaluation of groundwater potential of Musi River catchment using DRASTIC index model*. In B. R. Venkateshwar, M. K. Ram, C. S. Sarala, & C. Raju (Eds.), Hydrology and watershed management. Proceedings of the international conference 18– 20, 2002 (pp. 399–409). Hyderabad: B. S. Publishers.

Babiker, I. S., Mohammed, M. A. A., Hiyama, T., & Kato, K. (2005). A GIS-based DRATIC model for assessing aquifer vulnerability in Kakamigahara Heights, Gifu Prefecture, central Japan. Science of the Total Environment, 345, 127–140.

Barber, C., Bates, L. E., Barron, R., & Allison, H. (1993). *Assessment of the relative vulnerability of groundwater to pollution: A review and background paper for the conference workshop on vulnerability assessment.* Journal of Australian Geology and Geophysics, 14(2/3), 1147–1154.

De Dieu Bazimenyera J., Zhonghua T. (2008). *A GIS-based DRATIC model for assessing groundwater vulnerability in shallow aquifer Hangzhou-Jiaxing-Huzhou Plain*, China. Research Journal of Applied 3 (8): 550–559.

Dixon, B. (2004). *Prediction of groundwater vulnerability using integrated GIS-based neuro-fuzzy techniques*. Journal of Spatial Hydrology (St. Petersburg), 4(2).

Dixon, B. (2005). *Groundwater vulnerability mapping: A GIS and fuzzy rule based integrated too*l. Applied Geography, 25(4), 327–347.

Dixon, B., Scott, H. D., Dixon, J. C., & Steele, K. F. (2002). *Prediction of aquifer vulnerability to pesticides using fuzzy rule-based models at the regional scale*. Physical Geography, 23, 130–152.

Durbude, D. G., Naradrajan, N., & Purandara, B. K. (2003). *Mapping of ground water quality parameters in GIS environment*. In B.

Etienne Ake, G., Al. (2009). *Contribution des Méthodes de Vulnérabilité Intrinsèque DRASTIC et GOD à L'Etude de la Pollution par les Nitrates dans la Région de Bonoua (Sud-Est de la Côte d'Ivoire)*. Research Journal of Applied 3, 157–171.

Fazal, S. (2005). *Urban expansion: A threat to crop land. A GIS based study of Aligarh City, India*. In J. Livingstone (Ed.), Trends in agriculture and soil pollution research (pp. 191–204). New York: Nova Science Publications.

Hamza, M.H., Added, A., Ben Mammou, A., Abdeljaoued, S., Rodrý´ guez, R., 2004. *Evaluation de la vulnérabilité a la pollution potentielle par les pesticides, de la nappe côtière alluvionnaire de la plaine de Metline-Ras Jebel-Raf Raf, Nord-Est tunisien, selon la méthode DRASTIC appliquée par les systèmes d'information géographique*, La Houille Blanche Revue Internationale de l'Eau 2004/ 2005, 86–94.

Hamza, M.H., Al. (2007). *A GIS-based DRASTIC vulnerability and net recharge reassessment in an aquifer of a semi-arid region (Metline-Ras Jebel-Raf Raf aquifer, Northern Tunisia)*. Journal of Environmental Management 84. p.12-19.

Lodwick WA, Monson W, Svoboda L., (1990), *Attribute error and sensitivity analysis of map operations in geographical information systems: suitability analysis*. Int J Geogr Inf Syst; 4(4):413– 28.

Murat V., Martel R., Michaud Y., Therrien R., (2000). *Étude comparative des méthodes d'évaluation de la vulnérabilité des aquifères à la pollution : application aux aquifères granulaires du piémont laurentien, Québec*. 53e conférence canadienne de géotechnique, 15-18 Octobre 2000, Montréal. 411-418.

Mohammadi, K., Niknam, R., Majd, V. J. (2008). Aquifer vulnerability assessment using GIS and fuzzy system: a case study in Tehran–Karaj aquifer, Iran. Environ Geol. 437-446.

Napolitano P, Fabbri AG., (1996), *Single-parameter sensitivity analysis for aquifer vulnerability assessment using DRASTIC and SINTACS HydroGIS 96: application of geographical information systems in hydrology and water resources management*. Proceedings of Vienna Conference. IAHS Pub, vol. 235,. p. 559–66.

Rahma, A. (2008). *A GIS based DRASTIC model for assessing groundwater vulnerability in shallow aquifer in Aligarh, India*. Applied Geography 28. p. 32-52

Rao, R. Venkateshwar, M. K. Ram, C. S. Sarala, & C. Raju (Eds.), (2002), *Hydrology and watershed management*. Proceedings of the international conference 18– 20, (pp. 568–577). Hyderabad: B.S. Publishers..

.

APPLICATION OF GPS SENSING TECHNIQUE FOR SUN-EARTH COUPLING STUDIES

W. Suparta[1]

ABSTRACT:
Sun-Earth coupling studies is one channel projections to explain certain physical mechanisms of how solar activity exerts their influences on severe weather or changes in global climate towards improved global forecast models and space weather prediction. Measurements of atmospheric precipitable water vapour (PWV) and the ionospheric total electron content (TEC) at Husafell, Arctic vantage point from satellite at L-band signals using the Global Positioning System (GPS) technology is addressed in this paper. In this study, the lower and upper atmosphere represented by PWV and TEC respectively, is employed as a climate and solar activity parameters to enlighten Sun-Earth connection. The diurnal variation of both PWV and TEC, and its possible connection to the solar activity during the September 2008 campaign are presented. Day-to-day changes both parameters and their diurnal cycle pattern measured in this region were clearly influenced by solar activity, indicates a reasonable coupling between upper and lower atmosphere.

Keywords: *GPS, sun-earth, PWV, TEC, Husafell station (HUSA)*

1. INTRODUCTION

The Sun is the source of the energy that causes the motion of the atmosphere and their energy clearly drives the Earth's climate and controls the weather. Recently, it has been convincingly demonstrated that the results of investigations of solar radiation and cosmic ray flux variability, primarily the impact of solar radiation variations and space weather processes on the troposphere, stratosphere, especially mesosphere, lower thermosphere and lower ionosphere, and also the role of solar activity in determining long-term trends of the greenhouse effect origin (*Lastovicka, 2005*). These studies clear showed that the variable solar radiative and particle output affects the Earth's atmosphere and climate in many fundamental ways. One key element that is very often taken as evidence of a response is the similarity of the periodicities between solar activity indices and different meteorological parameters. However, understanding solar influences on climate requires improved specification of both the amplitudes and timescales of solar radiative output changes on climatological timescales and the climate sensitivity to small insulation changes (*Lean and Rind, 1997*). Moreover, weather changes in space and ground were very fast, hazardous and strong damage not only on economic, socio-politic, geographic and ecological even it can be changing mentality of human activities. It is paramount important to study the extreme weather or super geomagnetic storms in short-term measurements, which can be used representatively to understand the solar response to climate forcing. The comprehensive understanding of its distribution will have a major impact on a better planning of resources as well as the key to a better understanding of global climate change (*Suparta et al., 2009*), and quantifying their impats can be useful for analysis and modeling purposes.

Sun-Earth coupling due to its transport energy that occurs throughout the Sun-Earth system is fundamental science to space physics, aerospace and satellite communication,

[1] *Institute of Space Science (ANGKASA), Universiti Kebangsaan Malaysia (National University of Malaysia), 43600 Bangi, Selangor Darul Ehsan, Malaysia, Email: wayan@ukm.my*

meteorology and terrestrial climate cycle, and affecting human being in the humanosphere. Water vapour in the lower atmosphere is one of the most fundamental of all climate variables due to its importance as a natural resource and its role in atmospheric dynamics. High or low frequency natural variability of water vapour is an important factor in global change issues because it may obscure human influence on hydrologic variations. It is possible to measure the influence of solar activity on water vapour variability inferred from ionospheric disturbances by using GPS measurements, as GPS signals were very sensitive to the water vapour and ionospheric effects. GPS receivers that originally installed for geophysical and geodetic applications can also be used to measure the atmospheric precipitable water vapour (PWV) with high spatial and temporal resolution in the atmosphere. GPS sensing technique has also been widely used as a powerful tool to accurately measure the ionospheric total electron content (TEC). Therefore, one parameter used to study Sun-Earth coupling by means of GPS observation is PWV and TEC, respectively. This is possible because GPS receivers gather energy from direct signal that travels between the GPS satellite and receiving antenna on the ground. Measurements of both parameters at L-band frequencies are encouraged and promising technology complement for future satellite missions.

Here, we demonstrate the measurements of atmospheric PWV and ionospheric TEC using GPS sensing. The work aimed at measuring the PWV content and vertical TEC based on the GPS receving system. For this work, the observation and investigation are made at the Northern hemisphere Arctic vantage point. North pole as a part of IPY (International Polar Year) programme and is a great challenge to provide suitable platforms for the studies of solar-climate relationship and provides a key to explain the causes of change and prediction of the global climate system. Additionally, the challenge to conduct atmospheric research at Arctic would provide us the opportunity to study the upper and lower atmospheric science and investigate the ionosphere and water vapour characteristics at the Northern Hemisphere. Hence results from polar-equatorial-polar can be comparable. For this purpose, GPS signals for a week period during the September 2008 campaign is processed to determine the vertical TEC (VTEC), and the PWV is determined by using same GPS signals and surface meteorological data. At same period, the possibility influences of solar activity as external factors driving of weather change to the PWV variation on daily analysis are also presented. The analysis is supported by a GPS Spider and GNSS QC softwares to easy processing and checking quality of the data.

2. METHODOLOGY

Iceland at North Pole is the second largest island in Europe, located at geographic coordinates between latitude 63°24´N and 66°33´N and between longitude 13°30´W and 24°32´W, touches the Arctic Circle. In this work, Husafell station (HUSA) situated at a distance of about 135 km from Reykjavik center was chosen as a observation site to study the Sun-Earth coupling. Beside study changes in global climate and the effect of geospace environment on ionospheric activity in both hemispheres, HUSA location is one observatory for an ideal studies on conjugacy and non-conjugacy effects, since its to have magnetic conjugate pair with Syowa station in the Antarctic region (South Pole). The location of HUSA is shown in Figure 1.

At HUSA, the measurements system employed for this work consists of a GPS receiving system and a ground meteorological system (so-called GPS PWV system). The system is shown in Fig. 2 with broadband meteorological sensors is collocated with GPS

receiver. The GPS was installed on 6 September 2008 under collaboration between Universiti Kebangsaan Malaysia (UKM) and National Institute of Polar Research (NIPR) and between UKM and Science Institute, University of Iceland (SIUI). It consists of a Leica GRX1200 Pro GPS reference station with a high performance permanent dual-frequency GPS receiver, a AT504 chock-ring antenna and a HP note book contains of a Leica GPS Spider (GPS reference station software) for data logging. The dual-frequency Leica choke-ring antenna was fully equipped by a dorne margolin with weather-protection radome. It was employed due to its improved their accuracy, more resistant to radio frequency (RF) jamming and it is exacting standards features in superior satellite tracking (GPS and GLONASS) at all elevation angles and superior multipath rejection with uncompromised phase center stability (<1 mm).

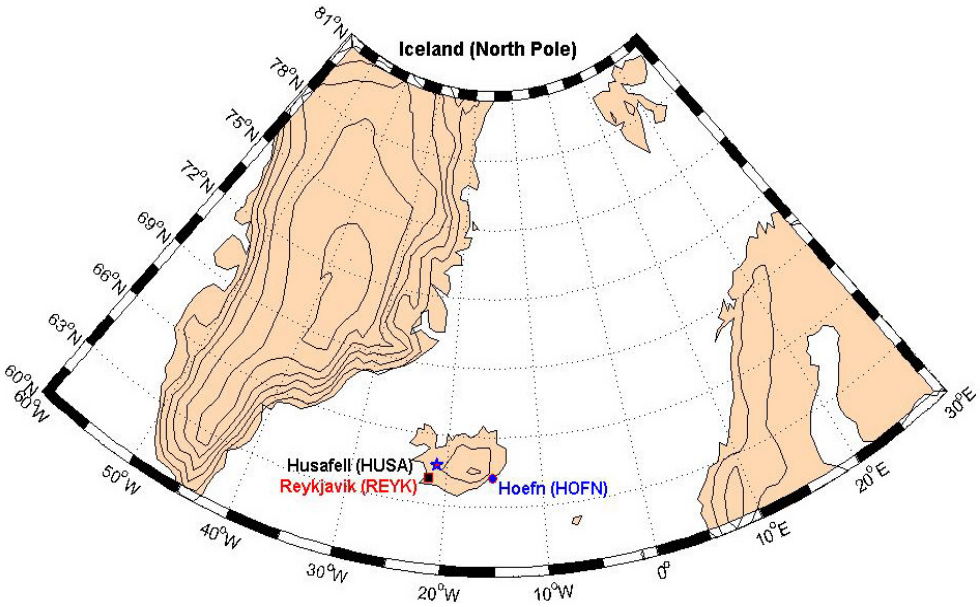

Fig. 1 Location of Husafell station (HUSA), Iceland (North Pole)

The ground meteorological system is employed the Paroscientific broadband MET4A sensors to accurately measure the surface pressure (in bar), air temperature (in degrees Celsius) and relative humidity (in percent). A site to install the GPS PWV system is at around 15 m Northwest at behind of farmer main house, or 3 m North from All Sky cameras antennas of NIPR. Both systems were fixed on the ground in a base pillar with a height of 5.20 m. In other word, the GPS station at HUSA is located at geographical coordinates 64.67°N latitude, 21.03°W longitude (Geomagnetic: 65.26°N, 67.04°W) with geodetic height of 220.20 m at sea level. As shown in the Fig. 2, the GPS receiver, meteorological system and the note book were housed inside the NIPR Husafell observatory. The GPS receiver was set to track GPS signals with a one-second sampling period and the cutoff elevation angle was set to 15° to maintain the quality of the data. The GPS receiver recorded the data in UT time, which Local Time (LT) at Husafell, Iceland is

equal to Greenwhich Mean Time (GMT) or UT time. The meteorological system was set logged at 1-min sampling period. The third surface meteorological measurements and the GPS signals is then used to determine the PWV. On the whole, the GPS PWV system is maintained by a farmer under SIUI coordination for all year round for a five years duration beginning from September 2008 to August 2013. At the moment, the collected data are sent by SIUI to the authors in CD or flash memory forms every three month.

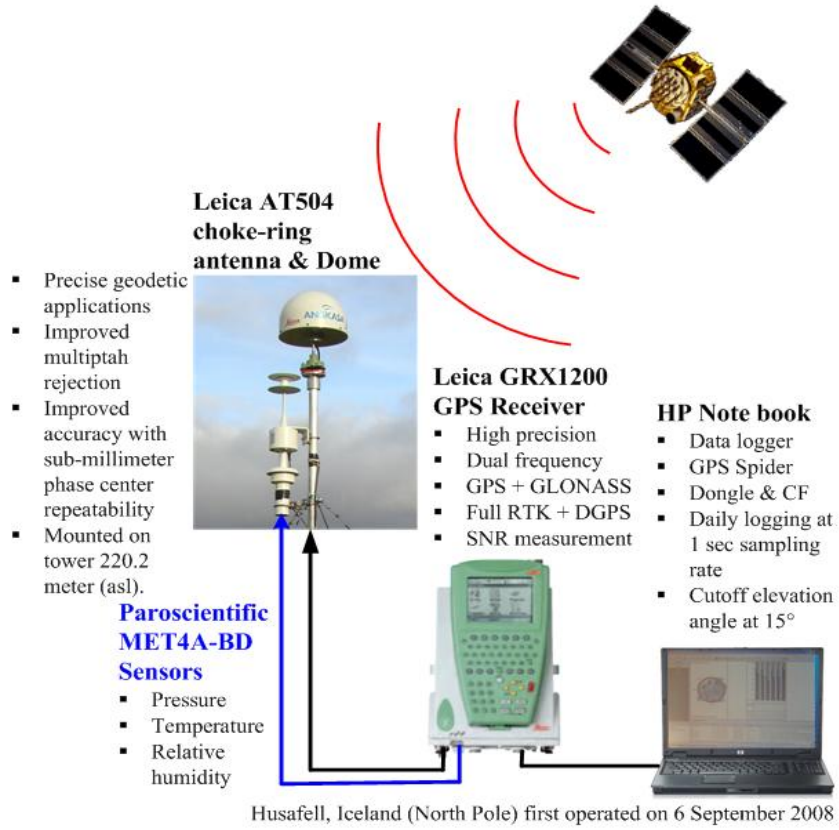

Fig. 2 Ground-based GPS PWV measurement system at Husafell, Iceland (North Pole)

Based on the GPS PWV setup, the data are collected and stored into three subdirectories. The first two subdirectories were created by Leica GPS Spider to store the raw data (in MDB format) and RINEX files. The last one subdirectory was created by meteorological system to store the surface pressure, temperature and relative humidity measurements. GPS signals were converted automatically into RINEX format using the GPS Spider routine developed by Leica Geosystems. Both MDB and RINEX files were set to 1-hour and daily saving, respectively to easier processing the data. The RINEX observation files are produced in Hatanaka format (d-file compression) and were processed with a 30 second average for purposes analysis. The surface meteorological data at this station are saved in 'Data Files' subdirectories. The data processing and analysis programs

to produce the PWV data developed by author were used Tropospheric Water Vapour Program (*TroWav*) which was written in Matlab (*Suparta, 2005*). The algorithms of the *TroWav* is weather-related signals delays-based to calculate the PWV. It includes satellite elevation angle, Zenith Tropospheric Delay (ZTD), Zenith Hydrostatic Delay (ZHD), Zenith Wet Delay (ZWD) and mapping function calculations. Detail calculation of PWV using the GPS meteorology and the models adopted, readers are referred to Suparta et al. (2008). The GPS PWV product at HUSA for this measurement is available at one-min interval. For monitoring of the ionospheric TEC along the path from satellite to the receiver, Slant TEC (STEC) measurements are taken from different GPS satellites observed at arbitrary elevation angles and is can be calculated by employing differential techniques. However, the entire effect of the integral over the electron density along the zenith direction is frequently corrupted by instrumental biases. Therefore, the absolute TEC determination due to the instrument time delay errors are corrected by employed CODE bias obtained from Bern university data center (*ftp://ftp.unibe.ch/aiub/CODE/*). Detail a method for calculating the absolute TEC can be found elsewhere (e.g. *Abdul Rashid et al., 2006*). The GPS TEC product at HUSA for this measurement is available at 30s interval.

3. RESULTS AND DISCUSSIONS

Geospace characterization on the possible teleconnection between the Sun and Earth's climate is conducted along the earth-satellite slant-path link medium at L-band frequencies measured from GPS signals. Based on these measurements, two major results presented here are lower atmosphere and upper atmosphere parameters, respectively. To ensure the PWV and TEC data is accurate enough to be used in global climate and space weather studies, both results are verified using the GPS data obtained from the nearby HUSA station: Reykjavik (REYK) and Hoefn (HOFN) stations. The ZTD results as a major component in PWV determination was validated with ZTD product at REYK (64.14°N, 21.95°W) and HOFN (64.26°N, 15.19°W). Both the ZTD were obtained from the CODE/AIUB (Center of Orbit Determination Europe/Astronomical Institute University of Berne, Switzerland) data center, as the DCB (Differential Code Bias) solution accessible for TEC. The PWV result at HUSA was compared with the PWV generated from NOAA Reanalysis. The analyses are presented as follows:

3.1 Assesment of ZTD

A ZTD parameter plays an important role in analyzing microwave space-geodetic measurements. The ZTD should be properly estimated for accurate PWV quantification. For this work, ZTD product from CODE/AIUB is employed to compare the ZTD result at HUSA. Figure 3 shows the superimposed their comparison in 2-hour average, together with the scatterplot of their relationship. ZTD value at HUSA (Fig. 3a) is ranging between 2.359 and 2.404 m with mean value of 2.38 m. It is lower than ZTD at HOFN (2.39~2.445 m) and REYK (2.364~2.430 m), however its variation seem almost similar pattern. The averages of ZTD different between the stations are about 4.5 cm, which corresponds to 7.0 mm of PWV (1 mm PWV equal to 6.4 mm ZTD). High and low of ZTD in that location constantly, is influenced by many complex factors such as regional weather patterns and local topographical conditions, affect the way that tropospheric patterns are formed and circulated. As seen on 7, 9 and 10 September, ZTD peaks occurred during afternoon is due to falling the air pressure associated with cloudy and heavy precipitation develops. Moreover, ZTD at HOFN on 9 and 10 September and ZTD at REYK on 7 September were

seen the highest due to stormy weather occurring along upward motion in the atmosphere through the North Atlantic Ocean. A moderate correlation between ZTD and ZTD_{CODE} with correlation coefficient of 0.67 is clearly seen in Fig. 3b, which are all significance at the 99% confidence level. Although both sites used to compare ZTD results were not close in Husafell region, their trend relationship tends to linear indicates a tropospheric event at that time not so much different.

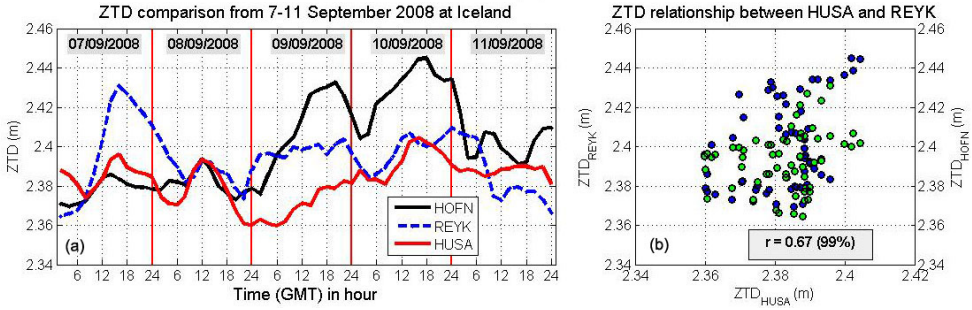

Fig. 3: The ZTD results at HUSA compared to the ZTD_{CODE} at HOFN and REYK for the period of 7-11 September 2008 and their relationships

3.2 Lower atmosphere results

Fig. 4 shows the day-to-day variation of lower atmosphere parameters during the campaign. Analysis results showed that the ZHD variation in **Fig. 4a** follows the surface pressure variation with a mean value of 2.234 m. The ZWD (Fig. 4c) as part component of water vapour in the atmosphere is about 11.09 cm, which follow the ZTD variation (**Fig. 4b**). The PWV content was observed high with a maximum value of 23.2 mm (~17 mm, on average). Their values were also comparable with PWV map spatially over Iceland region (see Fig. 5), which in daily mean, its value was ranged from 12.53 to 23.24 mm (17.34 mm, on average). The PWV uncertainty demonstrates high accuracy ranging from 0.47 mm to 1.72 mm for one-week campaign.

As shown in **Fig. 4d**, the consistency of GPS-derived PWV is fairly good with standard deviation errors were found to be 1.25 to 4.54 percent, which are all within 1~2 mm accuracy. The PWV value was twice bigger of about 5-10 mm compared to the PWV at Antarctica at same season. The high of PWV content in that area is due to the ocean current activity called the North Atlantic drift carries relatively warm waters along Iceland's shores. As a consequence, climatic conditions are relatively moderate across most of the island. Interesting to note that day-to-day PWV variation at HUSA is starting to increase at 11:00 GMT, maxima between 14:00 and 16:00 GMT and start to decrease at 17:00 GMT. On the other hand, their pattern was follows the Sun activity as surface temperature increased at those times. This pattern was quite different with day-to-day PWV variation in the Antarctic region as the weather rapidly changing over time. By comparing **Figs. 4b** and **4c** respect to the **Fig. 4d**, it closely the PWV variation was consistent influenced by both ZTD and ZWD. In Fig. 4d, the PWV pattern was shown a diurnal cycle, higher during dayside (the Sun activity is high) and lower during night-side (the Sun activity is low), indicates the PWV profiles at HUSA are strongly influenced by diurnal variation of slant path length of GPS satellites as well as solar activity.

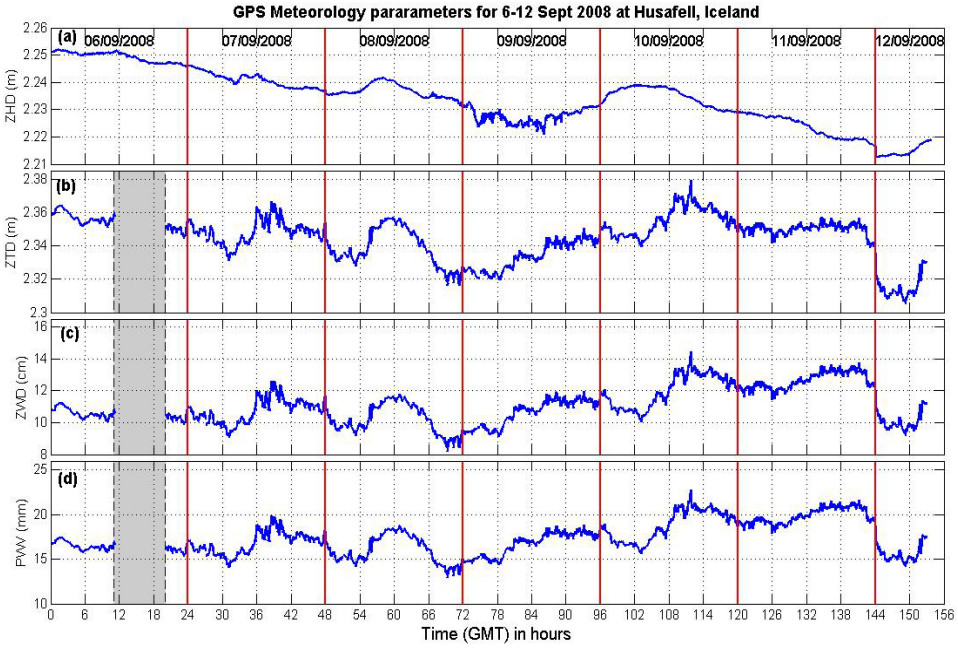

Fig. 4 Day-to-day lower atmosphere variation for the period from 6 to 12 September 2008 at Husafell, Iceland. The shaded area on 6 September is the time maintained of the GPS system.

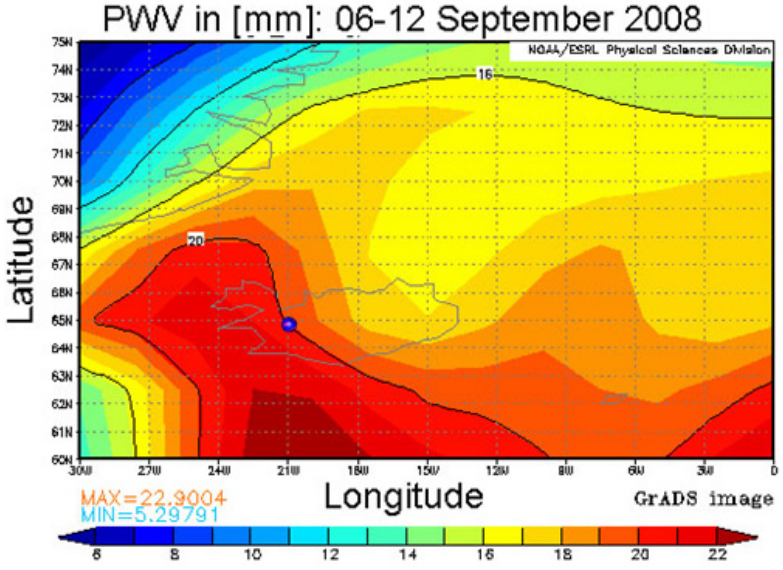

Fig. 5 PWV map generated from the NOAA/ESRL CPC Merged Analysis of Precipitation (CMAP). The globe marked in the figure is Husafell site at Iceland

3.3 Upper atmosphere results

Figure 6 shows the day-to-day ionospheric TEC variation from 6 to 12 September 2008 based on a one-minute average. The data almost exhibit a similar variation with VTEC value vary between 5.0 and 13.9 TECU (~10 TECU on average). All maximum peaks during the day were occurred at 17:00 GMT, except on 7 September 2008, it was distinctive and peaked at around 19:00 GMT. As shown in the figure, the unique minimum peak was occurred at 12:00 GMT for 9 and 11 September 2008, respectively with observed value of about 8.3 TECU. While for the other days at same time, the minimum peak was between 9.7 and 10.2 TECU (~0.5 TECU). The unique VTEC fluctuation value during the period is probably due to effects of atmospheric disturbance to the distribution of the ionization and recombination processes in the ionosphere along signal path-length. The TEC profiles showed in Fig. 6 was varies systematically with typical amount radiation received by the Sun, whereas ionization increases during sunlight atmosphere and decreases on the shadowed side.

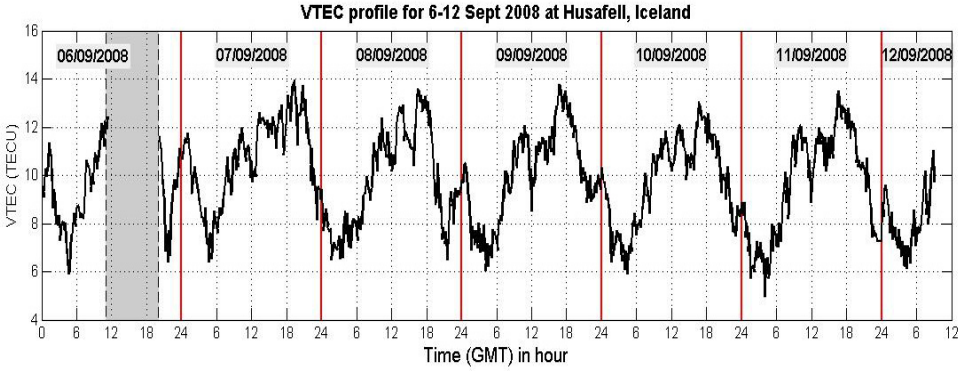

Fig. 6 Daily VTEC vartiation for the period of 6-12 September 2008 at Husafel, Iceland

Looked at hour-to-hour temporal and spatial variations of VTEC values presented in **Fig. 7**, it appear that VTEC value at HUSA point in the TEC map (10 to 30 degrees longitude and 60 to 70 degrees latitude) was very low starting from 00:00 GMT to 03:00 GMT and from 22:00 to 23:00 GMT (night-time) with value ranged between 0 and 4 TECU. The high VTEC values on the map (the Sun was very active) are seen starting from 08:00 to 12:00 GMT (dayside) with value ranging from 5 to 20 TECU. At usual days, the average peak TEC value was occurred between ~14:00 and 17:00 GMT, this phenomenon was known as the equatorial anomaly ('Fountain Effect'), which is a diurnal cycle activity of the Sun (e.g. Tsurutani et al., 2006). The high and low activity of VTEC variation along the signal path depends on the ionization and recombination of particles as well as on the transport processes in the ionosphere. The recombination process is dependent on the collision rate between the particles, and is thereby a function of density, pressure and temperature. The TEC value seen varies systematically with time of day, season and geographical position (latitude and longitude), and is affected by solar and geomagnetic activities (Rishbeth, 1997).

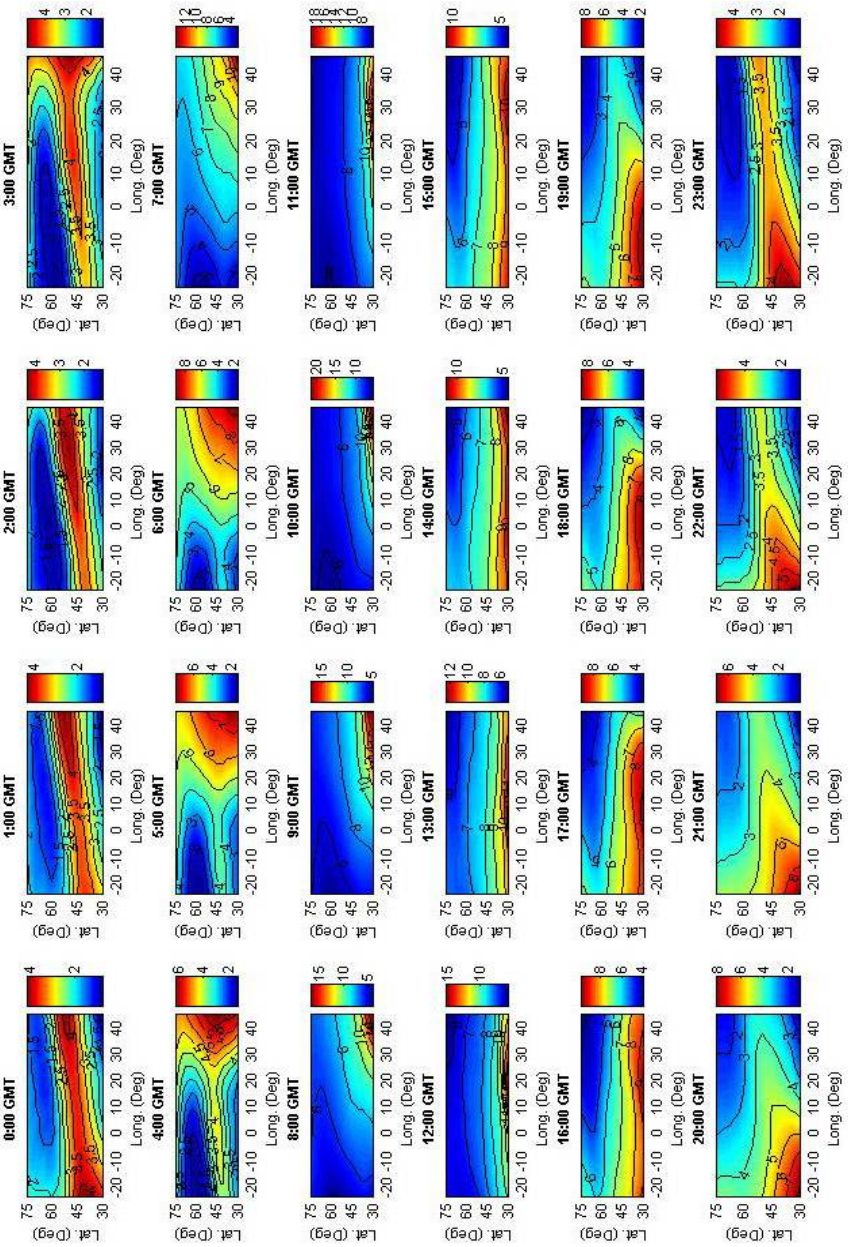

Fig. 7 VTEC values on TEC map for 10 September 2008

3.4 Preliminary coupling between lower and upper atmosphere

From **Figs. 5** and **6**, TEC variation was shown a clear diurnal cycle, following the Sun activities. The TEC profiles showed in **Fig. 7** is amount emission from the Sun, which is correlated with the number of sunspots and geomagnetic activities communicated via solar wind. Solar wind is a good conductor in supplying energy from the Sun to the Earth and it will be causes disturbances in the geomagnetic field as well ionospheric storm. From the figure, it is clear that the intensity of TEC affecting the Earth's atmosphere varies with typical diurnal rotation of the earth, so the strongest ionization is occurring on the dayside (sunlight atmosphere) of the Earth, while the shadowed (night) side is less affected by the radiation. The low measured of VTEC value during the campaign is associated with minimum state of 23rd solar cycle. Noticeable that ionospheric disturbances as well as TEC during the intense of geomagnetic field period most often take place during the active periods of the Sun's 11-year sunspot cycle. During the campaign period, the sunspot number obtainable from SEC NOAA was measured zero, except on 11 September 2008, which is available with value of 12.

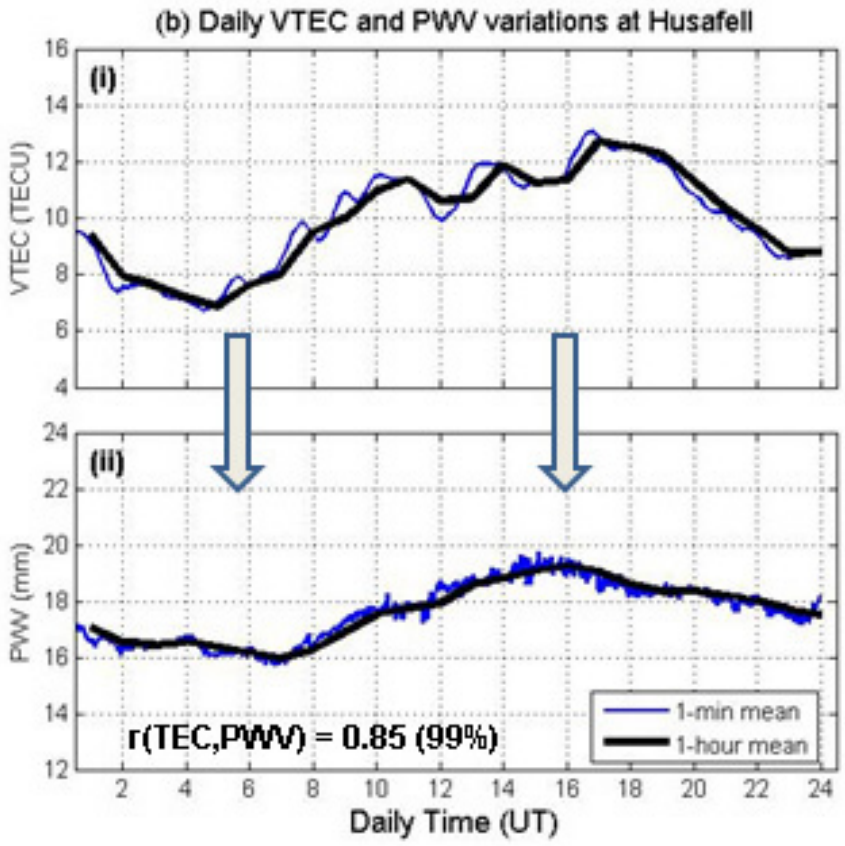

Fig. 8 Solar activity forcing on PWV

As shown in **Fig. 7b**, the PWV exhibits the usual diurnal variation of a minimum (TEC depletion) in the pre-sunrise hours (07:00 GMT), and a maximum (TEC enhancement) 15:00 GMT. The TEC rapidly rises from its morning minimum till about 11:00 GMT, decreased at 12:00 GMT and then continues to rise at a slower rate to reach maxima value at around 13:00 GMT, then again minimum between 14:00 and 16:00 GMT, it continues to be higher for the next few hours before reach the daytime peak level at around 17:00 GMT to develop a diurnal cycle. The unique daily variation was occurred between 11:00 and 16:00 GMT (~5 hrs), where VTEC variation was dropped slowly and tends to oscillates. On the other hand, by correlating **Figs. 7a** and **7b**, it can be seen that PWV is clearly forced by solar activity, although morphology PWV change sometimes does not follow the time TEC variation. On the other hand, there was lagged or leading time between TEC and PWV connection caused very complex phenomena occurred between the ionosphere and troposphere layers. Interestingly, a strong correlation or possible coupling between TEC and PWV with correlation coefficient of 0.85, which significance at the 99% confidence level was clearly observed. This indicated PWV amplifies warming, as the temperature rises and the ice melts, more Sun's energy absorbed by ground or ocean and magnifies the warming. However, this phenomena is interesting to be investigated further that how much the contribution of coupling processes and unknown driving factor as well as on the transport processes in the ionosphere to the solar-influenced climate change.

CONCLUSIONS

A GPS receiver collocated with broadband meteorological shows excellent agreement in measuring ionospheric TEC and atmospheric PWV employed for Sun-Earth coupling studies. The brief and guidance technique presented in this paper could be applied to data from existing thousand of GPS receivers that exist worlwide could be used to create a global Sun-Earth coupling network. The preliminary results and analyses at Husafell Arctic vantage point desribed here are encouraging, further studies is needed to determine the effects of severe weather or geomagnetic storm on GPS propagation signals in both hemispheres to solicit investigation for a better understanding of their changes in relation to the local weather and global climate towards improved global climate systems as well as space weather prediction.

REFERENCES

Abdul Rashid, Z.A., Momani, M.A., Sulaiman, S., Mohd Ali, M.A., Yatim, B., Fraser, J.G., Sato, N., (2006), *GPS ionospheric TEC measurement during the 23rd November 2003 total solar eclipse at Scott Base Antarctica*, Journal of Atmospheric and Solar-Terrestrial Physics, Vol. 68 , No. 11, 1222–1236

Lastovicka, J., (2005), *Preface*, Journal of Atmospheric and Solar-Terrestrial Physics, Vol. 67, Issues 1-2, pp. 1

Lean, J., Rind, D., (1998), *Climate forcing by changing solar radiation*, Journal of climate, Vol. 11, No. 12, pp. 3069-3094

Rishbeth, H., (1997), *Long-term changes in the ionosphere*, Advances in Space Research, Vol. 20, No. 11, 2149 –2155

Suparta, W., (2005), *GPS TroWav Tool for Atmospheric-Terrestrial Studies*, unpublished

Suparta, W., Abdul Rashid, Z.A., Mohd Ali, M.A., Yatim, B., Fraser, J.G., (2008), *Observations of Antarctic precipitable water vapor and its response to the solar activity based on GPS sensing*, Journal of Atmospheric and Solar-Terrestrial Physics, Vol. 70, 1419-1447

Suparta, W., Mohd Ali, M.A., Yatim, B., Fraser, J.G., (2009), *Analysis of GPS sensed PWV and its response to the terrestrial winds over Antarctica*, Journal of Physics and Chemistry of the Earth, Vol. 34, Issues 1-2, 72-87

Tsurutani, B.T., Mannucci, A .J., Iijima, B., Guarnieri, F.L., Gonzalez, W.D., Judge, D.L., Gangopadhyay, P. , Pap, J., (2006), *The extreme 2003 solar flares (and Bastille Day, 2 0 0 0 Flare), ICMEs and resultant extreme ionospheric effect: a review*, Advances in Space Research, Vol. 37, No. 8, 1583–1588.

RECHERCHE SUR LES ANNEES PLUVIOMETRIQUES EXTREMES DANS LE CENTRE DU BENIN (AFRIQUE DE L'OUEST)

I. Yabi[1], F. Afouda[1], M. Boko[1]

ABSTRACT: Study of the extreme rainfall years in the centre of Benin
The present research studies the frequency and magnitude of extreme rainfall years with high rainfall variability that characterizes the study area since the 1970s.
The data concern the high rainfall (daily, monthly, seasonal and annual) of four (4) stations from ASCNA-Cotonou and covering the period 1941-2000. The use of descriptive statistics (mean, quartile, etc.) and the frequency analysis, were used to process data collected.
The results indicate that extreme rainfall years (surplus and deficits) are alternated with no apparent periodicity. In addition, the extreme rainfall was more frequent during the 1971-2000 series of thirty especially during the rainy season in comparison to the 1941-2000 series.

Keywords*: Center of Benin, extreme rainfall, frequency, agriculture, impacts***.**

RÉSUMÉ :
La présente recherche s'intéresse à la fréquence des années pluviométriques extrêmes en rapport avec la forte variabilité pluviométrique qui caractérise la région d'étude depuis les années 1970.
Les données utilisées concernent les hauteurs pluviométriques (saisonnières et annuelles) de quatre (4) stations extraites du fichier de l'ASCENA-Cotonou et couvrant la période 1941-2000. L'utilisation de la statistique descriptive (moyenne, quartile, etc.) et de l'analyse fréquentielle, ont permis de traiter les données collectées.
Les résultats attestent que les années pluviométriques extrêmes (déficitaires et excédentaires) s'alternent sans aucune périodicité apparente. En outre, les extrêmes pluviométriques ont été plus fréquents au cours de la série trentenaire 1971-2000 notamment pendant la saison pluvieuse en comparaison avec la série 1941-2000.

Mots clés: *Centre du Bénin, extrêmes pluviométriques, fréquence, agriculture, incidences.*

1. INTRODUCTION

L'Afrique de l'ouest est affectée depuis plus de trois décennies par une variabilité pluviométrique sans précédent, du reste depuis le siècle passé. En effet, la plupart des recherches climatologiques ont montré que les totaux pluviométriques annuels des décennies 1970 et 1980 sont caractérisés par des baisses sensibles (*Nicholson, 1980 ; Sircoulon et al., 1986 ; Le Borgne, 1990 ; Paturel et al., 1995 ; Brou et al., 1999*).

Au Bénin, la tendance climatique est identique à celle de l'Afrique de l'ouest. Le pays connaît depuis la fin des années 1960, une forte variabilité pluviométrique. Celle-ci se manifeste, en particulier, par une modification du régime des précipitations et par une diminution des hauteurs annuelles (*Bokonon-Ganta, 1987 ; Boko, 1988 ; Afouda, 1990 ; Houndénou, 1999 ; Yabi, 2002 ; Ogouwalé et al., 2005 ; Yabi et Afouda, 2007*).

Mais, dans ce contexte de tendance générale à la baisse, il survient par moments de fortes pluviométries génératrices d'inondations, parfois désastreuses voire dramatiques sur

[1] *Laboratoire Pierre PAGNEY "Climat, Eau, Ecosystème et Développment " (LACEEDE), Département de Géographie, Université d'Abomey-Calavi (République du Bénin.*

les plans socioéconomiques notamment agricoles (IPCC, 2007). Dans un contexte où l'agriculture pluviale constitue la principale occupation et procure l'essentiel des revenus des populations, toutes perturbations pluviométriques menacent la sécurité alimentaire capable d'entrainer des troubles socio-économiques voire politiques dans les sociétés (*Boko, 1988*).

Plusieurs travaux ont été consacrés à l'étude de l variabilité pluviométrique au Bénin en général et dans le Centre du Bénin en particulier (*Boko, 1988 ; Afouda, 1990 ; Yabi, 2002*), mais les aspects relatifs à l'étude des pluviométries extrêmes ont été peu abordés. Dès lors, quelques préoccupations méritent des approches de réponses. En effet, quelle est la fréquence et l'ampleur des extrêmes pluviométriques annuels dans le Centre du Bénin ? La présente recherche tente répondre à cette interrogation.

2. DÉMARCHE MÉTHODOLOGIQUE

2.1. Données utilisées et reconstitution des valeurs manquantes

Les données utilisées sont relatives aux hauteurs pluviométriques annuelles et saisonnières (la saison pluvieuse) des quatre (4) stations situées dans la région d'étude (**Fig. 1**).

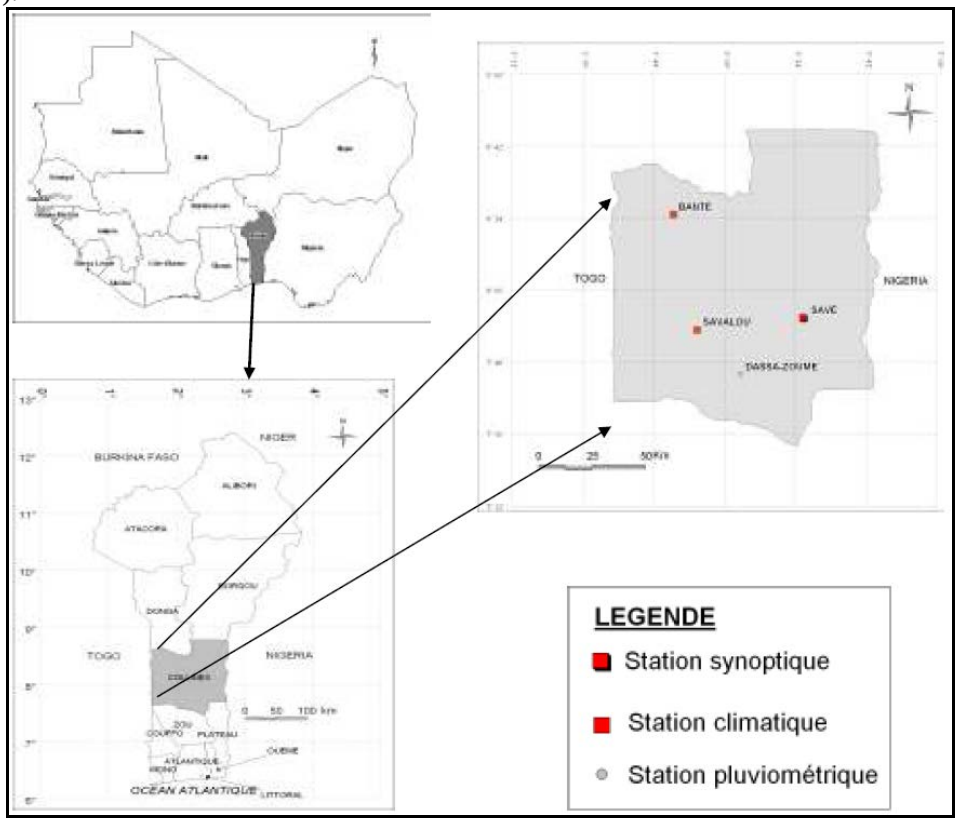

Fig.1 Situation géographique du secteur de l'étude et localisation des stations étudiées

Ces données ont été extraites du fichier de l'Agence pour la Sécurité et la Navigation Aérienne (ASECNA). La période considérée s'étend de 1941 à 2000 (60 ans) sauf à Savalou où les données exploitables ne remontent qu'en 1951.

Seule la station synoptique de Savè est exempte de lacune, les autres comportent quelques données manquantes. Les valeurs manquantes ont été reconstituées par la méthode des moindres carrés (*Houndénou, 1999*). Elle est basée sur le calcul de régression multiple entre les séries lacunaires et les séries complètes des stations situées dans un environnement géographique proche. Le calcul de la régression pour la période 1941-2000 a permis de combler 1,6 % du total d'observations.

2.2. Démarche méthodologique

Afin de mieux affiner les analyses, la période étudiée a été subdivisée en deux séries trentenaires, à savoir 1941-1970 et 1971-2000. La première série étant réputée plus pluvieuse et la seconde caractérisée par une fréquence des années sèches (*Yabi, 2002 ; Ogouwalé et al., 2005*). L'utilisation de la statistique descriptive (moyenne arithmétique, quartiles, médianes, etc.) a permis d'effectuer des analyses comparatives. Pour identifier les années pluviométriques extrêmes, la méthode de l'analyse fréquentielle a été utilisée (*Benzarti et al., 2004*). Ainsi, les années dont la fréquence au non dépassement est supérieure ou égale à 90 %, sont considérées comme des années extrêmement pluvieuses ; au contraire, les années dont la fréquence au non dépassement est inférieure ou égale à 10 %, sont considérées comme des années extrêmement sèches. La sélection de chaque type d'année est faite aux échelles annuelle et saisonnière.

La fréquence des années pluviométriques extrêmes (FAPE) excédentaires ou déficitaires est calculée suivant le protocole ci-après:

$$\mathbf{FAPE = (NAPE/NTA)*100}$$

- avec :

NAPE : nombre d'années pluviométriques extrêmes ;

NTA : nombre total d'année étudiées.

3. RÉSULTATS

3.1. Caractéristiques pluviométriques générales au cours de chaque série

3.1.1. A l'échelle annuelle

Les caractéristiques pluviométriques annuelles au cours des séries 1941-1970 et 1971-2000 sont illustrées dans la **Fig. 2**.

L'analyse de la figure 2 montre que les valeurs moyennes et maximales sont globalement élevées au cours de la première série (1941-1970) alors que les valeurs minimales sont plutôt faibles. Cette observation montre qu'à l'échelle annuelle, la série 1941-1970 est plus pluvieuse et confirme que les décennies 70 et 80 sont caractérisées des déficits pluviométriques en comparaison aux décennies 50 et 60.

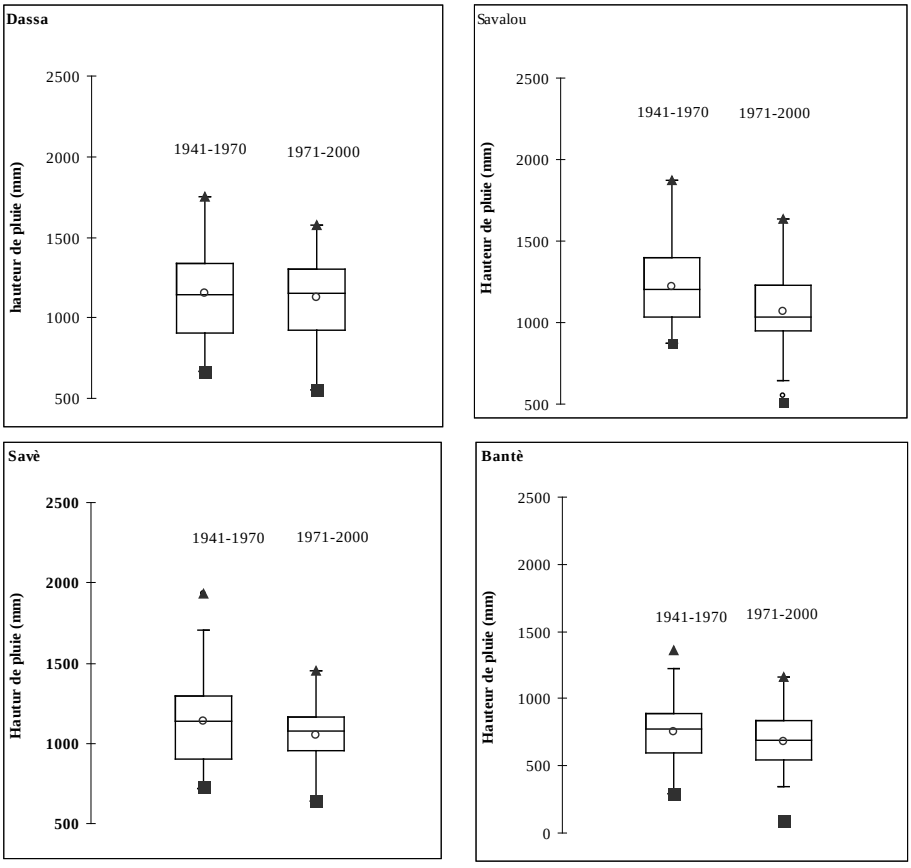

Fig. 2 Caractéristiques pluviométriques annuelles selon lés périodes 1941-70 et 1871-2000 dans les quatre stations. Le premier quartile (q1), la médiane (q2) le troisième quartile (q3) sont respectivement représentés par les barres horizontales inférieure, centrale et supérieure. Les points inférieur, central et supérieur de chaque boite représentent respectivement les valeurs minimum, moyenne et maximale de chaque série

3.1.2. A l'échelle saisonnière

La figure 3 montre la répartition des hauteurs de pluie au cours de la saison pluvieuse par station étudiée.

L'examen de la figure 3 révèle qu'à l'échelle saisonnière, les valeurs moyennes (moyenne et médiane) sont globalement plus élevées au cours de la série 1941-1970. Quant aux valeurs extrêmes (minima et maxima), elles sont plus prononcées durant la série 1971-2000. Ainsi, les plus faibles valeurs minima et les plus fortes valeurs maxima sont enregistrées au cours de cette série.

Il convient d'analyser la fréquence et l'ampleur des années pluviométriques extrêmes tant aux échelles annuelle que saisonnière.

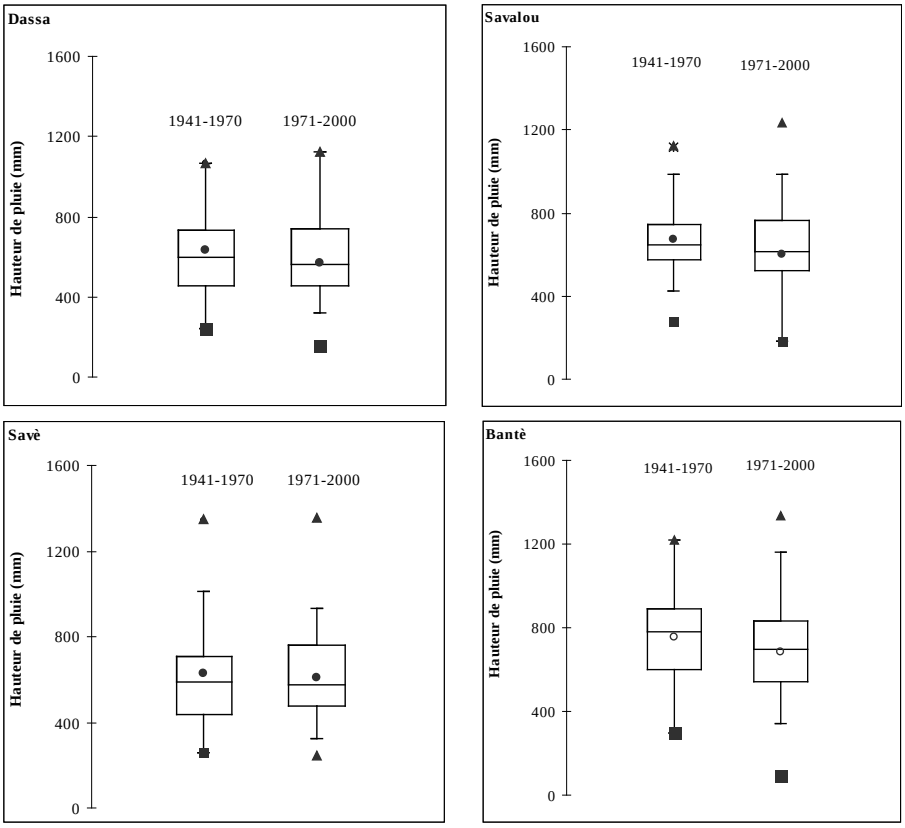

Fig. 3 Caractéristiques pluviométriques saisonnière suivant chaque série trentenaire. Le premier quartile (q1), la médiane (q2) le troisième quartile (q3) sont respectivement représentés par les barres horizontales inférieure, centrale et supérieure. Les points inférieur, central et supérieur de chaque boite représentent respectivement les valeurs minimum, moyenne et maximale de chaque série.

3.2. Fréquences des années pluviométriques extrêmes

3.2.1. A l'échelle annuelle

Le tableau 1 résume la fréquence des années pluviométriques extrêmes suivant chaque série étudiée.

La fréquence totale des années extrêmes varie entre 23 % et 30 % et la station de Bantè enregistre la forte valeur (30 %). Globalement, il n'y a pas de différence importante entre les valeurs de fréquence (des années sèches et pluvieuses) suivant les deux séries trentenaires. Au regard de cette observation, on peut déduire qu'à l'échelle annuelle, la fréquence des années pluviométriques extrêmes n'a pas connu une évolution notable entre les deux séries.

Tableau 1 ***Fréquence des années pluviométriques extrêmes (sèches et pluvieuses) à l'échelle annuelle***

Stations	1941-1970			1971-2000		
	Sèches	**Pluvieuses**	**Total**	**Sèches**	**Pluvieuses**	**Total**
Dassa	13 %	13 %	26 %	13 %	10 %	23 %
Savalou	13 %	13 %	26 %	13 %	13 %	26 %
Savè	13 %	10 %	23 %	13 %	13 %	26 %
Bantè	17 %	13 %	30 %	13 %	10 %	23 %

3.2.2. A l'échelle saisonnière

L'évolution des fréquences des hauteurs pluviométriques saisonnières extrêmes est résumée dans le tableau 2. Les années extrêmement sèches ont été plus fréquentes entre 1971 et 2000 par comparaison à la série 1941-1970. De même, la fréquence totale des années pluviométriques extrêmes a quasiment doublé au cours de la période 1971-2000 par rapport à la période 1941-1970. Ces constats permettent de conclure qu'à l'échelle saisonnière (saison pluvieuse) les années pluviométriques extrêmes (sèches et pluvieuses) sont de plus en plus fréquentes.

Tableau 2 ***Evolution de la fréquence des hauteurs pluviométriques saisonnières extrêmes.***

Stations	1941-1970			1971-2000		
	Sèches	**Pluvieuses**	**Total**	**Sèches**	**Pluvieuses**	**Total**
Dassa	10 %	13 %	23 %	20 %	17 %	37 %
Savalou	10 %	10 %	20 %	20 %	20 %	40 %
Savè	13 %	10 %	23 %	20 %	17 %	37 %
Bantè	10 %	13 %	23 %	20 %	20 %	40 %

Dans un contexte d'agriculture pluviale, la multiplication d'années pluviométriques extrêmes de saison pluvieuse rend vulnérable la production agricole. En effet, les années extrêmement sèches se manifestent par déficit hydrique prononcé pour les différentes cultures, ce qui affecte sérieusement leur rendement alors que les années de fortes pluviométries se manifestent par excédent hydrique important capable de provoquer des inondations désastreuses pour les cultures. Dans l'un ou autre cas, les activités agricoles se trouvent handicapées sans oublier les autres répercussions socioéconomiques.

CONCLUSION

La présente recherche a permis de constater que les années pluviométriques extrêmes (sèche et pluvieuse) sont de plus en plus fréquentes dans le Centre du Bénin. La saison pluvieuse est la plus affectée par ces anomalies pluviométriques.

Ces perturbations pluviométriques rendent vulnérables l'agriculture pluviale qui est la principale activité des populations étant donné qu'elles affectent principalement la saison pluvieuse dont dépend le rendement des cultures.

Ces constats invitent les différents acteurs du monde rural à définir des mesures d'atténuation et d'adaptation conséquentes capables de faire face à la nouvelle donne pluviométrique de la région d'étude qui, au demeurant, abritent deux des principaux greniers du Bénin.

BIBLIOGRAPHIE

Afouda F., (1990), *L'eau et les cultures dans Bénin central et septentrional : Etude de la variabilité des bilans de l'eau dans leurs relations avec le milieu rural de la savane africaine*. Thèse de doctorat nouveau régime. Paris IV-Sorbonne. 428 p.

Benzarti Z., Ben Boubakar H. et Henia L., (2004), *Circulations méridiennes et extrêmes pluvio-thermiques en Tunisie*. Acte du XVII^{ème} Colloque de l'Association internationale de Climatologie, Université de Caen (France), pp. 117-121.

Boko M., (1988), *Climat et communautés rurales du Bénin : Rythmes climatiques et rythme de développement*. Thèse d'Etat ès lettre, Dijon 607p.

Bokonon-Ganta E., (1987), *Les climats de la région du Golfe du Bénin*. Thèse de Doctorat du 3ème cycle. Institut de Géographie, Université de Paris-Sorbonne, Paris, 248 p + annexe.

Brou Y.T, Servat E. et Paturel J.E., (1999), *Contribution à l'Analyse des inter-relations entre activités humaines et variabilité climatique : cas du sud-forestier ivoirien*. CR Acad Sci (Paris) ; **327**(sér II a).

Houndénou C., (1999), *Variabilité climatique et maïsiculture en milieu tropical humide, diagnostic et modélisation*. Thèse de doctorat Unique, UMR 50 80 du CNRS, climatologie de l'espace tropicale, 341 p.

IPCC, (2007), *The Physical Science Basis. Contribution of Working Group I to the Fourth Assessment Report of the Intergovernmental Panel on Climate Change*. Cambridge University Press, Cambridge, United Kingdom and New York, NY, USA, 996 p.

Le Borgne J. (1990), *La dégradation actuelle du climat en Afrique entre Sahara et Équateur*. In : Richard JF, éd. La dégradation des paysages en Afrique de l'Ouest. Paris ; Dakar : Aupelf ; Coopération Française ; Union internationale pour la conservation de la nature (UICN) ; Orstom-ENDA-TM, Documentation française ; Presses Universitaires de Dakar.

Nicholson S. E. (1980), *The nature of rainfall fluctuations in subtropical West Africa*. In Mon Wea Rev, **108**, pp. 473-87.

Ogouwalé E. Yabi I. et Boko M., (2005), *Singularité de la variabilité pluviométrique entre les 9 et 10ème parallèle au Bénin (Afrique de l'ouest)*. In actes des 2 ^{ème} journées Scientifiques Internationales des Universités Nationales du Bénin, Tome 2, pp 62-71.

Paturel J.E, Servat E., Kouamé B., Masson J. et Lubes H. (1995), *La Sécheresse en Afrique de l'Ouest non sahélienne (Côte d'Ivoire, Togo, Bénin)*. Sécheresse, **6**, pp. 95-102.

Sircoulon J.(1986), *La sécheresse en Afrique de l'Ouest. Comparaison des années 1982 - 1984 avec les années 1972 - 1973*. Cahiers hydrologiques Vol XXI, **N° 4**, ORSTOM, Bondy ,pp.75 - 92.

Yabi I. (2002), *Particularités de la variabilité pluviométrique entre 7° et 8°N au Bénin*. Mémoire de maîtrise de Géographie FLASH - UAC, Abomey-Calavi. 96p.

Yabi I. et Afouda F., (2007), *Variabilité pluviométrique du début de la saison agricole et mesures d'adaptation dans le département des Collines au Bénin (Afrique de l'ouest)*. Actes du 1er colloque de l'UAC des Sciences, Cultures et Technologies, Géographie : pp. 315 327

AIMS AND SCOPE

Geographia Technica is a journal devoted to the publication of all papers on all aspects of the use of technical and quantitative methods in geographical research. It aims at presenting its readers with the latest developments in G.I.S technology, mathematical methods applicable to any field of geography, territorial micro-scalar and laboratory experiments, and the latest developments induced by the measurement techniques to the geographical research. *Geographia Technica* is dedicated to all those who understand that nowadays every field of geography can only be described by specific numerical values, variables both of time and space which require the sort of numerical analysis only possible with the aid of technical and quantitative methods offered by powerful computers and dedicated software. Our understanding of *Geographia Technica* expands the concept of technical methods applied to geography to its broadest sense and for that, papers of different interests such as: G.I.S, Spatial Analysis, Remote Sensing, Cartography or Geostatistics as well as papers which, by promoting the above mentioned directions bring a technical approach in the fields of hydrology, climatology, geomorphology, human geography territorial planning are more than welcomed provided they are of sufficient wide interest and relevance.

Targeted readers:
The publication intends to serve workers in academia, industry, and government.
Students, teachers, researchers and practitioners should benefit form the ideas in the journal.

GUIDANCE FOR AUTHORS

Submission

Articles and proposals for articles are accepted for consideration on the understanding that they are not being submitted elsewhere. Three copies of all articles and proposals for articles should be sent to: The Editor, at the following address: **editor@studiacrescent.com** . The site hosts the submitted articles for free (PDF).

Content

In addition to full-length research contributions, the journal also publishes Short Notes, Books and Software Reviews, Letters to the Editor; however the editors wish to point out that the views expressed in the book reviews are the personal opinion of the reviewer and do not necessarily reflect the views of the publishers. Each year two volumes are scheduled for publication. Papers in English or French are accepted. The articles are printed in black and white, but each issue is accompanied by a mini CD containing the paper in extenso and full color graphics. The papers shall be reviewed by two anonymous peers. The link between author and reviewers is mediated by the Editor.

Format

Paper Size must be 17 cm x 24 cm, the margins: Top - 5.7 cm, Bottom - 5 cm, Left - 4 cm, Right - 4 cm. **The font** to be used is : Times New Roman. Font sizes vary, according to the following uses: **the title** must be written with11 bold big letters, **the author** 10 bold big letters, the "Abstract" word with 9 bold normal letters, the **abstract contents** 9 normal, the **article text** must be written with10 normal, the title of the **chapter** with 10 bold big letters, the title of the **table** 9 bold-centered, the **figures** : 9 normal and the **bibliography** with 11 bold big letters.
For your ease, we have provided a dummy article, formatted as required at our Guides for authors page at **http://studiacrescent.com/publishing/main-page/guides-for-authors**.